TRIBOLOGICAL BEHAVIOUR OF POLYMER NANOCOMPOSITES CONTAINING TUNGSTEN BASED NANOPARTICLES

A Thesis submitted to
the Graduate School of Engineering and Science of
İzmir Institute of Technology
in Partial Fulfillment of the Requirements for the Degree of

MASTER OF SCIENCE

in Materials Science and Engineering

By
Kazım KARAL

July 2007
İzmir, Turkey

We approve the thesis of **Kazım KARAL**

Date of Signature

…….. **06 July 2007**
Assoc. Prof. Dr. Metin TANOĞLU
Supervisor
Department of Mechanical Engineering
İzmir Institute of Technology

…….. **06 July 2007**
Prof. Dr. Orhan ÖZTÜRK
Department of Physics
İzmir Institute of Technology

…….. **06 July 2007**
Assoc. Prof. Dr. Funda TIHMINLIOĞLU
Department of Chemical Engineering
İzmir Institute of Technology

…….. **06 July 2007**
Prof. Dr. Muhsin ÇİFTÇİOĞLU
Head of Department
İzmir Institute of Technology

…….
Prof. Dr. M. Barış ÖZERDEM
Head of the Graduate School

ACKNOWLEDGEMENTS

I am very grateful to my supervisor Assoc. Prof. Dr. Metin Tanoğlu for his advise, help and support. I would like to acknowledge The Scientific and Technical Research Council of Turkiye (TUBİTAK) for financial support for 105M065 project. I would also like to express my sincere thankfulness to Prof. Dr. M. Lütfi Övecoğlu, Prof. Dr. Mustafa Ürgen, Nil Ünal, Selim Coşkun and Vefa Ezirmik of İstanbul Technical University, Department of Metallurgical and Materials Engineering for all their help during my studies.

I would like express my appreciation to all my friends especially A.Tuğrul Seyhan, Çiçek Karşal, Erinç Sezgin and Mustafa Altındiş for their help, support and friendship. Finally, a special thank you goes to my mother, sisters, brother-in-law and Aslı Guruşçu. Without their constant support, this work could not have been accomplished.

ABSTRACT

TRIBOLOGICAL BEHAVIOUR OF POLYMER NANOCOMPOSITES CONTAINING TUNGSTEN BASED NANOPARTICLES

The use of nanostructured fillers in epoxy systems has a significant role on the development of thermosetting composites. Recent investigations on inorganic nanoparticles filled polymer composites reveal their significant potential in producing materials with low friction and/or high wear resistance.

In the present study, epoxy nanocomposites and fiber reinforced polymer (FRP) composites were prepared with the addition of tungsten based nanostructured particles which are produced by mechanical alloying. The effects of the nanostructured additives on the tribological, mechanical and thermal properties of composite laminates and nanocomposites were investigated. Composite laminates with and without filler were manufactured by using hand lay-up technique and cured under compression.

It was found that tungsten based particle loading has no significant effect on the flexural properties of the nanocomposites and the composite laminates, and the tensile properties of the nanocomposites. It was found that while the addition of 3 wt. % of nanoparticles increases the hardness values, it significantly improves the wear resistance of nanocomposites. Furthermore, the significant improvement on the wear resistance was observed with the addition of 3 wt. % W-SiC-C (24h mechanical milling) powder onto the surface of fiber reinforced epoxy. The worn surfaces were examined with scanning electron microscopy (SEM) and the results revealed that wear mechanisms are altered due to the presence of nanoparticles in the matrix. Differential scanning calorimetry (DSC) results showed that nanoparticles have no significant effect on glass transition temperatures (T_g) of nanocomposites. Incorporation of nanoparticles increased the thermo mechanical properties of nanocomposites and composite laminates; including the storage and loss modulus and T_g.

ÖZET

TUNGSTEN ESASLI NANOPARTİKÜLLER İÇEREN POLİMER NANOKOMPOZİTLERİN TRİBOLOJİK DAVRANIŞI

Nanoyapılandırılmış katkı maddelerinin epoksi reçine içerisinde kullanılması termoset kompozitlerin geliştirilmesinde ciddi bir rol oynamaktadır. İnorganik nanoparçacıklarla güçlendirilmiş polimer kompozitler üzerine yapılan son çalışmalar, bu kompozitlerin düşük sürtünme katsayısına sahip ve yüksek aşınma mukavemeti gösteren malzemelerin üretimindeki önemli potansiyeli ortaya çıkarmıştır.

Bu çalışmada, epoksi nanokompozitler ve fiber ile güçlendirilmiş polimer kompozitler, mekanik alaşımlama ile üretilmiş tungsten bazlı nano yapılı partiküller eklenerek hazırlanmıştır. Nano yapılı bu katkıların kompozit lamine yapılara ve nanokompozitlere tribolojik, mekanik ve termal özellikler bakımından etkileri incelenmiştir. Nano yapıda partikül katkılı ve katkısız kompozit lamine yapılar el yatırması yöntemi ile üretilmiş ve basınç altında kürleştirilmiştir.

Tungsten bazlı partiküllerin ilave edilmesi, lamine kompozit yapıların ve nanokompozitlerin eğme özelliklerine, ayrıca nanokompozitlerin çekme özelliklerine önemli bir etkisi olmadığı bulunmuştur. Nano parçaların sadece %3 ağırlık oranında eklenmesi nanokompozitlerin sertlik değerlerini arttırması yanında aşınma dayanımlarını da önemli ölçüde arttırdığı bulunmuştur. Bununla birlikte, %3 ağırlık oranındaki 24 saat mekanik işlem görmüş W-SiC-C tozunun fiber ile güçlendirilmiş epoksi yüzeyine eklenmesi ile aşınma dayanımında oldukça önemli iyileşme gözlenmiştir. Aşınmış yüzeyler taramalı electron mikroskopu (SEM) ile incelenmiştir ve sonuçlar aşınma mekanizmasının matriks içinde varolan nano parçalara bağlı olarak değiştiğini göstermiştir. Diferansiyel taramalı kalorimetri (DSC) sonuçları, nanokompozitlerin camsı geçiş sıcaklığına (T_g) nano parçaların önemli bir etkisinin olmadığını göstermiştir. Nano parçaların varlığı, lamine kompozit yapıların ve nanokompozitlerin dinamik mekanik özelliklerini arttırmıştır.

TABLE OF CONTENTS

LIST OF FIGURES viii
LIST OF TABLES xii

CHAPTER 1. INTRODUCTION 1

CHAPTER 2. POLYMER NANOCOMPOSITES 5
2.1. Nanostructured Materials and Their Producing Techniques 5
2.2. Tungsten 8
2.3. The Properties and Applications of Epoxy Resins 11
2.4. Fiber Reinforced Epoxy Composites 13
2.5. Epoxy Composites Containing Nanosized Fillers 17

CHAPTER 3. TRIBOLOGY FOR POLYMER NANOCOMPOSITES 20
3.1. Wear Mechanisms 20
3.1.1. Abrasive Wear 20
3.1.2. Sliding, Adhesive Wear and Friction Transfer 23
3.1.3. Fatigue Wear 25
3.1.4. Corrosive Wear 25
3.2. Tribological Applications of Composite Materials 25
3.3. Effect of Fillers on the Properties of Composites 27

CHAPTER 4. EXPERIMENTAL 39
4.1. Materials 39
4.2. Characterization of Tungsten based Powders 40
4.3. Preparation of Nanocomposites 40
4.4. Preparation of Fiber Reinforced Composites with Nanoparticles 41
4.5. Wear Test 42
4.6. Characterization of Mechanical Properties 44
4.6.1. Hardness Test 44
4.6.2. Flexural Test 45
4.6.3. Tensile Test 46

4.7. Characterization of Thermal Properties 47
4.7.1. Differential Scanning Calorimetry (DSC) 47
4.7.2. Dynamic Mechanical Analysis (DMA) 48
4.8. Microstructure Characterization 49
4.8.1. Scanning Electron Microscopy (SEM) 49
4.8.2. Optical Microscopy 49

CHAPTER 5. RESULTS AND DISCUSSION 50
5.1 Properties of Tungsten Based Powders 50
5.2. Properties of Nanocomposites 52
5.2.1. Wear Resistance 52
5.2.2. Flexural Properties 58
5.2.3. Tensile Properties 59
5.2.4. Thermal Properties 61
5.3. Fiber Reinforced Nanocomposites 65
5.3.1. Wear Performance 65
5.3.2. Flexural Properties 72
5.3.3. Thermomechanical Properties 75

CHAPTER 6. CONCLUSIONS 79

REFERENCES 81

LIST OF FIGURES

Figure		Page
Figure 1.1	Test Specimen Configurations	4
Figure 2.1.	a) A typical Spex shaker mill b) Tungsten carbide vial set consisting of the vial, lid, gasket, and balls	7
Figure 2.2.	Schematic view of a ball-powder-ball collision.	8
Figure 3.1.	Types of contact during abrasive wear. (a) Open two-body. (b) Closed two-body. (c) Open three-body. (d) Closed three-body	22
Figure 3.2.	Illustration of the four types of abrasive wear, (a) Low-stress abrasion (b) High-stress abrasion is almost always more severe than low-stress abrasion, (c) Gouging abrasion where material removal is caused by the action of repetitive compressive loading, (d) Polishing wear	23
Figure 3.3.	Comparison of the wear performances of various groups pf epoxy composites with 5 vol.% of nano-TiO_2 instead of the same amount of PTFE under a standard wear condition, i.e. 1 MPa and 1 m/s: (a) the specific wear rate measured with both P-o-D and B-o-R apparatuses, and (b) the frictional coefficient measured with P-o-D apparatus	29
Figure 3.4.	Flexural strength and unnotched Charpy impact strength of the neat epoxy (EP) and SCF or Aramid (Ar) filled composites (without PTFE)	31
Figure 3.5.	Specific wear rate (ws) and the coefficient of friction (l) of the neat epoxy (EP) and SCF or aramid (Ar) filled composites (without PTFE) under sliding conditions (block-on-ring)	32
Figure 3.6.	Flexural strength and unnotched Charpy impact strength of the epoxy resin and its composites	34
Figure 3.7.	Wear rate of the epoxy matrix composites filled with silica particles (□) 120 nm, 1 N; (◊) 510 nm, 1N; (♦) 120 nm, 2 N; (■) 510 nm, 2 N)	35

Figure 3.8. Relationship between stiffness and impact strength for some of the composites. The black line represents the traditional tendency. (●) The neat polymer. (▲) EP/TiO_2 nanocornposites. (■) EP/TiO_2/$CaSiO_3$ composites. (♦) EP/SiC_from earlier experiments. (X) EP containing hygrothermally decomposed polyurethane (HD-PUR, 40 wt %) 37
Figure 3.9. Effect of filler at 30 volume percent on epoxy composite wear 38
Figure 4.1. Schematic illustration of quadriaxial stitched non-crimp glass fibers 39
Figure 4.2. Production Steps of Polymer Nanocomposites and Glass Fiber Reinforced Nanocomposites 42
Figure 4.3. a)Tribometer (CSM instruments), b) 3D profilometer(Veeco Wyko NT 1100) 43
Figure 4.4. Wear test specimens; a) nanocomposites, b) fiber reinforced composites 43
Figure 4.5. Shimadzu™ micro hardness tester 44
Figure 4.6. Flexural test specimen under load 46
Figure 4.7. Tensile test specimen under load 47
Figure 4.8. Perkin Elmer Diamond DMA 48
Figure 4.9. DMA Specimens; a) nanocomposites, b) fiber reinforced nanocomposites 49
Figure 5.1. XRD patterns of a) W powder, b) W-SiC-C powder (6h mechanically alloyed), c) W-SiC-C powder (24h mechanically alloyed), d) W-B_4C-C powder (10 h mechanically alloyed) 50
Figure 5.2. SEM images and particle size distributions of (a) W-SiC-C (6h), (b) W-SiC-C (24h), (c) W-B_4C-C (10h) 51
Figure 5.3. Comparison of the specific wear rates of nanocomposites containing (a) 3 wt. % and (b) 5 wt. % tungsten-based powders. The wear rate for neat epoxy is also given. 53
Figure 5.4. Comparison of the Friction Coefficient values of nanocomposites containing (a) 3 wt. % and (b) 5 wt. % tungsten-based powders. The μ values for neat epoxy are also given in the Figures. 54

Figure 5.5. The surface topology of worn surfaces: (a) 3D profile of the wear track of the neat epoxy, (b) 3D profile of the wear track of the epoxy matrix composite filled with 3 wt. % W-SiC-C (24h) powder 55
Figure 5.6. SEM images of worn surfaces of (a) neat epoxy, (b) 3wt.% W/epoxy (c) 3 wt. % W-SiC-C (24h)/epoxy, (d) 5wt. % W/epoxy and (e) 5 wt. % W-SiC-C (24h)/epoxy..... 56
Figure 5.7. Microhardness of neat epoxy and its nanocomposites containing (a) 3wt. %, (b) 5 wt. % tungsten based powders..... 57
Figure 5.8. Flexural Strength and modulus values of composites containing 3 wt. % powder 58
Figure 5.9. Flexural Strength and modulus values of composites containing 5 wt. % powder 59
Figure 5.10. Tensile Strength and modulus values of composites containing 3 wt. % powder 60
Figure 5.11. Flexural Strength and modulus values of composites containing 5 wt. % powder 61
Figure 5.12. At 3 wt. % loading rate (a) Storage Modulus of epoxy nanocomposites (b) Storage Modulus values at 20 ^{0}C 62
Figure 5.13. At 5 wt. % loading rate (a) Storage Modulus of epoxy nanocomposites (b) Storage Modulus values at 20 ^{0}C 63
Figure 5.14. Comparison of Tan δ values of epoxy nanocomposites containing (a) 3wt. % and (b) 5 wt. % tungsten based powders..... 64
Figure 5.15. Glass Transition Temperatures (T_g) of epoxy nanocomposites containing (a) 3wt. %, (b) 5 wt. % of tungsten based powders 65
Figure 5.16. Comparison of the specific wear rates of fiber reinforced nanocomposites containing 3 wt. % of tungsten-based powders..... 66
Figure 5.17. Comparison of the specific wear rates of fiber reinforced nanocomposites containing 5 wt. % of tungsten-based powders..... 67
Figure 5.18. Comparison of the Friction Coefficient values of non-crimp glass fabric reinforced epoxy-based nanocomposites containing (a) 3 wt. % and (b) 5 wt. % tungsten-based powders 68

Figure 5.19. The surface topology for worn surfaces of non-crimp fabric reinforced (a) neat epoxy (b) epoxy nanocomposite containing 5 wt.% W-SiC-C (24h) powder 69
Figure 5.20. SEM images of worn surfaces of glass fabric reinforced composites containing epoxy matrix with (a) no powder addition (neat epoxy), (b) 3wt.% W, (c) 3 wt. % W-SiC-C (24h), (d) 5wt. % W and (e) 5 wt. % W-SiC-C (24h)..... 71
Figure 5.21. Microhardness of fiber reinforced epoxy nanocomposites containing (a) 3wt. %, (b) 5 wt. % of tungsten based powders 72
Figure 5.22. Flexural Strength and modulus values of glas fiber reinforced composites containing 3 wt. % powder 73
Figure 5.23. Flexural Strength and modulus values of composites containing 5 wt. % powder 74
Figure 5.24. Optical micrographs of a) Fiber reinforced composite without filler, b) Fiber reinforced composite containing 5 wt. % of W..... 75
Figure 5.25. At 3 wt. % loading rate (a) Storage Modulus of fiber reinforced epoxy composites (b) Storage Modulus values at 20 ^{0}C 76
Figure 5.26. At 5 wt. % loading rate (a) Storage Modulus of fiber reinforced epoxy composites (b) Storage Modulus values at 20 ^{0}C 77
Figure 5.27. Comparison of Tan δ values of fiber reinforced epoxy nanocomposites containing (a) 3wt. % and (b) 5 wt. % tungsten based powders..... 78

LIST OF TABLES

Table		Page
Table 2.1.	Properties of Tungsten	10
Table 2.2.	Thermosetting resin comparison.	12
Table 2.3.	Fiber Types and Their Some Properties.	13
Table 3.1.	Tribological Applications of Polymer Composite Materials	26
Table 3.2.	Under the Constant Sliding Velocity (1 m/s), the Influence of the Normal Force on the Variation of the Wear Rate, Coefficient of Friction, and the Formation of Transfer Films	33
Table 5.1.	The Volume Loss Values of Nanocomposites	52
Table 5.2.	The Volume Loss Values of Fiber Reinforced Composites	66

CHAPTER 1

INTRODUCTION

Polymer composites have gained great interest as high-performance structural materials for aerospace, defence, marine, automotive and civil engineering applications over the past few decades. This is due to their dimensional stability with high strength to stiffness ratio and good thermal properties. With the advent and application of nanotechnology, polymer nanocomposites are also promising development of next generation material systems for various applications. Most of the work carried out in the area of polymer nanotechnology has been focussed on the improvement of thermal, mechanical, optical and barrier properties of thermosetting and thermoplastic polymer systems (Chowdhury et al. 2006). However, there is a lack of information on the tribological behaviour of the polymer nanocomposites.

High performance polymer composite materials have been also used as sliding elements for engineering applications under hard working conditions. The required materials need to provide unique mechanical and tribological properties combined with a low specific weight and a high resistance to degradation in order to ensure safety and economic efficiency (Chang et al. 2005).

Epoxy resins are widely used in industrial applications owing to their high mechanical and adhesion characteristics as well as their chemical resistance, together with their curability in a wide range of temperatures without the emission of volatile by products. Because of these advantages of epoxies, they find significant use in many applications including paints and coatings, adhesives, industrial tooling and composites, electrical systems and electronics, consumer and marine as well as aerospace.

There is a number of ways to modify epoxies by adding various fillers such as talc, silica and alumina, besides flexibilizers, viscosity reducers, colorants, thickeners, accelerators and adhesion promoters. These modifications are made to reduce costs, to improve performance, and to improve processing convenience. In order to improve the friction and wear behaviour of an epoxy material, one of the traditional concepts is to reduce its adhesion to the counterpart material and to enhance its hardness, stiffness and compressive strength. This can be achieved quite successfully by using special fillers that exhibit a good compatibility with liquid epoxy resins (Zhang et al. 2004).

Fillers play a substantial role in the production of polymeric materials (Bloom et al. 2003). Common filler types include glass, carbon and aramid fibers as well as particles such as ceramic and metal powders that can be chosen with respect to design of interest.

Fillers can alter the physical, rheological, chemical resistance, thermal, optical and electrical properties of a polymeric component. In addition to the electrical and thermal conductivity, wear and corrosion resistance of polymers can be increased with the addition of metallic fillers (Bloom et al. 2003), short fibers and some others (Chang and Zhang). The particles in these applications are generally of micrometer size. Use of nanoparticles as fillers in polymer composites has been attracting attention from materials scientists, technologists and industrialists (Xing and Li 2004).

The modification of the polymer composite surfaces and thus the improvement of their wear properties have been gained importance. The main reason of that, more and more industrial components such as bushings, cams, gears, rollers, wheels, brakes, conveyors, and sliding shoes, etc., are manufactured from short/continuous fiber reinforced composites, where friction and wear are key parameters to be taken into consideration (Hui and Zhong 2004).

In the recent years, with the intention of improving the tribological performance of the matrices, various types of nanoparticle filled polymer composites were developed and their performances were investigated. It has been observed that the inorganic fillers enhance not only the mechanical properties but also the tribological properties of polymers. In comparison with the conventional microscaled particles, nanoparticles were proved to have some special advantages for tribological applications. They provide (1) lower abrasiveness due to its reduced angularity; (2) a remarkable reinforcing effect, i.e., the enhanced modulus, strength, and toughness simultaneously; (3) better adhesion between the nanoparticles and the matrix due to its higher specific areas; and (4) a lower content of filler needed (Zhang et al. 2002, Xian et al. 2006).

Although the reinforcement effect upon the stiffness, toughness, and wear performance of the composites can be determined by the properties of the composite constituents, these properties depend strongly on the microstructure represented by the filler size, shape, and the homogeneity of particle distribution.

It is important for various applications to study the reinforcement effect of nanofillers in polymer matrices to interpret the mechanism of the improvement in the final mechanical properties.

The realization of the expected enhancements in ultimate performance of composites can only be achieved, if the nanoparticles are well dispersed in the surrounding polymer matrix. Due to their high specific surface area, nanoparticles in general tend to exist in agglomerated form within polymers. The particle attraction is thus caused by adhesive forces resulting from the material's surface energy. The smaller the particles, the more difficult it appears to break down these agglomerates and to accomplish a homogeneous distribution within the surrounding matrix. In order to attain the goal, an appropriate mixing technology which covers either application of high shear to disperse the involved powders within polymers or direct incorporation of chemically surface modified fillers must be utilized. This process is necessary in order to transfer the nanoparticles from the agglomerated state into a homogenously dispersed state. While for thermoplastic matrices mainly twin screw extrusion is the method for manufacturing nanocomposites, another mixing technology must be taken into account for low viscosity liquid thermosetting resin systems. This dispersion technique works such that a metal disc rotates with high speed inside the resin/particle mixture implying high shear energy. Another way to disperse nanoparticles is the application of ultrasound vibration, which also helps to improve the dispersion state of nanoparticles (Chang et al. 2005).

In the present study, the first objective was to develop tungsten based nanoparticle added epoxy nanocomposites with a good particle dispersion. Fabrication of glass fiber reinforced composites using nanocomposite suspensions as a matrix was the second goal. The third objective was to characterize the effect of filler type and content on the tribological, thermal and mechanical properties of the prepared nanocomposites and composite laminates. Tungsten and tungsten based nanoparticles were prepared by ball milling technique in collobration with İstanbul Technical University, Department of Metallurgical and Materials Engineering under a TÜBİTAK project. In that manner, the tungsten based nanostructured powders were incorporated into epoxy resin to obtain particle/resin suspensions. The prepared suspensions were used to process both nanocomposites and fiber reinforced composites. Composite laminates with and without filler were fabricated by hand lay-up technique. Additionally, as an innovative approach single top surface of the composite laminates were impregnated with epoxy suspensions to obtain functionalized surfaces. The flexural properties, the friction coefficient and the specific wear rate of the nanocomposites and composite laminates, the tensile strength and modulus of the

nanocomposites were measured to evaluate the effects of the particles on the mechanical properties. By utilizing dynamic mechanical analyser (DMA) and differential scanning calorimeter (DSC), thermal properties of the composites were investigated. The worn surfaces of specimens were investigated through scanning electron microscopy (SEM) to reveal the wear mechanisms. The structure of tungsten based powders was investigated through X-ray diffraction (XRD). The void contents and the structure of nanocomposites and laminates were examined based on optical microscopy and SEM, respectively.

In Figure 1.1, specimen configurations prepared in this study are illustrated. In the literature, to our knowledge there is limited work on the investigation of tribological behaviour of particle filled (especially tungsten based nanopowder) polymer composites and fiber reinforced nanocomposite system. In addition, the preparation of tungsten based nanoparticle added thermoset system for wear properties are relatively new. Therefore, the project has original contributions to the literature.

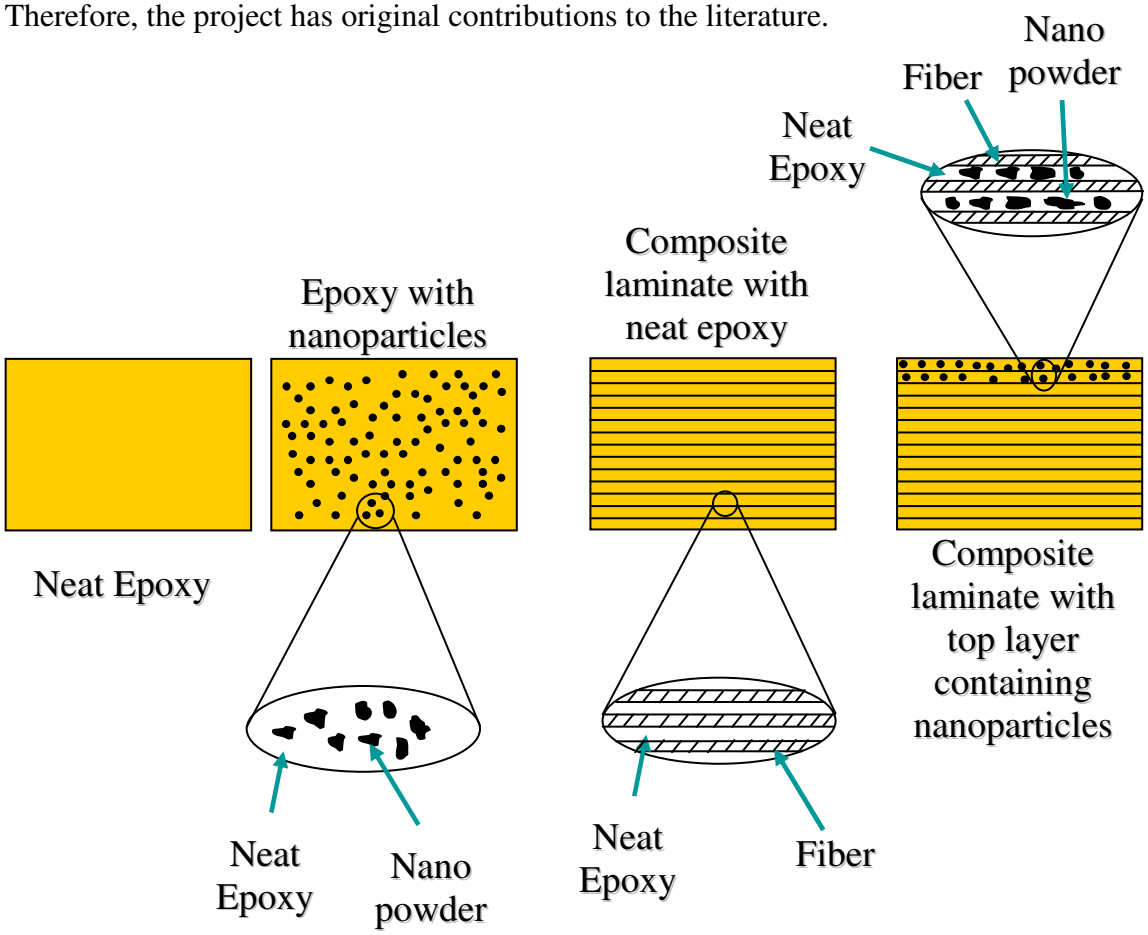

Figure 1.1. Test Specimen Configurations

CHAPTER 2

POLYMER NANOCOMPOSITES

Polymer nanocomposites are usually defined as the blend of a polymer matrix and additives that have at least one dimension in the nanometer range. The additives can be one-dimensional (examples include nanotubes and fibres), two-dimensional (which include layered minerals like clay), or three-dimensional (including spherical particles). Over the past decade, polymer nanocomposites have attracted considerable interests in both academia and industry, owing to their outstanding mechanical properties like elastic stiffness and strength with only a small amount of the nanoadditives (Becker and Simon 2006). For example, considerable improvement in the mechanical and tribological properties can be achieved in polymers with the addition of very low content of nano-fillers such as nanostructured form of clay, tungsten and carbon fibers.

2.1. Nanostructured Materials and Their Producing Techniques

In general, nanostructured materials with grain sizes less than 100 nm have been offering enhanced combinations of physical, mechanical and magnetic properties as compared to their conventional micro-sized equilavents (>1 μm) because of their extremely small size of the grains and a large fraction of their atoms located in their grain boundaries.

Mechanical Alloying (MA), a well known process to fabricate various nanocrystalline materials including several amorphous, metal nitrides, metal carbides and alloys, has been considered as a very powerful technique due to its simplicity and relatively inexpensive equipment (El-Eskandarany et al. 2000). In order to produce mechanically alloyed powders, different types of high-energy milling equipment such as spex shaker mills, planetary ball mills, attritor mills and commercial mills are used. They have different capacity, efficiency of milling and additional arrangements for cooling, heating, etc (Suryanarayana 2001, Goff 2003).

Commonly spex shaker mills are used for laboratory investigations. About 10±20 g of the powder is milled at a time depending on the density of starting constituents (Goff 2003). The common variety of these mills has one vial, containing

the sample and grinding balls, secured in the clamp and shakes the milling container in three-mutually perpendicular directions at about 1200 rpm resulting in powder microstructural refinement with time (Suryanarayana 2001, Goff 2003). Ball-ball and ball-container collisions continually trap and refine the powder constituents with time ultimately leading to an overall homogeneously dispersed microstructure (Goff 2003). There are various vial materials suitable for the spex mills, for instance; Hardened steel, alumina, tungsten carbide, zirconia, stainless steel etc. In figure 2.1, a typical spex mill and tungsten carbide vial set can be seen.

The planetary ball mill in which a few hundred grams of the powder can be milled at a time is another popular mill for conducting MA experiments. It is called the planetary ball because its vials make a planet-like movement. The centrifugal force produced by the vials rotating around their own axes act on the vial contents, consisting of material to be ground and the grinding balls. So, powders are trapped between the rotating balls and the walls of the vial and refined. The frequency of impacts is much more in the spex mills, the linear velocity of the balls in this type of mill is higher than that in the Spex mills, though.

Mechanical Alloying is an advanced fabrication process that can produce ultra-fine and homogenous powders (Ryu et al. 2000). MA of powder mixtures is used to produce nanocrystalline materials with a grain size of few nanometers. Moreover, this technique can be used to induce chemical (displacement) reactions in powder mixtures at room temperature or at much lower temperatures than normally required to synthesize pure metals (Suryanarayana et al. 2001).

In any mechanical alloying process, starting powder constituents are first mixed or blended according to the required stoichiometry for the given composite formulation. Then, they are put in the milling container with the appropriate ball charge and milled until a steady state of homogeneous dispersion is achieved (Goff 2003). The central event of MA is the ball-powder collisions (Fecht 2002). Microstructural refinement during the MA process occurs due to the repeated welding, fracturing, and rewelding of the dry powder constituents during their impact between ball-ball and/or ball-container collisions.

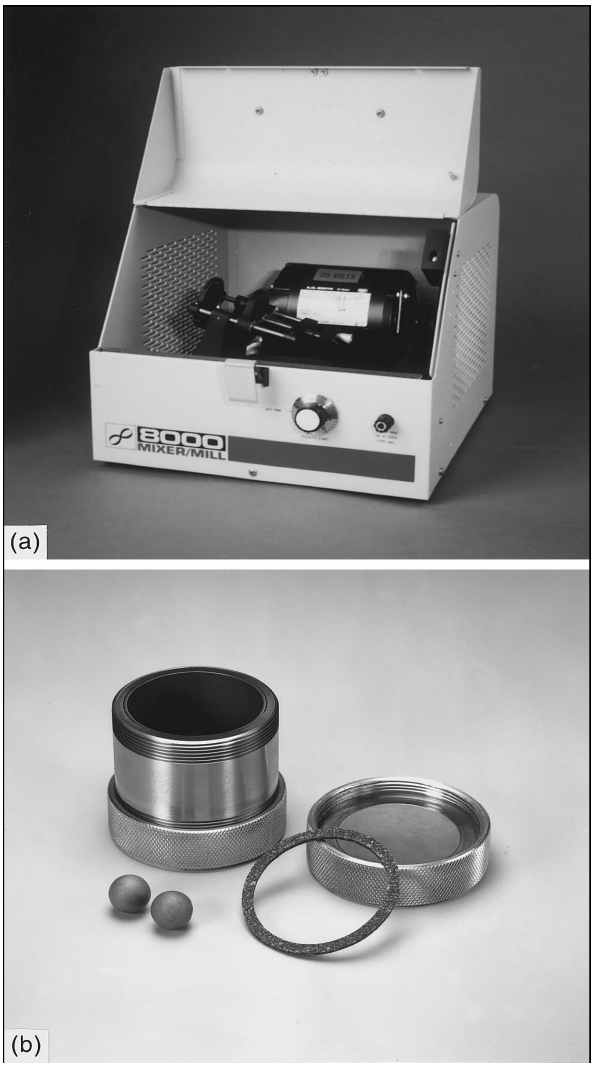

Figure 2.1. a) A typical Spex shaker mill b) Tungsten carbide vial set consisting of the vial, lid, gasket, and balls (Source: Suryanarayana 2001).

Whenever two balls collide, typically, around 1000 particles with an aggregate weight of about 0.2 mg are trapped during each collision (Fig. 2.2). The force of the impact plastically deforms the powder particles leading to work hardening and fracture (Suryanarayana 2001, Fecht 2002). Also, this severe working of powders produces a very fine grain size and substructural strengthening via high dislocation density and fine subgrain size.

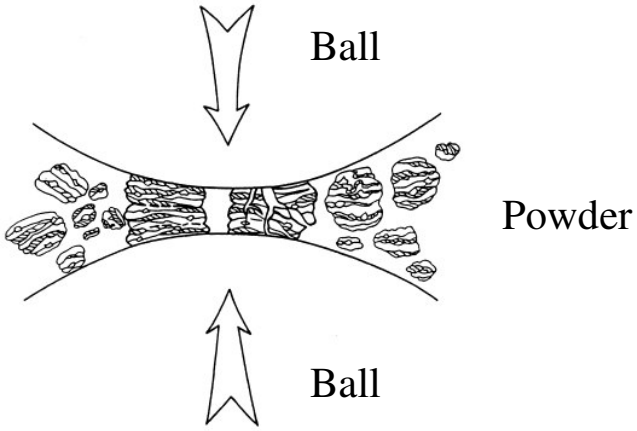

Figure 2.2. Schematic view of a ball-powder-ball collision.
(Source: Suryanarayana 2001)

In this process, lattice defects are produced by pumping energy into powder particles of typically 50 μm particle diameter. This internal refining process with a reduction of the average grain size by a factor of 10^3-10^4 results from the creation and self organization of small-angle and high-angle grain boundaries within the powder particles during the mechanical deformation process (Fecht 2002). In the elemental processes leading to formation of nanostructures;

i) The deformation is firstly localized in shear bands which contain a high dislocation density (Fecht 2002). Their typical width is approximately 0.5-1 μm (Suryanarayana 2001).

ii) At a certain level of strain within the high strained regions, these dislocations annihilate and recombine to small-angle grain boundaries separating the individual grains, which results in a decrease of the lattice strain.

iii) With the continuing process, deformation occurs in shear bands located in previously unstrained parts of the material. The grain size decreases steadily, as the shear bands come together. The small angle boundaries are replaced by higher angle grain boundaries, thus forming dislocation-free nanostructured grains (Suryanarayana 2001).

2.2. Tungsten

A distinguish property of the refractory metals is melting temperature well above the melting temperature of the common alloying bases, iron, cobalt, and nickel. When the refractory metals are considered to be those metals melting at temperatures above

1850°C, twelve metals are in this group: W, Re, Os, Ta, Mo, Ir, Nb, Ru, Hf, Rh, V, Cr. Among these, Tungsten has superior properties like good high temperature strength, high elastic modulus, good corrosion resistance and low coefficient of thermal expansion (Song et al. 2002). These superior properties, tabulated in table 2.1 make tungsten an attractive material for many important applications (Song et al. 2003). A large number of tungsten alloys and composites were investigated in the past. The aim of alloying tungsten is to improve its chemical, physical and mechanical properties at both ambient conditions and at elevated temperatures. However, alloying of tungsten (W) has been relatively less studied than of some of the other refractory metals. Most of the tungsten used until now in aerospace applications has been in the unalloyed form, which is much easier and less expensive to produce and fabricate. Also, it has been found that, particularly at temperatures above 2200°C, the strengthening effects of many alloying agents decrease disproportionately (Lassner and Schubert 1999).

Tungsten is mainly consumed in three forms:

1. Tungsten carbide
2. Alloying additions
3. Pure tungsten

Tungsten carbide accounts for about 65% of tungsten consumption (Lassner and Schubert 1999). It is combined with cobalt as a binder to form the so-called cemented carbides, which are used in cutting and wear applications because of their high hardness, good wear resistance, good fracture resistance and high temperature strength (Zhang et al. 2003) Cemented carbides such as WC-Co and WC-Co-TiC are the most widely used material for metalworking. As a result, a considerable amount of research effort has been spent to develop alternative cemented carbide systems in order to improve the microstructure and mechanical properties of these materials (Acchar et al. 2004).

Table 2.1.Properties of Tungsten
(Source: Lassner and Schubert 1999)

Period	6
Atomic Number	74
Atomic Mass	183.85
Electronegativity	1.7
Space Group	Im3m
Lattice Parameter	3.16524 A^o
Density	19.25 g/cm^3
Melting Point	3422 ^oC
Boiling Point	5663 ^oC
Specific Heat	0.0317 cal/gK
CTE	4.32-4.68x10^{-6} K^{-1} (25 ^oC)
Tensile Strength	172.4 MPa
Young's Modulus	390-410 GPa
Shear Modulus	156-177 GPa
Bulk Modulus	305-310 GPa
Poisson' Ratio	0.28-0.30
Hardness	350-450 kg/mm^2

Characteristically, most of the carbides used in cermets have high hardness, good electrical and thermal conductivity, and high stability. The brittleness of carbides, however, has prevented their use as single-phase materials in highly stressed structural applications and has led to the development of metal-bonded composites (cemented carbides or cermets) (anonymous 2005). Metallic tungsten and tungsten alloy mill products account for about 16% of consumption. Tungsten and tungsten alloys dominate the market in applications for which a high-density material (19.3 g/cm^3) is required, such as kinetic energy penetrators, counterweights, flywheels, and governors. Other applications include radiation shields and x-ray targets. In wire form, tungsten is used extensively for lighting, electronic devices, and thermocouples (anonymous 2005; Lassner and Schubert 1999). The high melting point of tungsten makes it an obvious choice for structural applications exposed to very high temperatures. Tungsten is also used at lower temperatures for applications that can use its high elastic modulus, density, or shielding characteristics to advantage (anonymous 2005).

2.3. The Properties and Applications of Epoxy Resins

The first bisphenol-A epichlorohydrin based epoxy resin was synthesized by Pierre Castan of Switzerland and Sylvian Greenlee independently from the United States in the late 1930s. Application of epoxy resin began in 1943 and became most used in manufacturing operations and a few years later in 1946, the first industrially-produced epoxy resins were introduced to the market. The wide variety of epoxy resin applications include: coatings, electrical, automotive, marine, aerospace and civil infrastructure as well as tool fabrication and pipes and vessels in the chemical industry. Because of their low density of around 1.3 g/cm^2, good adhesive property, good thermal and environmental stability and high strength, epoxy resins became a promising material for high performance applications in the transportation industry, usually in the form of composite materials such as fiber composites or in honeycomb structures. In the aerospace industry, epoxy-composite materials can be found in various parts of the body and structure of military and civil aircrafts, with the number of applications on the rise (O. Becker and G. P. Simon 2006).

The material shows good performance in corrosion resistance and provides higher strength under normal operation conditions. Epoxy resins can be applied at room temperature and have high surface activity and good wetting properties for a wide variety of materials. Usually epoxy resins are available in a two part systems. These are Component A (adhesive resin) and component B curing agents (hardener). The mixing ratio depends on the application. Many types of curing agents are used with epoxy resins, such as polyamines, polyamides, polysulfide, and melamine formaldehyde. The properties of cured epoxy resins depend on the type of epoxy, curing agent and the curing process employed.

Studies have been conducted on common adhesive resins (epoxy, polyester and vinylester) under different operational environments. The objectives were to understand the behavior and response of the adhesive resins under different weather exposures. The study found that epoxy matrix has the following advantages over other resins.

1. Epoxy has wide variety of properties because of availability of large number of starting materials, curing agents and modifiers.

2. Epoxy provides higher strength retention under sustained loading compared to the polyester and vinylester.

3. Epoxy resin has low creep and low shrinkage properties.

4. Epoxy material shows good chemical resistance and solvents.

5. The material indicates excellent adhesion properties to a wide variety of fillers, fibers and other substrates.

Jamond and Malvar (Jamond and Malvar 2000) tested the specimens that were bonded with three different resins (epoxy, vinylester and polyester) and fabric materials. The specimens were exposed to different operational conditions. After mechanical tests, the specimens bonded with epoxy showed higher moduli of elasticity, compression strength and tensile strength compared to other specimens. Specimens bonded with epoxy resin showed no effect under ultraviolet radiation (UV) exposure compared to vinylester and polyester resin.

Table 2.2. Thermosetting resin comparison.
(Source: Monib 1998)

Resin System	**Advantages**	**Disadvantages**
Polyester	- Low Cost - Easy to process - Good chemical and moisture resistance - Fast cure time - Room temperature cure	- Flammable - Toxic smoke upon combustion - Average mechanical properties
Vinyl Ester	- Low cost - Easy of processing - Low viscosity - Room temperature - Moisture resistant - Good chemical properties	- Flammable - Smoke released upon combustion - Mechanical properties is not good as epoxies
Epoxy	- Excellent mechanical properties - Good chemical and heat resistance - Good adhesive properties with a large variety of substrates - Moisture resistant - Variet of compositions available - Good fracture toughness	- Expensive - Requires high processing temperatures to achieve good properties

2.4. Fiber Reinforced Epoxy Composites

In recent years, it is an attractive goal to obtain an epoxy-based composite with excellent tribological properties by incorporating the appropriate components such as fibers or particles. Fibrous reinforcements tabulated in Table 2.3 such as glass, carbon, graphite and aramid are widely used to obtain materials with excellent mechanical properties. On account of their good combination of properties, fiber reinforced polymer composites (FRPCs) are used for producing a number of mechanical components such as gears, cams, wheels, brakes, clutches, bearings and seals. Most of these are subjected to tribological loading conditions (Suresha et al. 2006).

Table 2.3. Fiber Types and Their Some Properties.
(Source: Suresha et al. 2006)

Fiber	Advantages	Disadvantages
E, S-Glass	High strength, low cost	Low stiffness, short fatigue life, high temperature sensitivity
Carbon	High strength, high stiffness	Moderate cost
Graphite	High stiffness	Low strength, high cost
Aramid	High tensile strength, high toughness	Hygroscopic, less interfacial strength

Carbon fiber reinforced composites have been widely used in the bearings without liquid lubricant. In most cases, there are two kinds of polymeric matrix used in carbon composite bearings: thermoplastic matrices such as polytetrafluoroethylene (PTFE) and high-density polyethylene (HDPE), and thermoset matrices such as epoxy and phenol. Although the tribological characteristics of thermoplastic matrix are better than that of thermosetting matrix, the mechanical properties of carbon/thermoplastic composites are lower than those of carbon/thermoset composites. Moreover, as thermoplastics have low surface energy, their adhesion properties to the other structural materials are low. For that reason, the carbon/thermoset composites are preferable for the bearing structure for high load capability (H.G. Lee et al. 2006).

B. Suresha et al. (Suresha et al. 2006) present an experimental study on friction and wear behaviour of Carbon/Epoxy (C-E) and Glass/Epoxy (G-E) composites when sliding against a hardened steel counterface under various loads and sliding velocities using a pin-on-disc test setup. This article highlights the friction and wear behaviour of

these composites run for a constant sliding distance, where in the C-E composites show lower friction and lower slide wear loss compared to G-E composites irrespective of the load or speed employed. It is concluded from the experimental results of wear loss that there is a strong inter-dependence on the friction coefficient and wear loss with respect to applied normal loads and sliding velocities. Increase in sliding velocity or decrease in the load results in lowering the coefficient of friction for all samples evaluated. Between the G-E and C-E composites, the later records lower coefficient of friction in view of its inherent material characteristics favoring the frictional properties. The slide wear behavior of C-E samples is greatly superior compared to G-E composites due to the presence of carbon fibers, which act as a self lubricating material. Also another key observation that emerges from this investigation is that friction and wear characteristics of fabric reinforced epoxy composite systems depend on the type of fabric material.

Some researchers have reported on the tribological aspects, referring to the effect of fiber orientation. In the composites with low volume fraction of fibers, the wear rate in the longitudinal direction is higher while for higher volume fraction, it is vice-versa. The effect of carbon fiber reinforcement on the friction and wear of composites with thermoplastic as well as thermosetting polymeric matrices has been studied. It has been reported that the wear rate of polymer composites depends upon the volume fraction of fiber used as well as their orientations.

The tribological behaviour of chopped glass fiber reinforced polyester (CGRP) composite sliding against smooth stainless steel counterface has been reported in the study of El-Tayeb et al. (N.S.M. El-Tayeb 2006). Although the sliding took place against smooth stainless steel counterface (adhesive wear), various wear mechanisms of abrasive nature were observed such as fiber fracture, fragmentation, micro-crack, peeling off, matrix failure and debris formation.

During sliding motion of composite bearings, the wear debris produced on the composite contact surface affects the tribologic behavior of composite bearings. In the work of Lee et al. (Lee et al. 2006); the composite surface with many micro-grooves was used for the wear test to remove wear debris continuously during sliding motion, since the previous researches do not give any clue for the directional property of friction and wear due to wear debris produced in composite surface during sliding motion. In their work, in order to investigate the effect of wear debris on the tribological behavior of flat composite surfaces, dry sliding tests were performed on the composite surfaces with many micro-grooves. The friction coefficients of the flat and the grooved

composite surfaces were measured with respect to fiber volume fraction using a pin-on-disk type wear tester, and their worn out surfaces were observed, from which the friction and wear mechanisms of composite surface were suggested. From the wear test result, it was concluded that the wear debris produced and compacted was the dominant factor to the friction and wear behavior of carbon fiber reinforced composites. Therefore, for the low friction and wear, the compaction of wear debris should be retarded, which may be achieved by producing many micro-grooves on the composite surface.

Larsen et al. (T.Ø. Larsen et al. 2007) tested PMCs based on an epoxy resin. In their study, the friction and wear behavior of two types of bidirectional fibrous reinforcement studied that are in the form of a plain glass fiber weave and a carbon/aramid (CA) hybrid weave. The tribological comparison between different PMCs are often conducted at only one or a few combinations of contact pressure (p) and sliding velocity (v) referred to as pv conditions. The latter is particularly interesting since the applicability of PMCs in applications involving high sliding speeds and/or high environmental temperatures is limited due to their inferior thermoresistant properties compared to metals and ceramics. The tribological data are obtained using a Pin-On-Disk apparatus under dry-sliding conditions against smooth steel surfaces at ambient temperature and humidity. An average decrease in the coefficient of friction μ of approximately 35% was found by substituting a glass fiber weave with a carbon/aramid hybrid weave in an epoxy-matrix. This reduction is considered to be due to the lubricating effect of carbon fibers as opposed to the abrasive nature of glass fibers. The coefficient of friction furthermore seems to be roughly independent of p and v. CA/EP shows superior wear behavior at the six mildest pv conditions with the wear rate lower than those for G/EP rates. The reason for this was related with the following main factors. The aramid fibers seem to inhibit microcracking of the resin, which in the case of glass and carbon fibers that leads to exposed fiber ends. These exposed, and brittle, fiber ends seem to be fragmented and broken easily relative to the tough aramid fibers, which are worn by a fibrillation mechanism. Furthermore, third-body abrasive wear caused by fragmented glass fibers probably also contributes significantly to the high wear rate found for G/EP. In the case of CA/EP, the specimen failed at a limiting pv factor of 3 MPa m/s, which probably is due to buckling of the aramid and carbon fibers as the supporting resin softens and decomposes. When G/EP was tested at the

same conditions, a similar failure was not observed, but decomposition of the resin and development of larger-scale cracks was evident.

Abrasive wear can occur as two-body abrasion (2BA), three body abrasion (3BA), or both. Further distinctions of 2BA abrasion can be defined as the type of wear that caused by hard protuberances on one of the two surfaces sliding over each other. The study of 2BA wear is usually carried under single and/or multi-pass abrasive wear conditions. In a single pass two-body abrasive (S-2BA) wear, the polymer specimen always faces fresh abrasive particles; hence, the wear volume increases linearly with sliding duration and load. On the other hand, under multi-pass two-body abrasive (m-2BA) wear conditions, which is likely common case in practical situation, the polymer specimen transversed on the same wear track (same path on the abrasive tips) until the total sliding duration was reached. Generally, the wear rate in single pass condition is higher than in multi-pass condition and the difference in the extent of wear is determined by the clogging effect. For 3BA, the hard particles are free to slide as well as roll between the two surfaces. The rate of material removal in 3BA is one order of magnitude less than that for 2BA and this is most likely because of the abrading time by the loose particles consumed in rolling rather than sliding. N.S.M. El-Tayeb and B.F. Yousif (El-Tayeb and Yousif 2007) investigated the tribological behaviour of chopped glass fiber reinforced polyester (CGRP) composite when subjected to abrasive wear tests using abrasive media. Their study took fundamental approach towards the investigation of the multi-pass two-body abrasive (m 2BA) wear behaviour of CGRP composite when abraded against waterproof silicon carbide (SiC) abrasive paper of three different grades. The aim of the study was to evaluate the effects of the grit size upon the abrasion wear performance of the CGRP composite in three different orientations of chopped strand mat (CSM) which are antiparallel, AP; parallel, P; and normal, N. Another aim has to investigate to what extent the CSM orientation enhances the abrasive resistance of CGRP. Also, the changing of wear mechanisms due to the attrition of the abrasiveness and changing their locations throughout the experiment was discussed. Furthermore, a light shed on the possibility of transition between two-body and three-body abrasion mechanisms was given. The wear rates were experimentally determined under dry condition for different loads (5–25 N) and rotational speeds (50 and 100 rpm), and the resulting wear mechanisms were microscopically examined and categorized. Experimental results showed that m-2BA wear rate of the CGRP composite increases substantially with increasing the size of the abrasive grits and rotational speed,

whereas it tends to decrease with increasing the applied normal load. A 20–70% decrease in the wear rate at higher load was evident for all orientations tested under sliding wear conditions. During the tests, abrasive grains in the SiC paper were remained rigidly attached to the paper. AP-orientation exhibited the lowest wear rate (best abrasive performance) as compared to P- and N-orientation. Fibers in AP-orientation enhanced by filling the fiber–matrix gabs with fine debris and this in turn increases the rigidity of the CSM against the side forces leading to less fiber damage. Wear mechanisms were categorized after microscopic observation of the abraded surfaces into five main types such as micro-cutting, micro-ploughing, micro-fracture and micro-cracking in the resin, and micro-fatigue.

2.5. Epoxy Composites Containing Nanosized Fillers

In the recent years, nanoparticle filled composites based on epoxy resins have been utilized as high performance materials for many applications in the aerospace, defence, automotive, shipping, electrical, electronic, medical and sporting good industries. In general, epoxy polymers do not exhibit good tribological properties because of its cross-linked molecular structure, which inhibits the formation of an efficient transfer film and results in a relatively high degree of brittleness (Lu 2005). Nanoparticle materials were found to possess unique physical, chemical and electromechanical properties, which have extensive potential application (Lin 2007). The method of using nanoparticles as fillers in epoxy matrix to improve the tribological performance of the resultant nanocomposites has attracted a great deal of attention from materials scientists, technologists and industrialists (Lu 2005). One of the extents of the reinforcement effect is determined by the properties of the composite components. The other extent of the reinforced effect depends strongly on the nanostructure represented by the filler shape, size, concentration and the homogeneity of particle distribution within matrix. It has been demonstrated that nanoparticles are able to provide polymer matrix with improved performance at proper concentration (Lin 2007). It is apparent that the incorporation of appropriate reinforcements into polymer matrix has a beneficial effect on its mechanical and tribological properties. Even at low filler contents, the addition of various nanosized fillers into polymer may cause an

improvement in the tribological characteristic owing to a change of the wear mechanisms.

G. Shi et al. (Shi et al. 2004) focused on the tribological behavior of the composites consisting of epoxy and nano-sized Al_2O_3 particles with different pretreatments. Before addition of the nanoparticles into the epoxy, the particles were pretreated by either silane coupling agent or graft polymerization to enhance the interfacial interaction between the fillers and the matrix polymer. The experimental results indicated that the frictional coefficient and wear rate of epoxy can be reduced even at low concentration of nano-Al_2O_3. In addition, the flexural modulus and flexural strength of epoxy were increased by the incorporation of nano-Al_2O_3 particles. The lowest specific wear rate, 1.6×10^{-6} mm^3/Nm, was observed for the composites with 0.24 vol. % of nano-Al_2O_3 grafted by polyacrylamide. The value was decreased by 97% as compared to the value of unfilled epoxy. The wear performance of the composites was not correlate with flexural modulus and flexural strength of epoxy, even though the incorporation of nano-Al_2O_3 particles leads to increase the static mechanical properties. In contrast, there was a positive correlation between wear resistance and impact strength. The increased impact toughness of the composites as a result of nano-Al_2O_3 incorporation correlates with a decrease in specific wear rate and low friction. Nano-Al_2O_3 particles was found to be quite effective in lowering frictional coefficient and wear rate of epoxy composites. Addition of nano-Al_2O_3 particles has changed the severe abrasive wear of unfilled epoxy into mild fatigue wear. In order to improve the tribological performance of epoxy, graft polymerization was found to be superior than silane treatment among the modification techniques of nanoparticles used in their work. Besides, the grafted nanoparticles accompanied by the homopolymer provided the more obvious lubrication effect than the ones only with grafting polymer.

Shao-Rong Lu et al. (Lu et al. 2005) focused on investigating the mechanical and tribological properties of the epoxy/SiO_2-TiO_2 composites. It was concluded that SiO_2-TiO_2 nanoparticles can significantly improve mechanical properties of the composites, which contains an optimum amount of nanoparticles (1.3–2.6 wt %). The impact strength and tensile strength were found to be almost 2–3 times higher than those for the pure epoxy resin. The mechanism for this improvement was ascribed to increase the interfacial strength between nanoparticles and epoxy matrix through chemical bonding. Results of FT-IR spectroscopy and atom force microscope (AFM) demonstrated that epoxy chains have been covalently bonded to the surface of the SiO_2-

TiO_2 particles. When the material is subjected to an impact test, the epoxy/SiO_2-TiO_2 composites have generated microphase separated for introducing of the SiO_2-TiO_2 particles, which may induce to crack propagation, and resulted in the performance of the epoxy/SiO_2-TiO_2 composites improved. It proves to be an effective way in lowering frictional coefficient and wear rate of epoxy composites. The results of experiment indicate that the wear mechanism of the composites changed from the adhesive wear to mild abrasive wear plus fatigue wear with the increase of the SiO_2-TiO_2 content, the wear and friction performance of composites have been greatly improved with the addition of SiO_2-TiO_2 nanoparticles.

CHAPTER 3

TRIBOLOGY FOR POLYMER NANOCOMPOSITES

The word tribology, derived from the Greek word “tribos” meaning rubbing, can be defined as interdisciplinary science and technology related to friction, wear and lubrication. The tribology section is concerned with developing and improving materials and surfaces that have low friction and high wear resistance for engineering applications. The commonly used materials in tribological components range from metals, alloys to ceramics, solid lubricants, polymers and composites. Tribological behavior of polymers is reviewed since the mid-20th century to the present day. Much research has been carried out on the tribology of polymers and its application in various industries with the application of polymers for tribological purposes increasing and extending into even more new areas (Zhang et al. 1998).

3.1. Wear Mechanisms

Wear is defined as damage to a solid surface that generally involves progressive loss of material and is due to relative motion between surface and a contacting solid, liquid, or gas. The changes in surface layer arise from mechanical stresses, temperature and chemical reactions. Polymers due to their specific structure and mechanical behavior are more sensitive to these factors. Wear has been classified in various ways. One of the simplest classifications of wear is based on the presence or absence of effective lubricants called as lubricated or nonlubricated wear. Another possibility is to classify wear on the basis of the fundamental mechanism that is operating. It is generally recognized that the most common types of wear can occur through four major mechanisms such as adhesion, abrasion, fatigue and corrosion.

3.1.1. Abrasive Wear

Abrasive wear occurs between the two surfaces which have hard particles or hard asperities that are forced against and move along a solid surface contact. Because of hardness differences between surfaces, abrasive wear is observed on both surfaces (In

other words, both surfaces are being subjected to abrasive wear). The rate at which the surfaces abrade depends on the characteristics of each surface, the presence of abrasives between the first and second surfaces, the speed of contact and other environmental conditions. Abrasive wear results in the softer material being removed from the track traces by the asperity during the motion of the harder surface.

For instance, an individual walking up the stairs of a building would be more likely to think that his/her shoes, rather than the stairs, were experiencing abrasive wear, whereas opposite opinion would have been considered. In short, loss rates are not inherent to a material. Abrasion is typically categorized according to types of contact, as well as contact environment. Types of contact include two-body and three-body wear. The former occurs when an abrasive slides along a surface, and the latter, when an abrasive is caught between one surface and another. Two-body systems typically experience from 10 to 1000 times as much loss as three-body systems for a given load and path length of wear. Contact environments (Figure 3.1) are classified as either open (free) or closed (constrained). Tests have shown that for a given load and path length of wear, the wear rate is about the same for both open and closed systems. However, measurements of the loss in closed systems will often appear higher than the loss in open systems. This probably occurs because most closed systems experience higher loads. Abrasion is often further categorized as being low stress abrasion, high-stress abrasion, gouging abrasion, and polishing abrasion. Each of these forms of abrasion is characterized by varying amounts of surface or subsurface damage (ASM Handbook; Friction Lubrication, and Wear Technology).

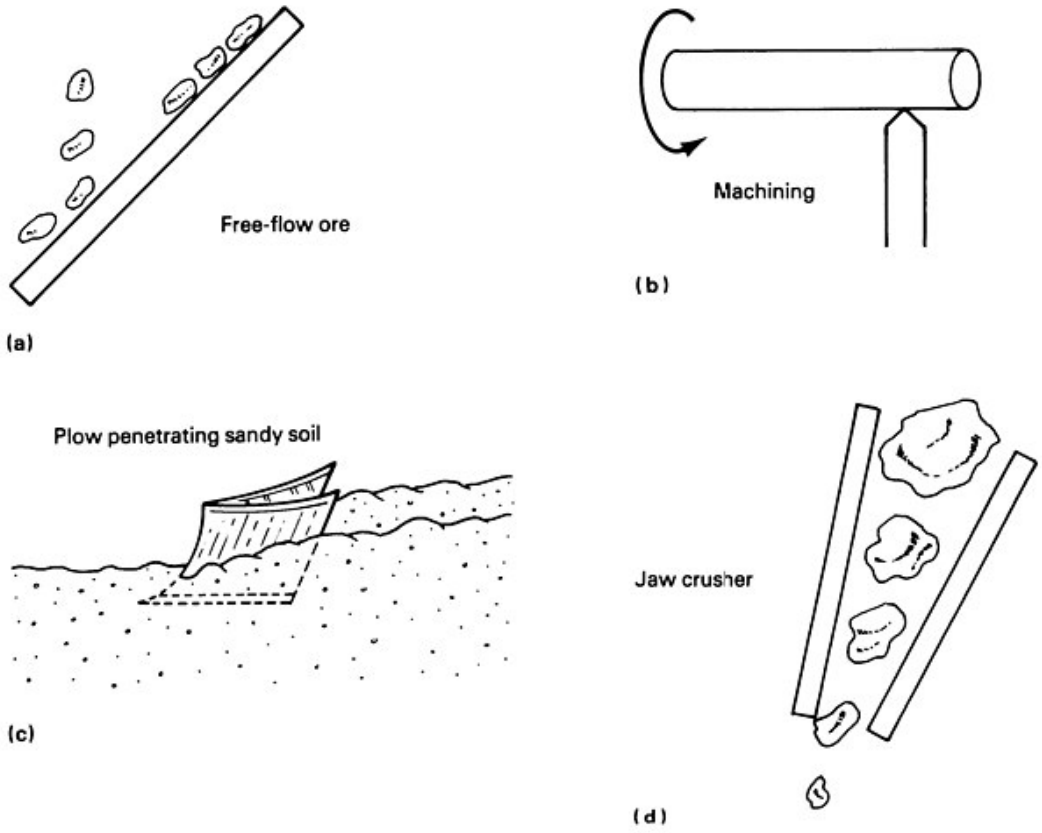

Figure 3.1. Types of contact during abrasive wear. (a) Open two-body. (b) Closed two-body. (c) Open three-body. (d) Closed three-body (Source: ASM Handbook; Friction Lubrication, and Wear Technology)

Low-stress abrasion (scratching) is defined as wear that take places clue to relatively light rubbing contact of abrasive particles with the metal. The criteria established for low-stress abrasion is that the forces must be low enough to prevent crushing of the abradant. Wear scars usually show scratches, and the amount of subsurface deformation is minimal. Consequently, the surface does not work harden appreciably. Many machine components such as bushings, seals, and chains that operate in dust will wear by low-stress abrasion. Figure 3.2(a) shows a surface that was subjected to low-stress abrasion.

High-stress abrasion is wear under a level of stress that is high enough to crush the abrasive. Considerably more strain hardening of the metal surface occurs. The abrasion of ore grinding balls is an example of highstress abrasion in the mining industry. Other examples include abrasion experienced by rolling-contact bearings, gears, cams, and pivots. Figure 3.2(b) illustrates this form of wear.

The gouging abrasion is used to describe the high-stress abrasion that results in great grooves or gouges on the worn surface (Figure 3.2c). It occurs on parts such as

crusher liners, impact hammers in pulverizers, and dipper teeth handling large rocks. Strain hardening and plastic deformation are the dominant factors.

Polishing wear is an extremely mild form of wear for which the mechanism has not been clearly identified, but that may involve extremely finescale abrasion, plastic smearing of microasperities, and/or chemical corrosion (Figure 3.2d). Surfaces that have been subjected to polishing wear are usually smoothed and brightened, but this smoothing or brightening requires material removal. It can cause loss of serviceability in some instances, for example, worn and slippery stair treads (ASM Handbook; Friction Lubrication, and Wear Technology).

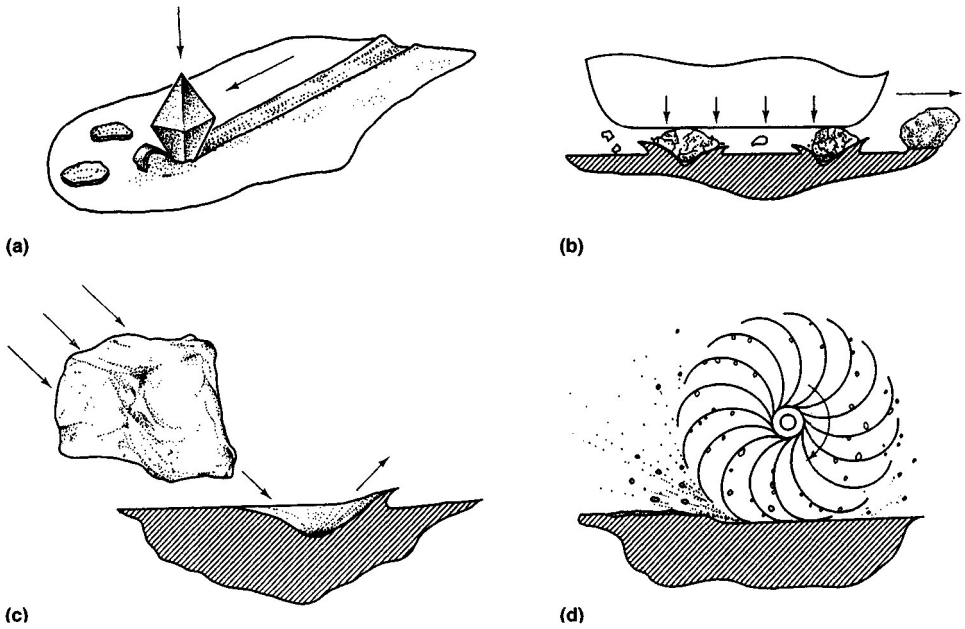

Figure 3.2. Illustration of the four types of abrasive wear, (a) Low-stress abrasion (b) High-stress abrasion is almost always more severe than low-stress abrasion, (c) Gouging abrasion where material removal is caused by the action of repetitive compressive loading, (d) Polishing wear (Source: ASM Handbook; Friction Lubrication, and Wear Technology)

3.1.2. Sliding, Adhesive Wear and Friction Transfer

Erosion, cavitation, rolling contact, abrasion, oxidative wear, fretting, and corrosion are traditionally excluded from the class of "sliding" wear problems even though some sliding may occur in some of these types of wear. In fact, sliding wear is a category of wear that is "left over" when all other types of wear are identified under

separate headings. Although adhesive wear is dubiously defined as sliding wear, the two are not strictly synonymous. Adhesive wear process progresses in formation of adhesion junction, its growth and fracture. A distinguishing feature of this wear is that transfer of material from one surface to another occurs due to localized bonding between the contacting solid surfaces. Adhesive wear denotes a wearing action in which no specific agency can be identified as the cause of the wear. Adhesion has been confirmed in the 1930s to be a major contributor to sliding resistance (friction) and was inferred in mechanics at least to be operative in wear as well. Thus, if no abrasive substances are found, if the amplitude of sliding is greater than that in fretting, and if the rate of material loss is not governed by the principles of oxidation, and so on, adhesive wear is said to occur. Adhesion is most clearly demonstrated in sliding systems when, for example, a shaft seizes in a bearing. Adhesion is not the cause of wear, but only the consequence of contact. Wearing occurs when interfaces in contact are made to slide and the locally adhered regions must separate. This separation may occur by one or two of the failure modes of solids, resulting in a very wide range of wear rate. The reason of defining and studying specific wear modes is to find ways to make longer the wear life of sliding systems. Each mode of wear can be resisted by the proper choice of material, lubricant, and method of operation (ASM Handbook; Friction Lubrication, and Wear Technology).

The phenomenon of friction transfer is observed for nearly all materials (metals, ceramics, and polymers) and their combinations. The point is that whether the transfer produces an influence on tribological behavior of the friction couple. In this case, the consequences of material transfer may be significantly distinct. If small particles of micrometer size are transferred from one surface to the other, then wear rate varies to only a small extent. Under certain conditions, the situations take place when thin film of soft material is transferred onto the hard mating surface, for example, polymer on metal. The transfer of polymer is the most important characteristic of adhesive wear for polymers. The transferred polymer fragment may exhibit a wide variety of forms depending on polymer properties and friction conditions or changes in roughness of both surfaces in contact. The roughness of polymer surface undergoes large variation during the unsteady wear until the steady wear is reached, while metal surface roughness is modified due to transfer of polymer (Myshkin et al. 2005).

3.1.3. Fatigue Wear

Fatigue is known to be a change in the material state due to repeated stressing which results in progressive fracture. Its characteristic feature is accumulation of permanent changes, which give rise to generation, and development of cracks. The similar process takes place at friction accompanying nearly all the wear modes. A friction contact undergoes the cyclic stressing at rolling and reciprocal sliding. In addition, each asperity of frictionsurface experiences sequential loading from the asperities of countersurface. In consequence, two varying stress fields are brought about in surface and sub-surface regions with different scales from the diameter of apparent contact area in the first case to that of local contact spot in the second. These fields are responsible for material fatigue in these regions that leads to the generation and propagation of cracks and the formation of wear particles. This process is named friction fatigue. Unlike the bulk fatigue, it spans only surface and sub-surface regions. The loss of material from solid surfaces owing to friction fatigue is referred to as fatigue wear. It has been known that the fatigue cracks are initiated at the points where the maximum tangential stress or the tensile strain takes place. The theoretical and experimental studies show that under contact loading the maximum tangential stress position is dependent on friction coefficient (Myshkin et al. 2005)

3.1.4. Corrosive Wear

Corrosive wear, which is frequently referred to simply as “corrosion”, is deterioration of material and its essential properties due to chemical or electrochemical reactions between a material and its environment. The term corrosion is generally used as a loss of an electron of metals reacting with water or oxygen. Corrosion also includes the dissolution of ceramic materials and can refer to discoloration and weakening of polymers by the sun's ultraviolet light.

Corrosive wear occurs when there is a combination of a wear state (abrasive or adhesive) and corrosive surroundings. Corrosive wear is indirect wear mechanism and can also be considered an accelerating mechanism for corrosion itself, because the motion of articulation can remove corrosive products and the protective passive layer sooner than interfaces with no relative motion. Release of corrosive products exposes a

greater surface (with less protection against corrosion) to further corrosion and so accelerates the removal of even more material.

3.2. Tribological Applications of Composite Materials

Tribology has to be taken into account in the modern industry. Many tribological components such as brakes, clutches, driving wheels, bolts, nuts, gears, cams, bearings and seals are applied in the machinery. The friction and wear appearing in these operations is one of the largest energy losses.

Although polymer materials have poor thermal conductivity, they can provide satisfactory performance for a wide range of applications; these can operate dry or with initial lubrication. Dry polymer material applications include car door hinges, office machinery, heat-sealing packaging machines, pneumatic equipment and aerospace applications.

The intention of this review is to present comprehensive information on entirely new phenomena that have been discovered and investigated over the past few years concerning the tribological properties of polymer matrix composites and their applications tabulated in Table 3.1 (Zhang et al. 1998). It was the first tribological application of polymer matrix composite when phenol-formaldehyde resin such as phenolic, reinforced with fibers and fabrics, was used to make bearings in 1930s (Park et al. 2006).

Table 3.1. Tribological Applications of Polymer Composite Materials
(Source: Friedrich and Reinicke 1998)

Field	Examples	Type of wear loading and requirements
Civil Eng.	Conveyors	
Mechanical Eng.	Seals	Sliding, minimize friction and wear
	Bearings	Sliding, minimize friction and wear
	Gear	Sliding, minimize friction and wear
	Turbine or Pump blades	Erosion, minimize wear
Medicine	Dental applications	Abrasion, minimize wear
	Hip replacements	
	Shaft	Fretting, minimize wear
	Cap	Sliding, minimize friction and wear
Automotive	Brakes	Sliding, minimize wear, optimize friction
	Tires	Abrasion, minimize wear, maximize friction

Abrasive wear is the most harmful among all the forms of wear and contributes almost 50% to the total wear. Polymers and the fibre reinforced polymers (FRPs) are most commonly used in highly abrasive systems such as conveyor aids, vanes, gears for pumps handling industrial fluids, sewage and abrasive contaminated water; bushes, seals and chute liners in agricultural, mining and earth moving equipments; roll neck bearings in steel mills subjected to heat, shock loading, water; and guides in bottle handling plants (Bijwe et al. 2001).

3.3. Effect of Fillers on the Properties of Composites

Polymer and polymer composites are used gradually more often as engineering materials for technical applications in which tribological properties are of considerable importance. Fillers (e.g., glass, carbon, asbestos, oxides and textile fibers) are incorporated within many polymers to improve their tribological performance. The reduction in wear is due mainly to preferential load support of the reinforcement components, by which the contribution of abrasive mechanisms to the wear of the materials is highly suppressed. Besides, the solid lubricant particles transfer fairly readily to a metal counterface, leading to the formation of a strengthened transfer film. Finally, some fillers are used to improve the poor thermal conductivity possessed by polymers, thereby facilitating dissipation of frictional heat. However, the composites filled with the micron particles usually need quite a large amount of filler to attain an evident improvement of wear resistance. (Zhang and Rong 2006)

B. Wetzel et al. investigated the influence of various amounts of micro- and nano-scale particles (calcium silicate $CaSiO_3$, 4–15 μm, alumina Al_2O_3, 13 nm) on the impact energy, flexural strength, dynamic mechanical thermal properties and block-on-ring wear behavior. In their work, the first step aimed to find out the best possible mechanical and tribological performance of the nano-refined polymer matrix as a function of the nanoparticle content (0.5–10 vol. % Al_2O_3). In a further step, the toughest nanocomposite matrix was chosen as a basis material to include conventional calcium silicate micro-particles (6.7 and 12.5 vol. % $CaSiO_3$). The combination of nanoparticles with conventional microparticles may induce synergistic effects by moving wear resistance to much higher levels. The addition of alumina nanoparticles simultaneously improves stiffness, impact energy and failure strain at low filler contents

(1–2 vol. %). Besides, a slight improvement of the wear resistance at 2 vol. % Al_2O_3. The flexural modulus and wear resistance increases higher levels introducing of calcium silicate microparticles into a nanocomposite matrix, which contains an optimum amount of nanoparticles (2 vol. %). Impact properties do not drop below the value for the neat matrix whereas the strain-to-break suffers significantly. Nanoparticles and microparticles are both able to improve the wear resistance of the epoxy matrix. The good wear performance of the $CaSiO_3$ composites may be the result of temporarily protecting microparticles which protrude out of the polymer surface and relieve the matrix from severe wear (Wetzel et al. 2002).

Z. Zhang et al. investigated enhancements of the wear resistance of a series of epoxy matrix composites, modified by polytetrafluoroethylene (PTFE) and graphite as internal lubricants, as well as reinforced by short carbon fiber (CF) and nano-TiO_2. They also investigated worn surfaces using a scanning electron microscope and an atomic force microscope. Wear properties of an epoxy matrix that were carried out on a block-on-ring apparatus indicated improvements introducing the fillers, e.g. PTFE, graphite and short-CF, as well as nano-TiO_2. The best wear-resistant composition was achieved, in the present study, by a combination of nano-TiO_2 with conventional fillers. As an example, epoxy + 15 vol. % graphite + 5 vol. % nano-TiO_2 + 15 vol. % short-CF exhibits a specific wear rate of 3.2 X 10^{-7} mm^3/Nm, which is about 100 times lower than that of the neat epoxy matrix. A content of 4–6 vol% nano-TiO_2 shows an optimum effect on the wear resistance of epoxy nanocomposites. Short carbon fibers play a key role to improve the wear resistance of polymer composites. A nanoscale rolling effect of nanoparticles may govern the significant enhancement of the wear resistance of the epoxy nanocomposites in the present study, which helps to protect the worn surface of the composites from more severe wear mechanism (Zhang et al. 2004).

L. Chang et al. investigated the tribological performances of epoxy-based nanocomposites, filled with short carbon fibre, graphite, PTFE and nano-TiO_2 in different proportions and combinations, by a pin-on-disk apparatus under different sliding conditions. Introducing spherical nano-TiO_2 (300 nm in diameter) into epoxy composites enhanced the wear resistance, especially at high contact pressure and high sliding speed, and consequently decreased the contact temperature and the frictional coefficient of fiber reinforced epoxy composites. An enhancement of the load-carrying capacity was achieved, which will promote these materials for the applications under more severe wear conditions. Under a standard sliding condition such as 1MPa and 1

m/s, if wear results of pin-on-disc and block-on-ring are compared, the lower wear rates resulted from the block-on-ring indicated to the good mechanical load-carrying capacity of nanocomposites. Epoxy filled with each 15 vol.% of graphite and short carbon fibre together with 5 vol.% nano-TiO_2 showed the lowest wear rate under a standard sliding condition. However, a composition with combined lubricants, i.e. each 5 vol. % of nano-TiO_2, graphite and PTFE, together with 15 vol.% of SCF, exhibited the highest wear resistance as seen in the Figure 3.3 (Chang et al. 2005).

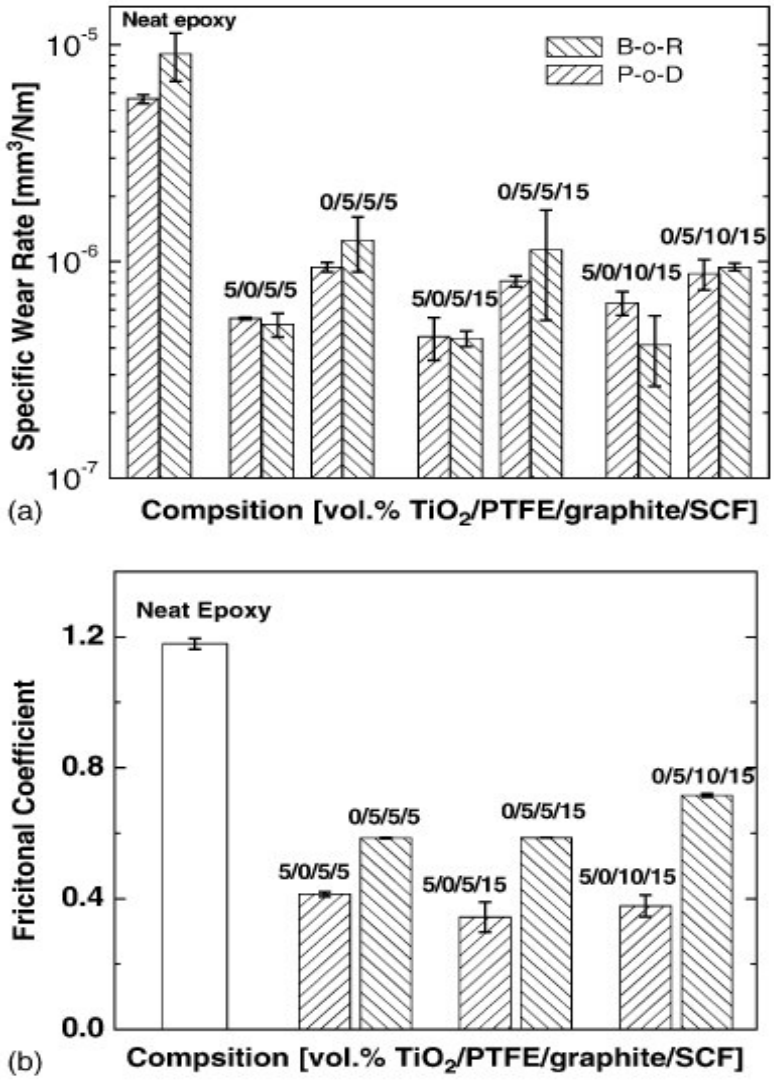

Figure 3.3. Comparison of the wear performances of various groups pf epoxy composites with 5 vol.% of nano-TiO_2 instead of the same amount of PTFE under a standard wear condition, i.e. 1 MPa and 1 m/s: (a) the specific wear rate measured with both P-o-D and B-o-R apparatuses, and (b) the frictional coefficient measured with P-o-D apparatus (Source: Chang et al. 2005).

L. Chang and Z. Zhang observed the micro-configurations of worn surfaces of selected compositions and the characterization of short carbon fibers (SCF) removal using SEM and AFM in order to understand the wear mechanisms involved in micro- and nanoscales. The improvement on the wear resistance of epoxy nanocomposites was generally associated with less fiber removal. There were some nanoscale grooves on the SCF surfaces, which might be scratched by the nanoparticles embedded in the counterpart surfaces. The behaviour of these grooves was strongly influenced by the sliding conditions. The rolling effect of the nanoparticles between the material pairs was investigated using SEM and AFM. This rolling effect helps to reduce the frictional coefficient during sliding, accordingly to reduce the shear stress and contact temperature. And this rolling effect protects as well the short carbon fibers from more severe wear mechanisms, especially at high sliding pressure and speed situations. As a result of sliding the nanocomposites against a very smooth disk, introducing of nanoparticles could not reduce the frictional coefficient. Moreover, it can be thought that there is no nano-TiO_2 detected on the counterpart surface after testing (Chang and Zhang 2005).

G. Xian et al. studied epoxy-based nanocomposites', containing graphite and nano-TiO_2, sliding and low amplitude oscillating wear behavior by adding short carbon fibers (SCF), aramid and polytetrafluoroethylene (PTFE) particles. The selected wear mechanisms were also studied based on the SEM analysis of the tribolayers formed on the surfaces of sliding bodies. Even though SCF impaired the low amplitude oscillating wear resistance the incorporation of SCF and aramid particles resulted in a remarkable enhancement in the sliding wear resistance. The further addition of PTFE to the SCF filled nanocomposites decreased the friction and wear under both wear conditions. However, an adverse effect of PTFE was found for the Aramid particles filled nanocomposites. The lowest wear rate and coefficient of friction showed the 2–4 vol% PTFE filled SCF nanocomposite under sliding conditions. Aramid particles containing nanocomposites (without PTFE) exhibited the best wear and friction behavior under low amplitude oscillating wear conditions among the selected composites. Both impact and flexural strength were impaired by introducing aramid into the nanocomposite containing TiO_2 and graphite, while inclusion of SCF was slightly beneficial to the flexural strength though damaging the impact strength as illustrated in Figure 3.4. On the other hand addition of PTFE impaired both these properties.

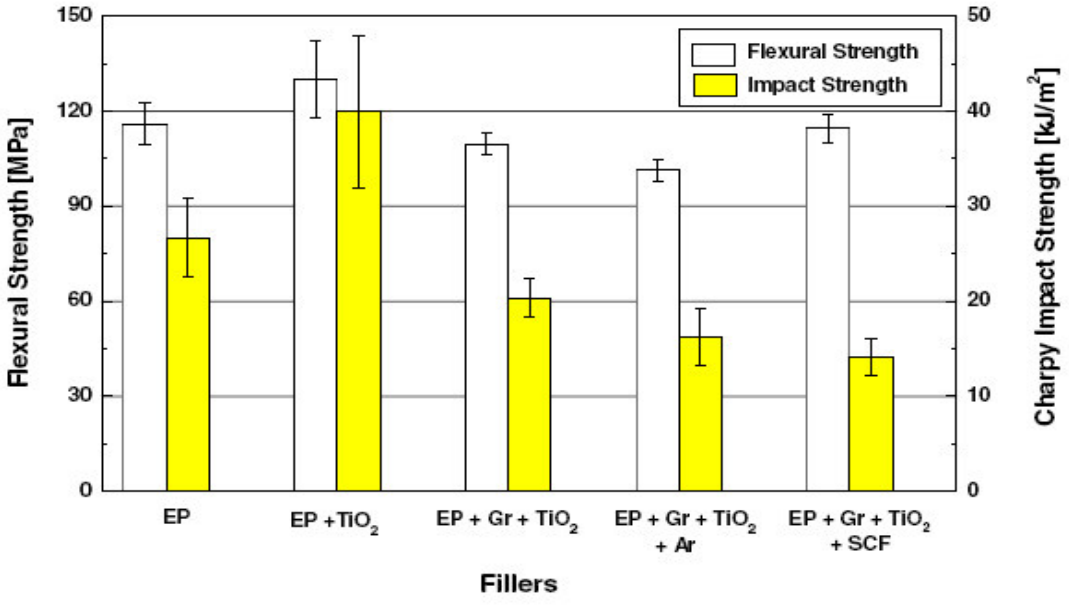

Figure 3.4. Flexural strength and unnotched Charpy impact strength of the neat epoxy (EP) and SCF or Aramid (Ar) filled composites (without PTFE) (Source: Xian et al. 2006).

Introducing aramid particles into the epoxy nanocomposite significantly improved the wear resistance under adhesive wear conditions. In contrast the further addition of PTFE significantly deteriorated both wear and friction. Although SCF in combination with PTFE proved very good for both wear and friction addition of SCF proved detrimental to both wear and friction as illustrated in Figure 3.5 (Xian et al. 2006).

While G. Xian et al. studied epoxy-based nanocomposites include graphite and nano-TiO_2 as filler with short carbon fibers (SCF), aramid and polytetrafluoroethylene (PTFE) particles, Xian, Walter, and Haupert also studied epoxy resin containing TiO_2 and graphite but under different various sliding load and velocity conditions without adding some other particles. It was also observed by mechanical measurements by Xian, Walter, and Haupert that the incorporation of TiO_2 significantly enhanced the flexural and impact strength of the neat epoxy and the graphite including epoxy. Although the incorporation of nano-TiO_2 was markedly diminished the wear resistance of the neat epoxy under severe sliding conditions (high velocity and normal load); this effect was significantly improved also under mild sliding conditions. As predicted, it caused to a higher friction coefficient

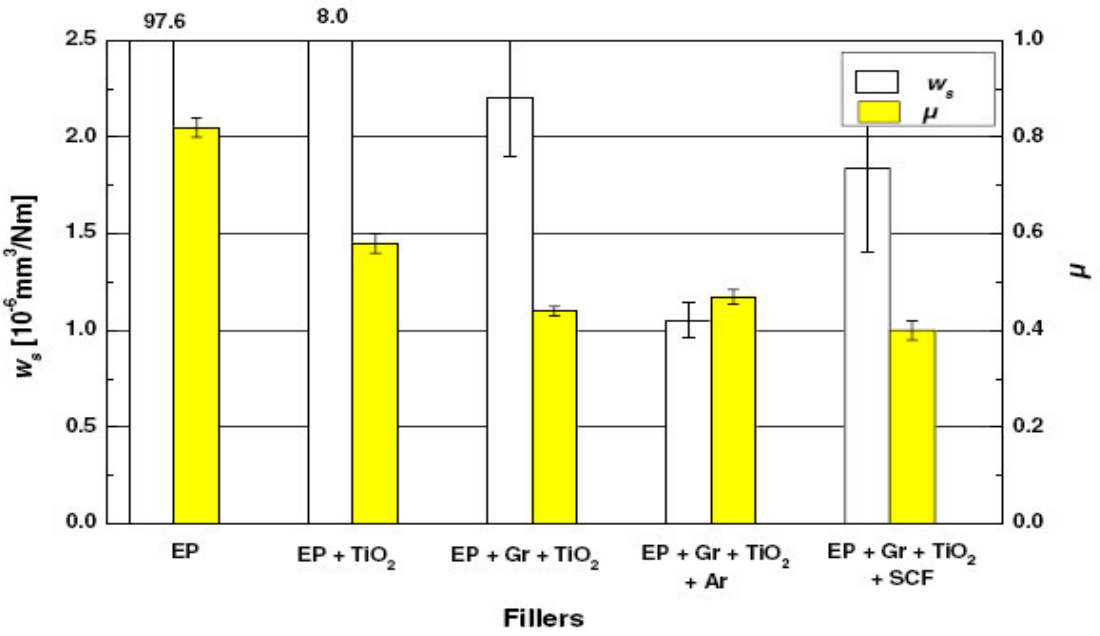

Figure 3.5. Specific wear rate (ws) and the coefficient of friction (l) of the neat epoxy (EP) and SCF or aramid (Ar) filled composites (without PTFE) under sliding conditions (block-on-ring) (Source: Xian et al. 2006).

than that of the neat epoxy on the contrary, under severe sliding conditions, nano-TiO_2 reduced the coefficient of friction of the neat epoxy. Under normal load, the graphite-filled epoxy showed more stable wear performance with the variation of the sliding conditions compared to the nano-TiO_2-filled epoxy. When the combination of nano-TiO_2 and graphite was studied, it was observed that it led to the lowest wear rate and coefficient of friction under the whole investigated conditions. The synergistic effect attributed to effective transfer films formed on sliding pair surfaces and the reinforcing effect of the nanoparticles. The influence of the normal force on the variation of the wear rate, coefficient of friction, and the formation of transfer films under the constant sliding velocity (1 m/s) was also compared in Table 3.2

Table 3.2. Under the Constant Sliding Velocity (1 m/s), the Influence of the Normal Force on the Variation of the Wear Rate, Coefficient of Friction, and the Formation of Transfer Films (Source: Xian, Walter, and Haupert 2006).

Materials	Force (N)	Wear rate (10^{-3} mm^3/m)	μ	Transfer film on cylinder	Transfer film on sample
Epoxy	10	0.48	0.62	No	No
	20	1.31	0.59	/	No
	30	2.11	0.58	/	No
	40	2.99	0.67	No	No
TiO_2/epoxy	10	0.07	0.83	Yes	/
	20	0.34	0.76	/	/
	30	1.79	0.51	No	No
	40	2.76	0.50	No	No
Graphite/epoxy	10	0.24	0.46	Yes	Yes
	20	0.36	0.40	Yes	Yes
	30	0.37	0.43	Yes	Yes
	40	0.52	0.39	Yes	Yes
Graphite/TiO_2/epoxy	10	0.02	0.35	Yes	Yes
	20	0.05	0.23	Yes	Yes
	30	0.08	0.25	Yes	Yes
	40	0.08	0.30	Yes	Yes

"/" means the transfer film is occasionally formed.

The nanometer-sized TiO_2 particles of low aspect ratio leads to low stress concentration and are able to prevent the propagation of cracks through the polymer. The flexural strength and the impact strength of the neat epoxy or graphite-filled epoxy were improved by adding a low content of nanometer- sized TiO_2 as shown in Figure 3.6

In addition to these studies, SEM analysis was examined. According to the results of SEM analysis, it was observed that the incorporation of nanometer-sized TiO_2 to the graphite-filled epoxy benefited the formation of transfer films on both contact surfaces. In combination with improved mechanical properties of the transferred material different wear mechanisms can take place, which are attributed to the synergism in terms of the improved wear resistance and reduced friction coefficient (Xian, Walter, and Haupert 2006).

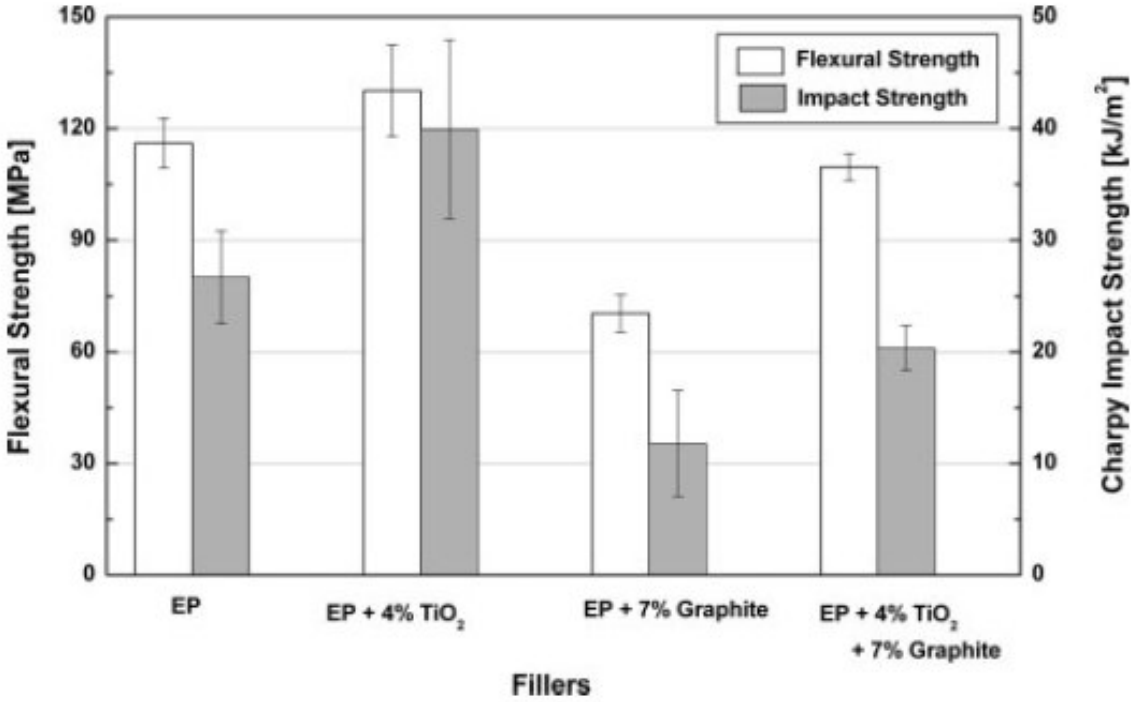

Figure 3.6. Flexural strength and unnotched Charpy impact strength of the epoxy resin and its composites (Xian, Walter, and Haupert 2006).

Xing and Li investigated the wear behavior of epoxy matrix composites filled with uniform sized sub-micron spherical silica particles differ from Xian et al.. They focused on the effect of particle size on the wear behavior of nanocomposites at low levels of filler content. Two distinct sizes of uniform sized silica particles (120 and 510 nm in diameter, respectively) were used as model fillers in the composite systems. Pin-on-disc wear test mode was used and the wear mechanisms were studied by scanning electron microscope (SEM) observations. Although the content of the fillers was at a relatively low level (0.5–4.0 wt. %) the wear rate of the composites was reduced dramatically as shown in Figure 3.7. It was found that the filler with smaller size seemed to be more effective in the improvement of the wear resistance of the composites (Xing and Li 2004).

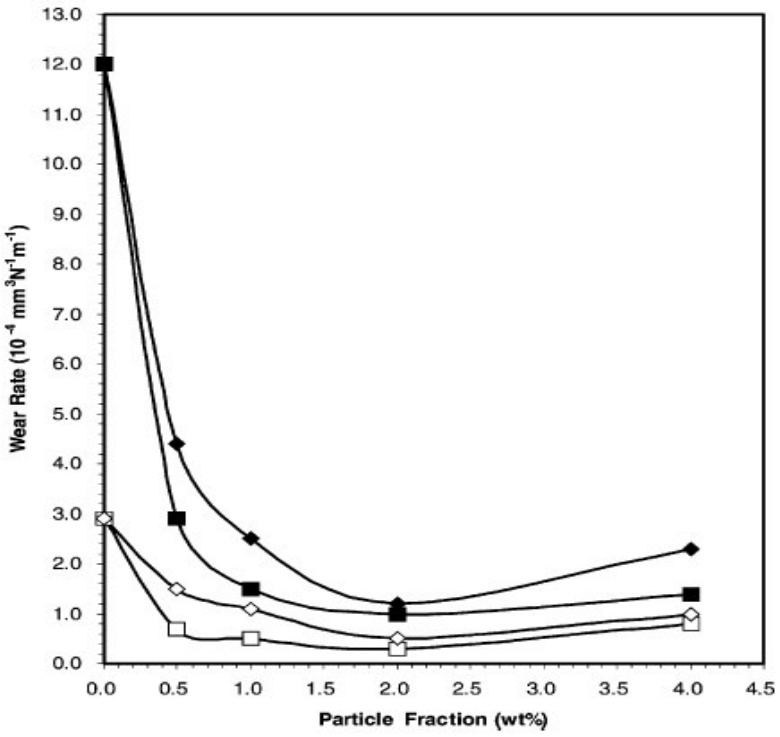

Figure 3.7. Wear rate of the epoxy matrix composites filled with silica particles (□) 120 nm, 1 N; (◊) 510 nm, 1N; (♦) 120 nm, 2 N; (■) 510 nm, 2 N) (Source: Xing and Li 2004)

G. Shi et al. (Shi et al. 2003) investigated the friction and wear resistance of epoxy composites that consist of low nanometer silicone nitride (Si_3N_4) particles. Under dry sliding wear conditions tribological performance and mechanical properties of the composite materials at rather low filler content (typically less than 1 vol. %) indicated improvement. Strong interfacial adhesion between Si_3N_4 nanoparticles and the matrix reduced damping ability and enhanced resistance to thermal distortion of the composites, and tribochemical reactions involving Si_3N_4 nanoparticles account for the reduced frictional coefficient and wear rate of the composites. Increasing the filler concentration flexural strength, flexural modulus and impact strength of nano-Si_3N_4/epoxy composites were increased. Because of high frictional surface temperature and contact pressure, some chemical reactions that cannot occur under normal circumstances are completed between the sliding counterfaces. The transfer film was formed in this way.

Inorganic fillers are known to improve the mechanical and tribological properties of polymers. Bernd Wetzel et al. (Wetzel et al. 2002) attempts to find the optimum performance of composites containing different amounts and types of

reinforcing nano- and microfillers in order to understand what role the inorganic fillers play on micro- and nanometer scales. Various amounts of micro- and nano-scale particles (titanium dioxide TiO_2. 200-400 nm, calcium silicate $CaSiO_3$, 4-15 μm) were introduced into an epoxy polymer matrix for its reinforcement. They investigated the effect of these particles on the impact strength, dynamic mechanical thermal properties and block-on-ring wear behavior. Nano-particles demonstrate the best improvement in stiffness, impact strength, and wear resistance of the epoxy at a nano-particle content of 4 vol% TiO_2. This nanocomposite was used as a matrix for the $CaSiO_3$, micro-particles, in order to find synergistic effects between the micro- and the nano-particles. A further improvement of wear resistance and stiffness are achieved, whereas the impact strength suffers. Geometrical properties of the particles, the homogeneous dispersion state, energy dissipating fracture mechanisms and a transition of wear mechanisms mostly contribute to the increase in performance. The mechanical and tribological properties are strongly influenced by the volume amount of incorporated fillers. The improved impact behavior may be ascribed to the nano-particles. Calcium silicate micro-particles, further incorporated into the toughest matrix (EP/TiO_2, 4 vol. %), showed good overall values at 3 vol % $CaSiO_3$. At higher filler loadings of calcium silicate micro-particles, impact strength is impaired, while stiffness and wear resistance are improved. In addition, nano-particles and micro-particles are both able to improve the wear resistance of the epoxy matrix. One of the reasons of the reduction in wear is the compacted wear debris layer that temporarily protects the composite surface from extreme wear. The other reason is the large $CaSiO_3$ particles that act as spacers towards the counterface and partially relieve the matrix from severe wear. Synergistic effects between TiO_2 nano-particles (matrix toughening) and $CaSiO_3$ micro-particles (stiffening) may play an important role in the property improvement because the wear behavior of polymer composites is influenced by stiffness and impact strength. Relationship between stiffness and impact strength is shown in the Figure 3.8. The mechanical and tribological properties are expected to improve further by a stronger coupling between the titanium dioxide nano-particles and the epoxy matrix.

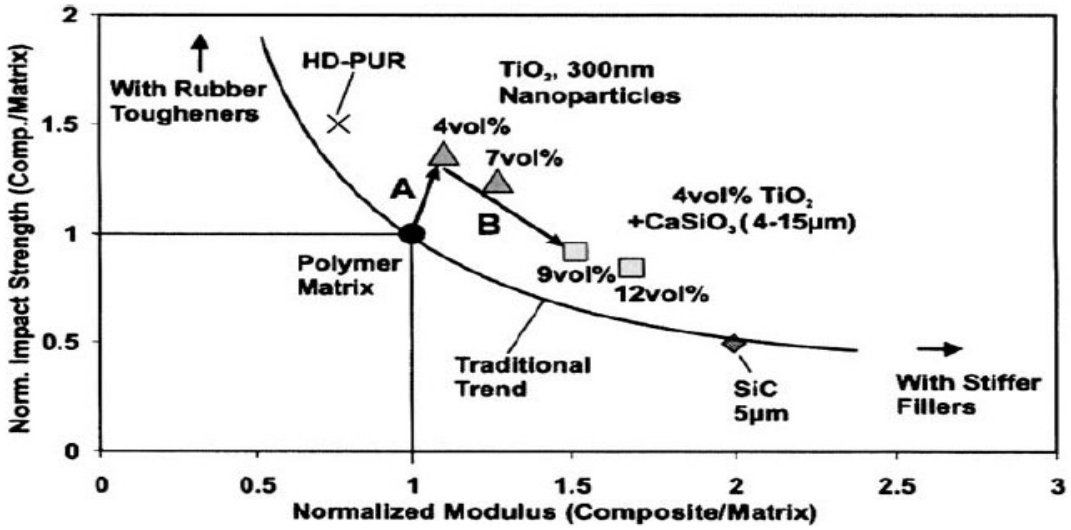

Figure 3.8. Relationship between stiffness and impact strength for some of the composites. The black line represents the traditional tendency. (●) The neat polymer. (▲) EP/TiO_2 nanocornposites. (■) EP/TiO_2/$CaSiO_3$ composites. (♦) EP/SiC_from earlier experiments. (X) EP containing hygrothermally decomposed polyurethane (HD-PUR, 40 wt %) (Source: Wetzel et al. 2002)

Treatment and modification of carbon fiber surface contribute to enhance the interfacial bonding between fiber and matrix. H. Zhang and Z. Zhang (Zhang and Zhang 2005) compared the wear performance of untreated and treated carbon fiber/epoxy (CF/EP) composites under various nominal contact pressures using a block-on-ring test apparatus. Two different kinds of surface treatments such as air oxidation and cryogenic treatment were concentrated on short carbon fibers (CF), which effectively improved the mechanical properties. After that these fibers were incorporated into epoxy matrix for wear investigations. It was found that under an appropriate air oxidative condition, the wear resistance of carbon fiber reinforced epoxy was significantly improved at low contact pressure, whereas that was reduced at high pressures which was ascribed to the damage of fiber mechanical properties after oxidation. On the other hand, carbon fibers preformed better at high sliding pressure after cryogenic treatment. Optimised oxidative treatment may significantly improve the wear resistance at low pv-factor, for instance 1 MPa m/s. However, negative effect occurred at higher pv values, e.g. P3 MPa m/s, which may due to the fiber damage after treatment. Cryogenic treatment performed very low wear rate at high sliding pressure, even they were not as good as untreated one at lower pressure. The improved fiber strength and interface strength may contribute to this effect.

P.D. Bloom et al. (Bloom et al. 2003) focused the use of novel quasicrystals (QC) as fillers in polymeric materials. In their research wear resistant of the epoxy filled with Al-Cu-Fe quasicrystalline powder is evaluated by pin-on-disk testing. In order to compare the results, epoxy samples filled with aluminum, copper, iron, aluminum oxide, and silicon carbide are tested. The use of Al-Cu-Fe QC powder, as filler in epoxy, maximizes the composite wear resistance while minimizing abrasion of the steel counterface. Wear mechanisms of the Al- Cu- Fe composites were characterized by scanning electron microscopy and X-ray photoelectron spectroscopy. The wear resistant of epoxy resins were improved with quasicrystalline Al-Cu- Fe powders. The low hardness of the ductile metal fillers resulted in increased wear coefficients compared to the unfilled epoxy resin. In contrast to ceramic materials and ductile metals, Al-Cu-Fe QC can be used to produce low weight, high wear thermoset parts such as bearings and gears for use in contact with steel mating surfaces. Furthermore, QC have good corrosion resistance and could be exploited as a wear-resistant filler for polymers in adverse service environments.

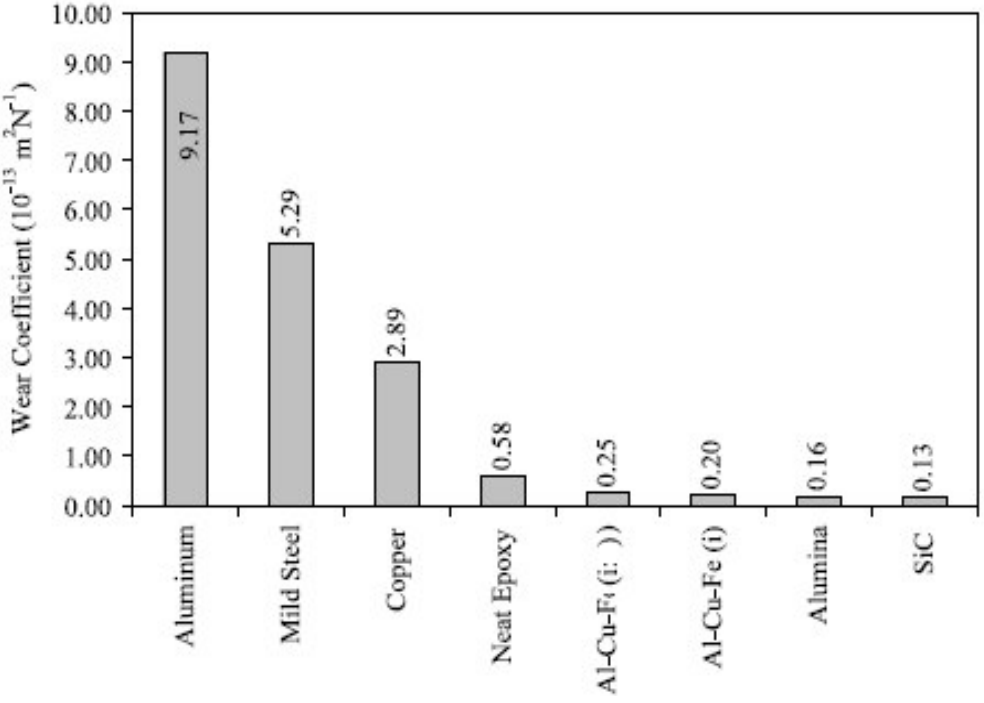

Figure 3.9. Effect of filler at 30 volume percent on epoxy composite wear
(Source: Bloom et al. 2003)

CHAPTER 4

EXPERIMENTAL

4.1. Materials

Bisphenol A-Epichlorhydrin based epoxy resin and its polyamine based curing agent provided from Aero Enercon Company were used for this study. Tungsten based nanostructured powders including W, W-B_4C-C (10 hours milling), W-SiC-C (6 hours milling), W-SiC-C (24 hours milling) were obtained to incorporate into epoxy resin. $0^o/+45^o/90^o/-45^o$ quadriaxial stitched non-crimp glass fibers (Metyx, Telateks Inc.), as schematically illustrated in Figure 4.1 were used as reinforcement constituent to fabricate fabric reinforced composite panels with nano-filler modified epoxy matrix.

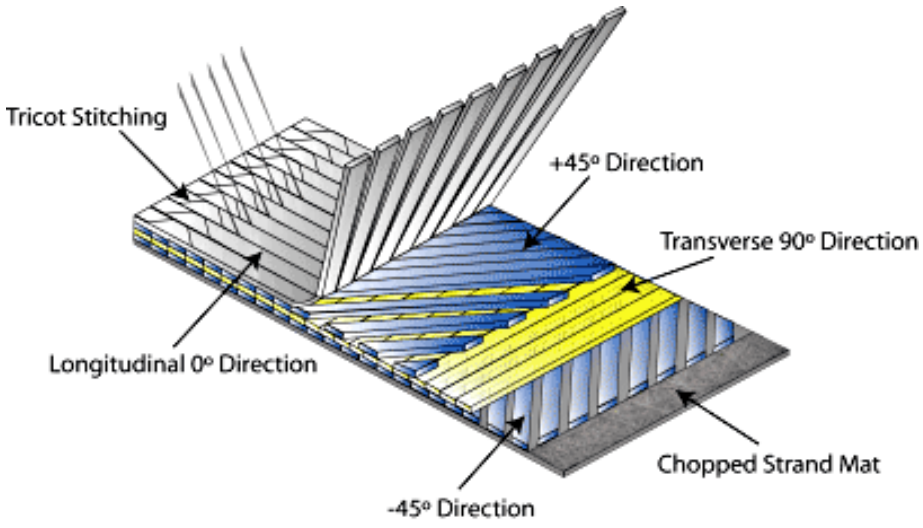

Figure 4.1. Schematic illustration of quadriaxial stitched non-crimp glass fibers (Source:Web_2)

The tungsten based nanopowders were prepared under a TÜBİTAK project in collobration with İstanbul Technical University (İ.T.U.), Department of Metallurgical and Materials Engineering and our research group. The powders were prepared through ball milling process. In this study, W, SiC, B_4C powders with average particle sizes of 14, 15, and 3 were used, respectively. Furthermore, graphite powder with an average particle size of 21 μm was used as a process control agent (PCA) to minimize cold

welding between powder particles and thereby to inhibit the agglomeration. In the experiments, powder mixtures of W-SiC-C and W-B_4C-C were mechanically alloyed in a tungsten carbide (WC) vial using a 8000D™ Spex mill with a speed of 1200rpm. WC balls with a diameter of ¼ inches were used as milling media. The balls-to-powder weight ratio was 10:1. The degree of the contamination of the milled powder with WC was determined by weighing the media before and after milling. W-SiC-C powder mixtures were mechanically alloyed for 6 and 24 hours as well as W-B_4C-C powder mixture was mechanically alloyed for 10 hours. High-purity argon was chosen as the milling atmosphere to prevent oxidation and contamination of the powder because the presence of air in the vial causes to produce oxides and nitrides in the powder, especially if the powders are reactive in nature.

4.2. Characterization of Tungsten based Powders

The microstructural and phase characterizations of tungsten based powders were carried out by scanning electron microscope (SEM) and X-ray diffraction (XRD) analyses techniques using Philips X'Pert Pro diffractometer, with CuKα radiation. Powdered samples were scanned in the interval of $2\Theta = 5°\text{-}80°$ at 40 kV and 30 mA.

4.3. Preparation of Nanocomposites

In order to prepare nanocomposites, tungsten based nanopowders at loading ratios of 3 and 5 wt. % were incorporated into epoxy resin. The schematic of nanocomposites processing is illustrated in Figure 4.2. To achieve uniform distribution of nano-powders within epoxy resin, each corresponding suspension was subsequently blended via mechanical stirrer at room temperature followed by sonication for 60 and 15 minutes, respectively. Afterwards, for 100 parts epoxy by weight, 35 parts amine curing agent was introduced into the mixtures and they were degassed by vacuuming. Finally, the compounds were casted into an open mold and cured at room temperature followed by post curing for 1 hour at 80 ^{0}C and 2 hours at 150 ^{0}C, respectively.

4.4. Preparation of Fiber Reinforced Composites with Nanoparticles

As an innovative approach, the resin suspensions, prepared as described in the section 4.3, containing various types of tungsten based nanopowders were used as a matrix on one surface of the non-crimp fabric reinforced composite laminates, whereas rest of composite layers were wet using neat epoxy resin. Composite laminates were fabricated by hand lay up technique. The procedure involves laying multiple plies on top of one another while spreading the resin between the adjacent fabrics in a mold. Prior to composite processing, mold surface was coated with a release agent in order to ease the peeling of the tool.

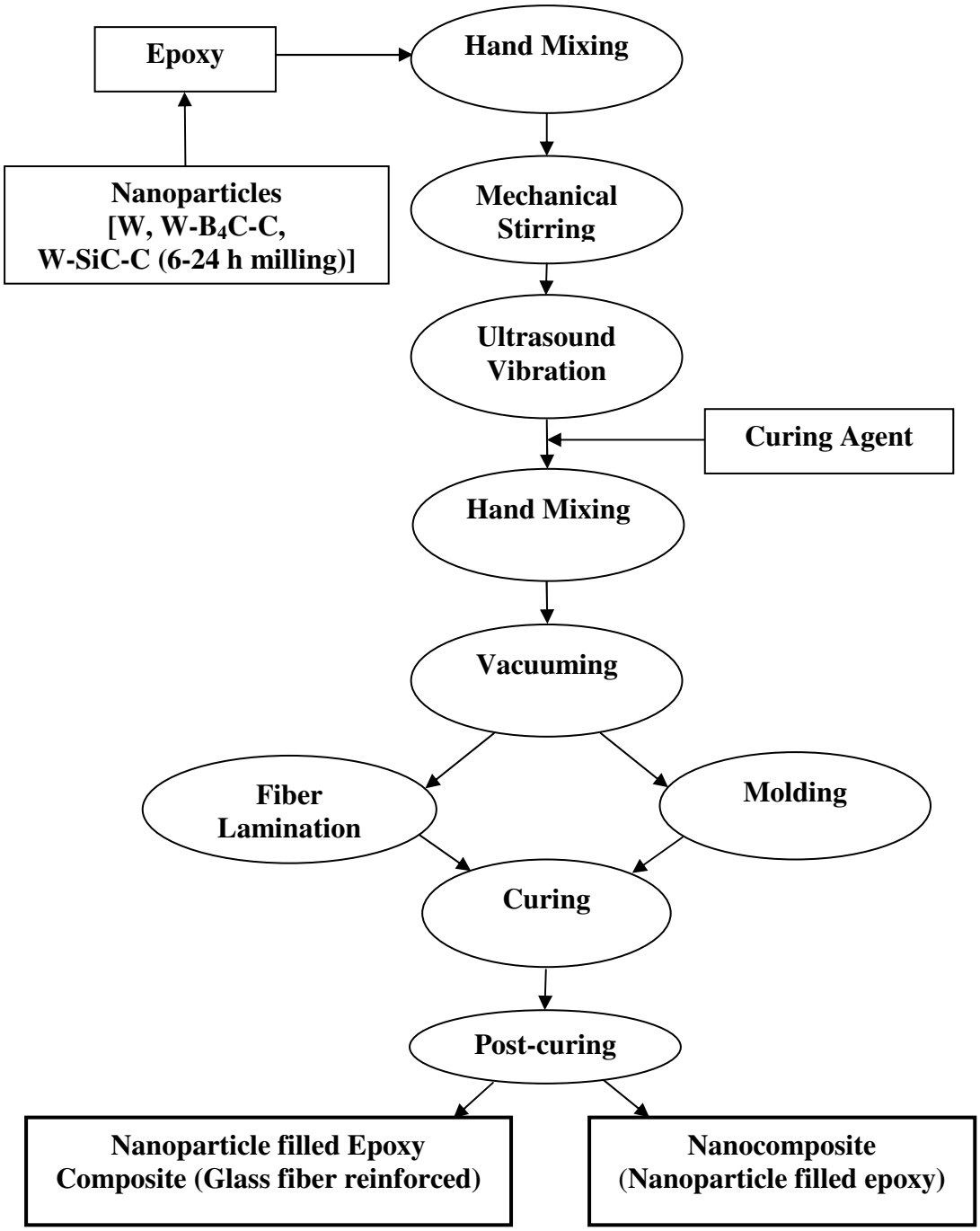

Figure 4.2. Production Steps of Polymer Nanocomposites and Glass Fiber Reinforced Nanocomposites

4.5. Wear Test

The pin-on-disk wear test technique, one of the most commonly used testing configurations, was conducted using the tribometer (CSM instruments, Figure 4.3.a) in

order to determine the effect of tungsten based nanopowders on friction coefficient and specific wear rate of the resultant nanocomposites.

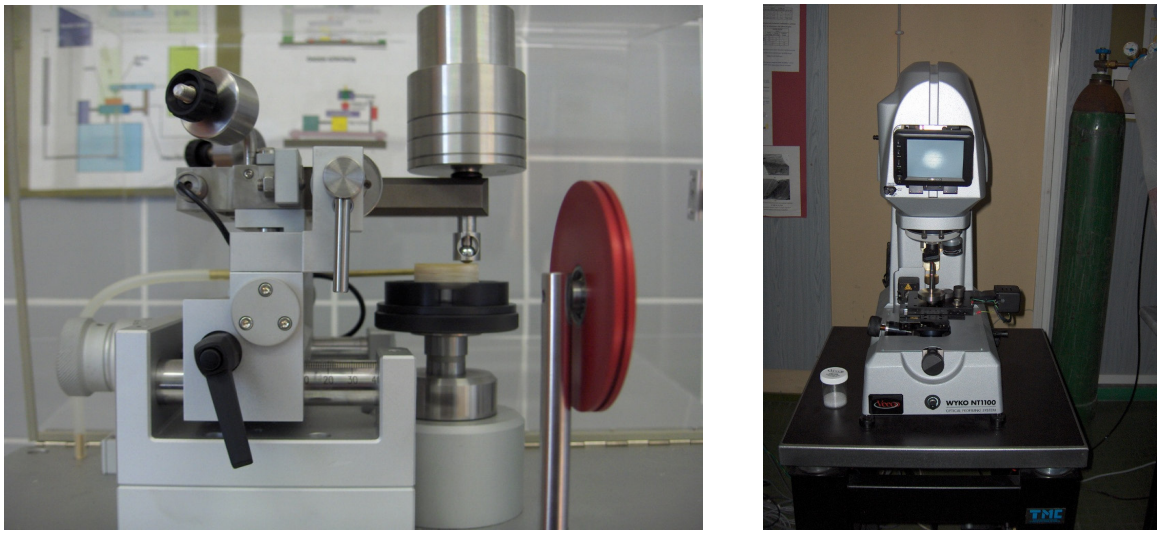

a **b**

Figure 4.3. a)Tribometer (CSM instruments), b) 3D profilometer(Veeco Wyko NT 1100)

Cylindrical test specimens shown in Figure 4-4 were prepared for wear testing. Nanocomposites were prepared by casting of resin suspensions into a silicone mold. The specimens with fiber reinforced laminates were prepared by sectioning from larger composite laminates.

a **b**

Figure 4.4. Wear test specimens; a) nanocomposites, b) fiber reinforced composites

In this wear test technique, 52100 steel balls with a diameter of 6 mm were used as the stationary pin material. A linear speed of 10 cm/s, with load of 4 N and wear track radius of 7.1 mm, a total linear distance of 1000 m were used during the wear testing. Friction coefficient values were determined by tribometer, as the ball was

sliding on the specimens. After a wear test was performed, 3D profilometer (Veeco Wyko NT 1100, Figure 4.3.b) was used to monitor the amount of volume loss from specimens and surface topography. The volume loss allows one to calculate the most important tribological property, the specific wear rate (W_S) of the material, by using the equation as below,

$$W_S = \frac{\Delta V}{L \cdot F_N} \quad \left(mm^3 / N \cdot m\right) \tag{4.1}$$

in which ΔV is the loss in volume, F_N is the normal load, and L is the sliding distance.

4.6. Characterization of Mechanical Properties

4.6.1. Hardness Test

Surface hardness values of the wear test specimens were measured by Shimadzu™ micro hardness tester with a Vickers indenter under a load of 1 kg for 15 seconds. Results of hardness tests were averaged out of 5 successive indentations.

Figure 4.5. Shimadzu™ micro hardness tester

4.6.2. Flexural Test

In order to investigate the effects of tungsten based nanofillers on flexural strength and modulus of the composites, the flexural test technique was used according to ASTM D 790M-86. The flexural test specimens were sectioned from nanocomposites and glass fiber reinforced nanocomposite laminates with 10 mm in width, 4 mm in depth and 80 mm in length. At least five specimens for both nanocomposites and laminates including 3 and 5 wt. % of W, W-SiC-C (6 h milling), W-SiC-C (24 h milling), W-B_4C-C particles were tested using the Schimadzu AGI universal test machine with the crosshead speed of 1.7 mm/min. During the test of fiber reinforced composites, the sides of the specimens that contain nanoparticales were placed onto the support fixtures. Three-point bending tests were performed for each specimen with a span to thickness ratio of 16 (Figure 4.6). Force vs. deflection at the center of the beam was recorded. The flexural strength, S, values were calculated using the equation below;

$$S = \frac{3PL}{2bd^2} \tag{4.2}$$

where P is the applied load at the deflection point, L is the span length, d and b are the thickness and the width of the specimen, respectively. The maximum strain in the outer fibers occurs at midspan and calculated as;

$$r = \frac{6Dd}{L^2} \tag{4.3}$$

where r is the maximum strain in the outer fibers, D is the deflection of the center of the beam. The Flexural modulus values, E_b, were calculated from;

$$E_b = \frac{L^3 m}{4bd^3} \tag{4.4}$$

where m is the slope of the tangent to the initial straight line portion of the load-deflection curve.

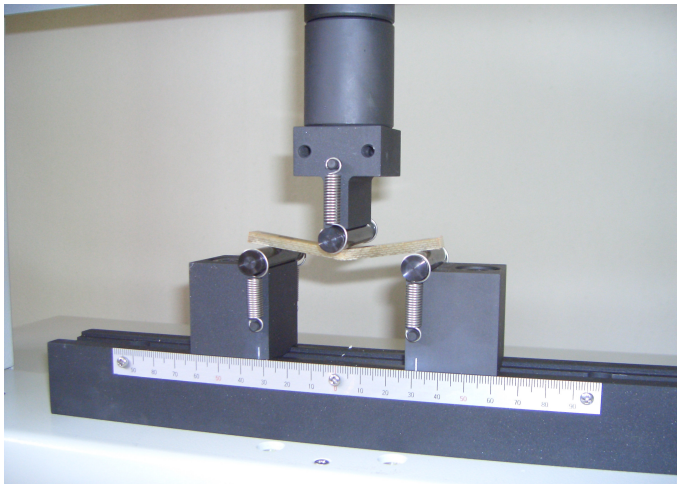

Figure 4.6. Flexural test specimen under load

4.6.3. Tensile Test

Tensile tests were applied only to nanocomposites without fibers. Tensile test technique, according to DIN EN 527.1/2. standard, was used to investigate the effect of nanofillers on the tensile strength and modulus of the nanocomposites. Test specimens were produced by casting in a silicone mold. At least five specimens were prepared for each type and content of nanoparticles (3 and 5 wt. %). Schimadzu AGI universal test machine was used for the tensile tests at a cross head speed of 1 mm/min (Figure 4.7). The tensile strength (σ_f) values were calculated using the following equation;

$$\sigma_f = \frac{F}{A} \tag{4.5}$$

where F is the applied load, and A is the cross sectional area of the specimen. Elastic modulus was obtained from the initial portion of stress (σ) - strain (ε) graphs based on the equation below is given by;

$$E = \frac{\sigma}{\varepsilon} \tag{4.6}$$

A video extensiometer was used to obtain strain values. Strain values (ε) were calculated from;

$$\varepsilon = \frac{(L - L_0)}{L_0} \tag{4.7}$$

where L_0 is the distance between gage marks on the samples at the beginning of the testing, and L is the distance between gage marks obtained with the extensiometer at a specific time during the extension.

Figure 4.7. Tensile test specimen under load

4.7. Characterization of Thermal Properties

4.7.1. Differential Scanning Calorimetry (DSC)

Differential scanning calorimetry (DSC) is a technique used for studying thermal transitions of polymers once they are heated. DSC can measure for instance the glass transition temperature and melting point of a polymer by detecting differences in the heat flow between the corresponding sample and reference. In the present study, TA instrument Q10 model DSC was used to investigate the effect of fillers upon the glass transition temperature (T_g) of resultant parts. In that manner, dynamic DSC measurements with a heating rate of 10°C/min from 25 to 180°C were performed under nitrogen atmosphere at a flow rate of 50 mL/min on the samples sectioned from larger

plates of neat epoxy resin and its related nanocomposites containing 3 and 5 wt % nanofillers. Glass transition temperatures were calculated by the midpoint method.

4.7.2. Dynamic Mechanical Analysis (DMA)

Dynamic mechanical analysis (DMA) is a thermal analysis technique used to measure changes in the elastic modulus (or storage modulus, E'), viscous modulus (or loss modulus, E'') and damping coefficient (Tan δ) of a material (especially polymers) as a function of temperature, time, or deformation frequency. The technique also is useful for qualitatively characterizing the glass transition temperature (T_g) of polymer and composite materials. DMA can recognize small transition regions that are beyond the resolution of DSC (Differential Scanning Calorimetry).

In this characterizing technique the test specimens were clamped into the Perkin Elmer Diamond DMA (Figure 4.8) apparatus between the movable and stationary fixtures and subjected to an oscillatory deformation while being heated at the controlled rate. The resonant frequency of the sample and mechanical clamp assembly was continuously monitored as a function of temperature. As the viscoelastic response of the material changed over some temperature range, the electrical energy required to maintain a constant level of sample deformation also changed and was continuously monitored.

Figure 4.8. Perkin Elmer Diamond DMA

The DMA specimens as shown in Figure 4.9*;* approximately 1 mm in thickness, 10 mm in width and 35 mm in length were sectioned from the nanocomposites and the composite laminates and tests were conducted with a strain rate of 0.1%. While testing, dual cantilever clamp were used and a heating rate of 2°C/min from 15 to 170°C was applied.

a **b**

Figure 4.9. DMA Specimens; a) nanocomposites, b) fiber reinforced nanocomposites

4.8. Microstructure Characterization

4.8.1. Scanning Electron Microscopy (SEM)

Phillips Scanning Electron Microscope (SEM) was used to investigate the dispersion state of particles in nanocomposites and the morphologies of worn surfaces obtained after wear test. The worn surfaces and cross-sections of specimens were sputter coated with a thin conducting layer of gold before examining with SEM.

4.8.2. Optical Microscopy

Nikon optical microscope was used to observe fiber alignment and to investigate the void content in the nanocomposites. Initially cold molded specimens were polished to obtain clear images.

CHAPTER 5

RESULTS AND DISCUSSION

In this chapter, the effect of the tungsten based powders on the tribological, mechanical and thermal properties of epoxy and glass fiber reinforced epoxy composites are presented. The specific wear rate of the resultant epoxy composite and the effect of the different filler types and contents on wear resistance were evaluated. The tensile, flexural strength and thermo-mechanical properties of the glass fiber reinforced epoxy composites and nanocomposites were also assessed.

5.1 Properties of Tungsten Based Powders

XRD patterns of tungsten (W) and mechanically alloyed tungsten based powders are shown in Figure 5.1. With the increasing time (from 6 h to 24 h) of mechanical alloying, peaks are broadened and heights of peaks are decreased, which are due to refining of grain size and increasing of internal strain resulted from mechanical alloying.

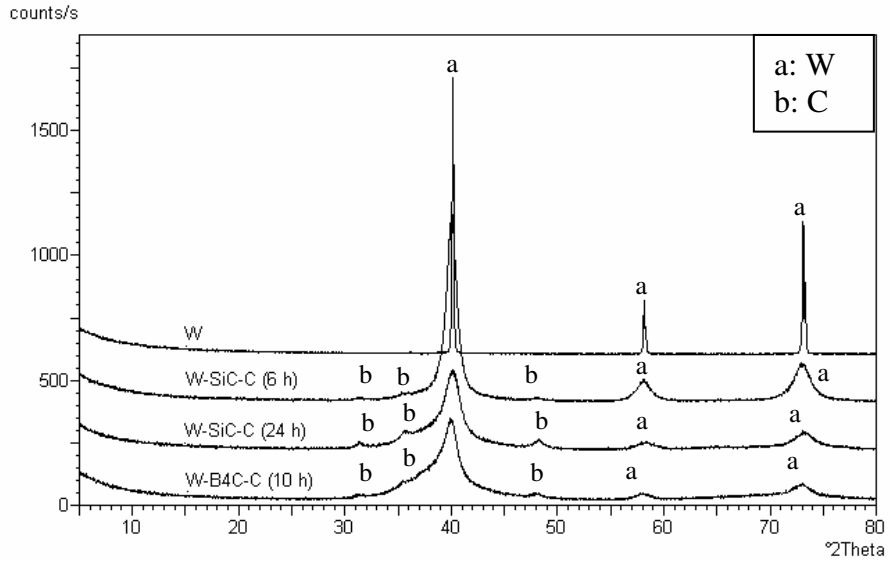

Figure 5.1. XRD patterns of a) W powder, b) W-SiC-C powder (6h mechanically alloyed), c) W-SiC-C powder (24h mechanically alloyed), d) W-B_4C-C powder (10 h mechanically alloyed)

SEM images of 6h and 24h mechanically alloyed W-SiC-C powders and 10 h mechanically alloyed W-B_4C-C powder are illustrated in Figure 5.2. The particle size analysis results of the powders are also given in Figure 5.2. As a result, average particle sizes of W-SiC-C (6h), W-SiC-C (24h), and W-B_4C-C (10h) were found to be 202 nm, 105 nm and 663 nm, respectively. Also, the images of 6h and 24h mechanically alloyed W-SiC-C powders show that the particle sizes of powders are decreasing with the increasing time of mechanical alloying. As observed in SEM images given in Figure 5.2.b., while the particle size of the powders becomes smaller, more volume of agglomerates occupy within micro-structures.

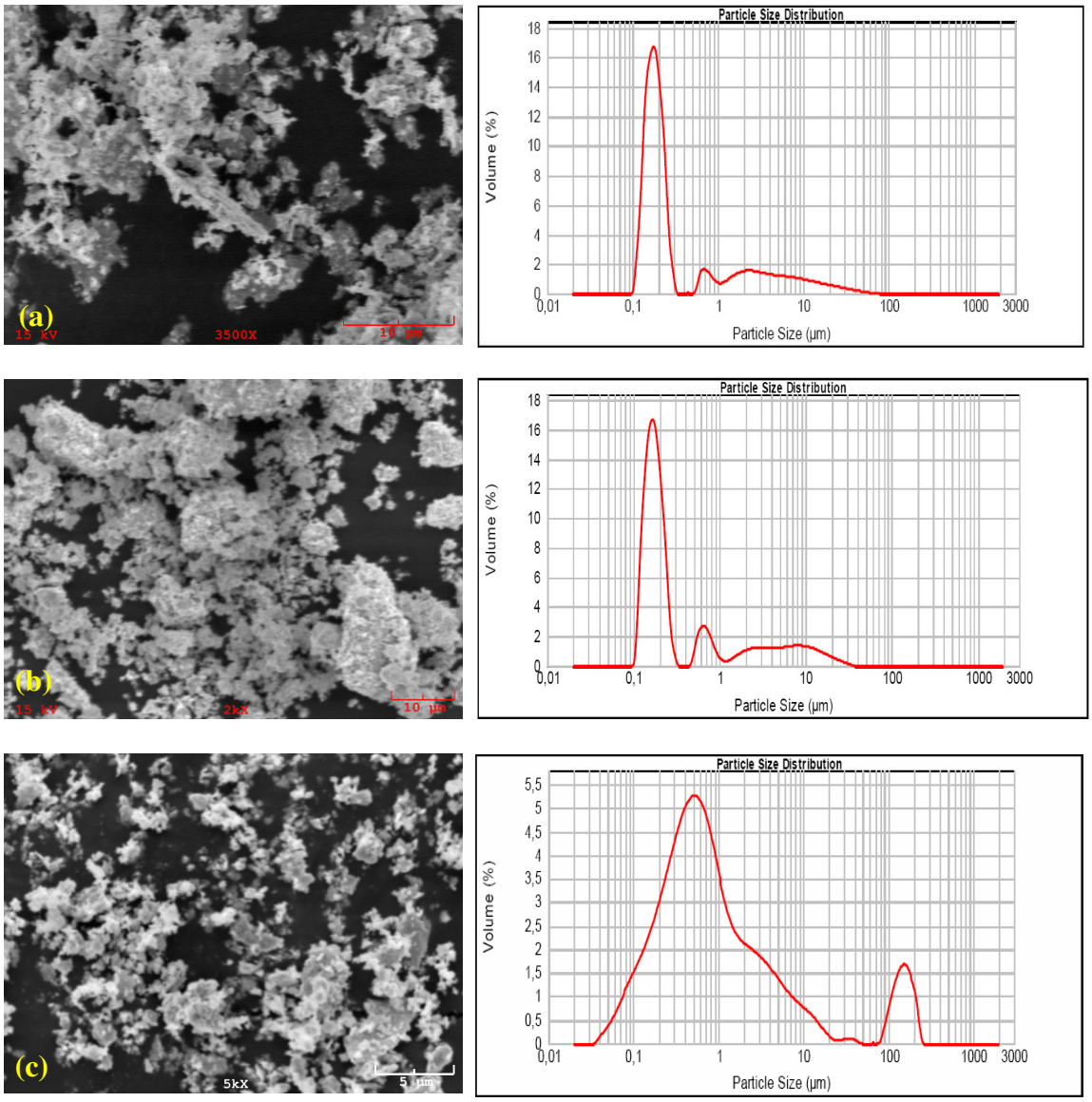

Figure 5.2. SEM images and particle size distributions of (a) W-SiC-C (6h), (b) W-SiC-C (24h), (c) W-B_4C-C (10h)

5.2. Properties of Nanocomposites

5.2.1. Wear Resistance

The volume loss values and the specific wear rates of neat epoxy and its corresponding nanocomposites containing various types of powders are given in Table 5.1 and Figure 5.3, respectively. Incorporation of fillers into epoxy matrix improves the wear resistance. No significant variation was observed between the specimens containing 3 and 5 wt. % of W and W-B_4C-C powders. This implies that the concentration of W and W-B_4C-C powders at the given loading rates have no significant effect on the wear rate values of the resultant nanocomposites. However, wear rate values of nanocomposites containing 6 and 24 hours mechanically milled W-SiC-C powders were altered the given powder content. Among all the specimens prepared, nanocomposites containing 3 wt. % W-SiC-C (24h) powder exhibited the lowest wear rate or highest wear resistance. The wear rate value of this nanocomposite is about 8 times better as compared to the value for neat epoxy.

Table 5.1. The Volume Loss Values of Nanocomposites

Nanocomposites	**Volume Loss (μm)**
Neat Epoxy	8.29×10^{-6}
3 wt % loading rate of powder	
W	1.67×10^{-6}
W-SiC-C (6 h)	1.35×10^{-6}
W-SiC-C (24 h)	1.02×10^{-6}
W-B_4C-C (10 h)	1.77×10^{-6}
5 wt % loading rate of powder	
W	1.63×10^{-6}
W-SiC-C (6 h)	1.93×10^{-6}
W-SiC-C (24 h)	1.76×10^{-6}
W-B_4C-C (10 h)	1.95×10^{-6}

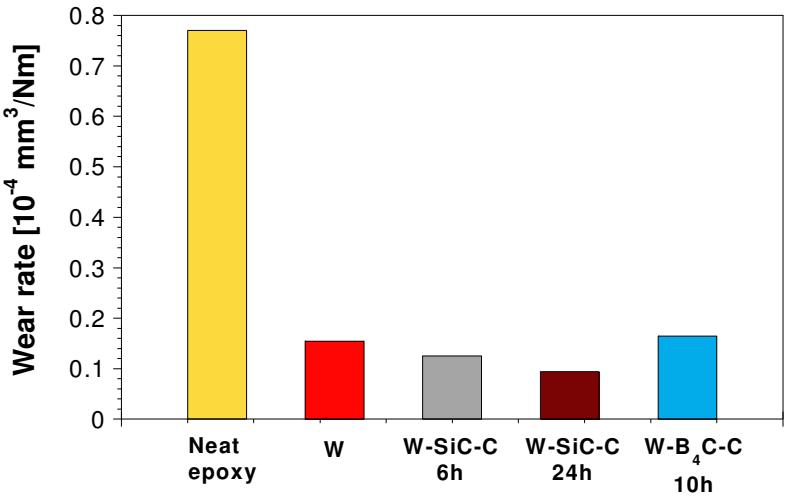

(a)

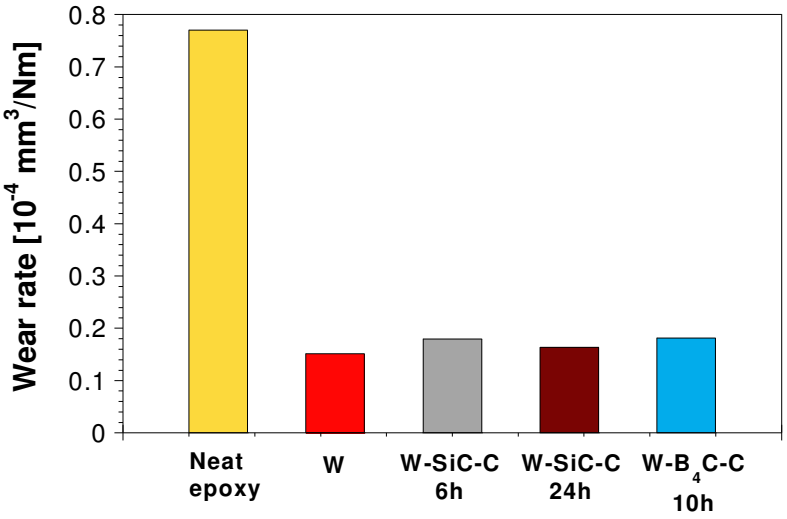

(b)

Figure 5.3. Comparison of the specific wear rates of nanocomposites containing (a) 3 wt. % and (b) 5 wt. % tungsten-based powders. The wear rate for neat epoxy is also given.

The friction coefficient values of neat epoxy and nanocomposites were obtained from tribometer and the effect of nanopowders on the friction coefficient values of composites is illustrated in Figure 5.4. The neat epoxy showed the highest friction coefficient values. During sliding, sudden drops were periodically observed in friction coefficient values for all specimens. Throughout the moving of the steel counterface on the specimens, produced wear debris took place on the specimen surface and this wear debris caused sudden drops in friction coefficient values. Comparing the neat epoxy with other nanocomposites, removal of the material from the surface or wear debris is much easier in neat epoxy. That is the reason why epoxy showed these sudden drops

more intensively than other specimens. The friction coefficient value of neat epoxy is approximately 0.6. At 3 wt. % loading rate, incorporation of each type of powders into epoxy resin lead to enhanced friction properties (reduced friction coefficient) relative to that of neat epoxy

.

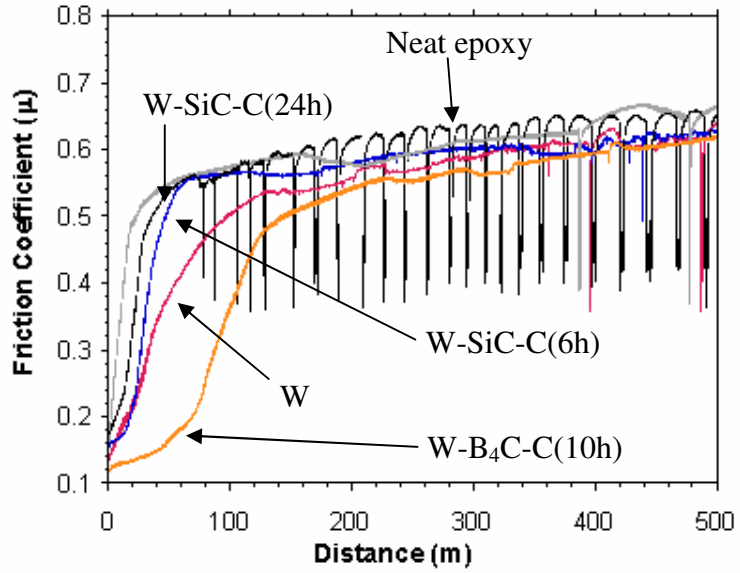

(a)

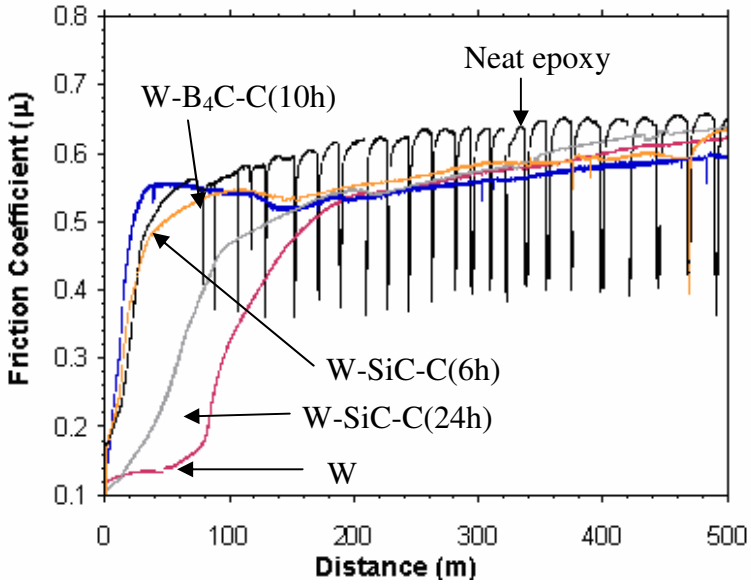

(b)

Figure 5.4. Comparison of the Friction Coefficient values of nanocomposites containing (a) 3 wt. % and (b) 5 wt. % tungsten-based powders. The μ values for neat epoxy are also given in the Figures.

The topographic images of neat epoxy and its nanocomposites containing 3 wt. % of W-SiC-C (24h) powder taken from 3-D profilometer are also illustrated in Figure 5.5. As observed in these 3-D images, neat epoxy possessed relatively higher wear rates (or lower wear resistance) as compared to its nanocomposites with 3 wt. % W-SiC-C (24h). It is in association with wear rate values. This result can be also attributed to the smallest particle size of W-SiC-C (24h) powders and their uniform dispersion within epoxy resin via high speed mechanical stirring. Furthermore, this powder has the highest volume fraction within epoxy resin because of its relatively lower density as compared to other powders used in this study. This may be also important factor on why nanocomposite containing W-SiC-C (24h) exhibited an enhanced wear resistance than those with other powders.

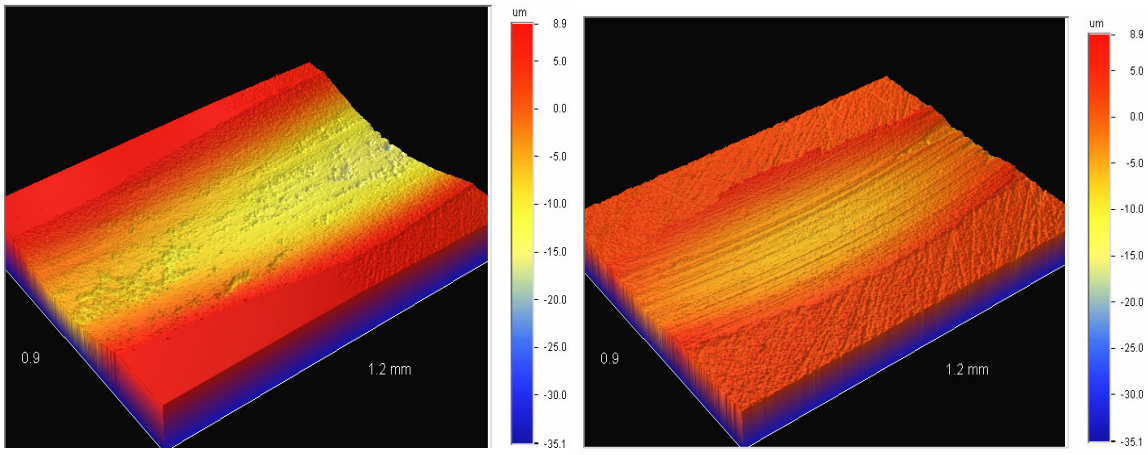

(a) **(b)**

Figure 5.5. The surface topology of worn surfaces: (a) 3D profile of the wear track of the neat epoxy, (b) 3D profile of the wear track of the epoxy matrix composite filled with 3 wt. % W-SiC-C (24h) powder

In order to interpret the involved wear mechanisms, worn surfaces of epoxy and its nanocomposites were examined using Scanning Electron Microscopy (SEM). Figure 5.6 shows the SEM micrographs of the worn surfaces of neat epoxy and its corresponding nanocomposites. Fatigue wear mechanism seems to be the dominative wear mechanism as a consequence of repeating high local stresses in the way of sliding. Moreover, surface roughness of the samples was found to increase along the sliding direction in both epoxy and its nanocomposites.

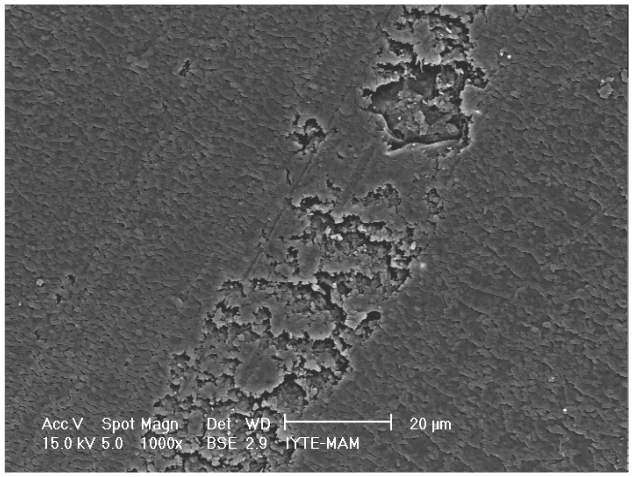

(a)

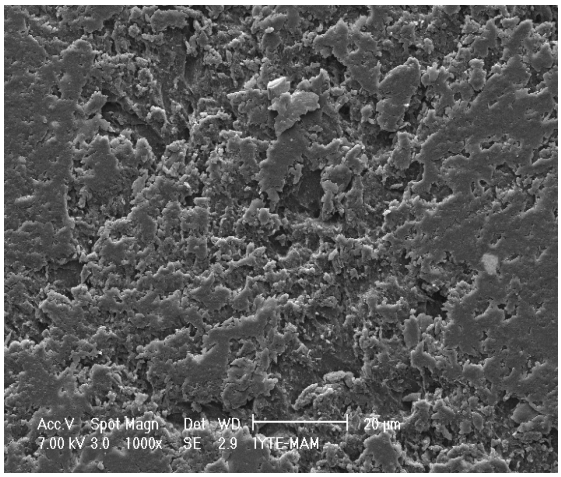

(b)

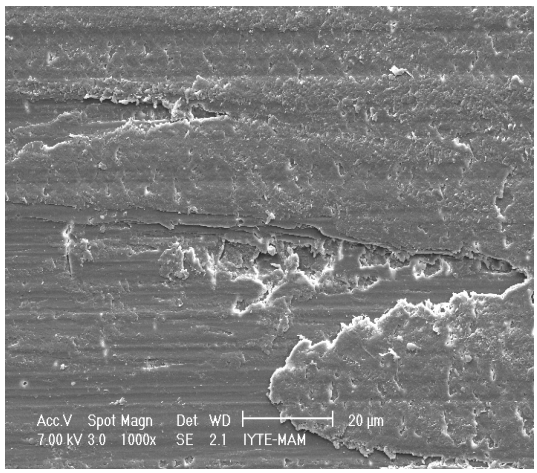

(c)

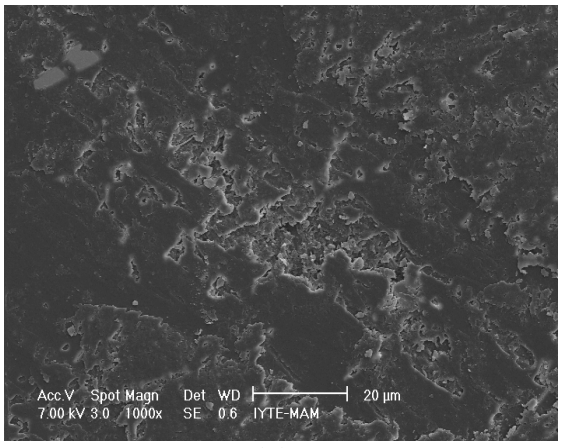

(d)

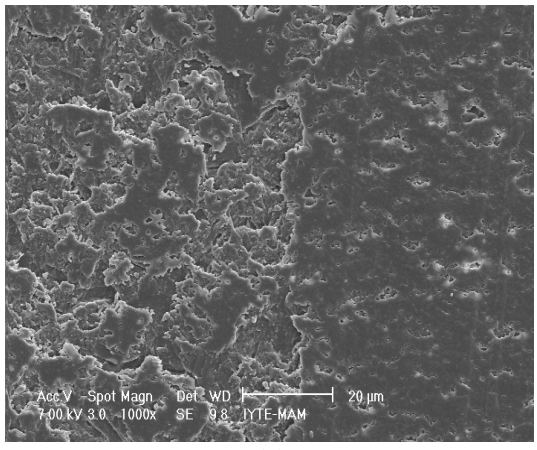

(e)

Figure 5.6. SEM images of worn surfaces of (a) neat epoxy, (b) 3wt.% W/epoxy (c) 3 wt. % W-SiC-C (24h)/epoxy, (d) 5wt. % W/epoxy and (e) 5 wt. % W-SiC-C (24h)/epoxy

In figure 5.7, vickers microhardness values of neat epoxy and nanocomposites are illustrated. It was observed that the hardness and wear resistance properties of

nanocomposites are related to each other. The nanocomposite containing 3 wt. % W-SiC-C (24h) powder has the highest hardness values, as similar the wear resistance (lowest wear rate) values. In the case of higher particulate content, agglomeration of the particles is rather severe, resulting in higher microhardness (Shi et al. 2003).

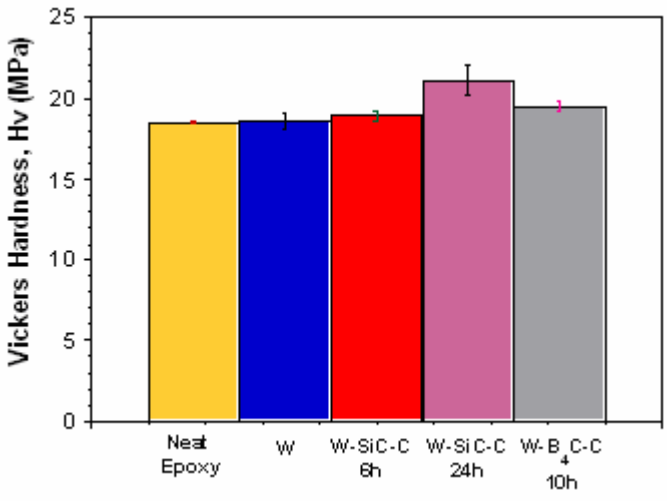

(a)

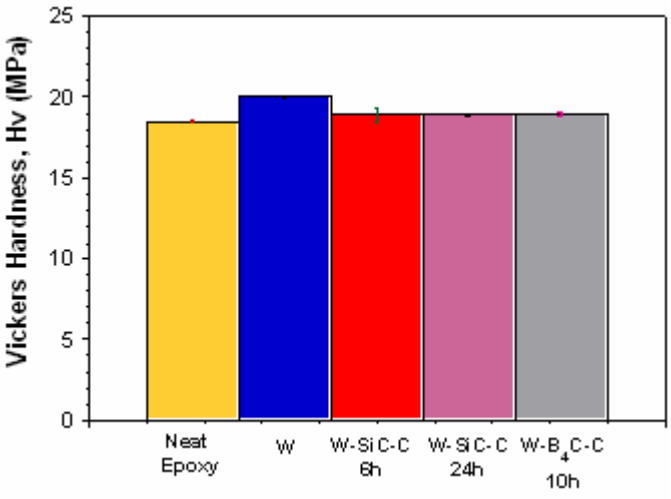

(b)

Figure 5.7. Microhardness of neat epoxy and its nanocomposites containing (a) 3wt. %, (b) 5 wt. % tungsten based powders

Even W-SiC-C (24h) powder does not have the lowest density, it has the smallest particle size among the other powders used in this study. Therefore, the increase in the hardness of the nanocomposite containing W-SiC-C (24h) powder can be ascribed the much more agglomeration due to its small particle size.

5.2.2. Flexural Properties

Figure 5.8 shows the measured flexural properties of epoxy resin and its nanocomposites containing various types of powders at 3 wt. % content. The flexural strength and modulus values of neat epoxy are 125 MPa and 3.39 GPa, respectively. W-SiC-C (24h) powder incorporated nanocomposites possessed relatively lower flexural strength and modulus as compared to neat epoxy resin and the other nanocomposites with different types of powder. Since W-SiC-C (24h) powder has the smallest particle size as compared to the other powders used in this study, it is expected that powders with smaller particle size exhibit relatively higher tendency to exist in more agglomarated form than those with greater particle size. From that point of view, the reduction in flexural strength and modulus of W-SiC-C (24h) powder modified nanocomposites may be attributed to high void content occupied within specimens.

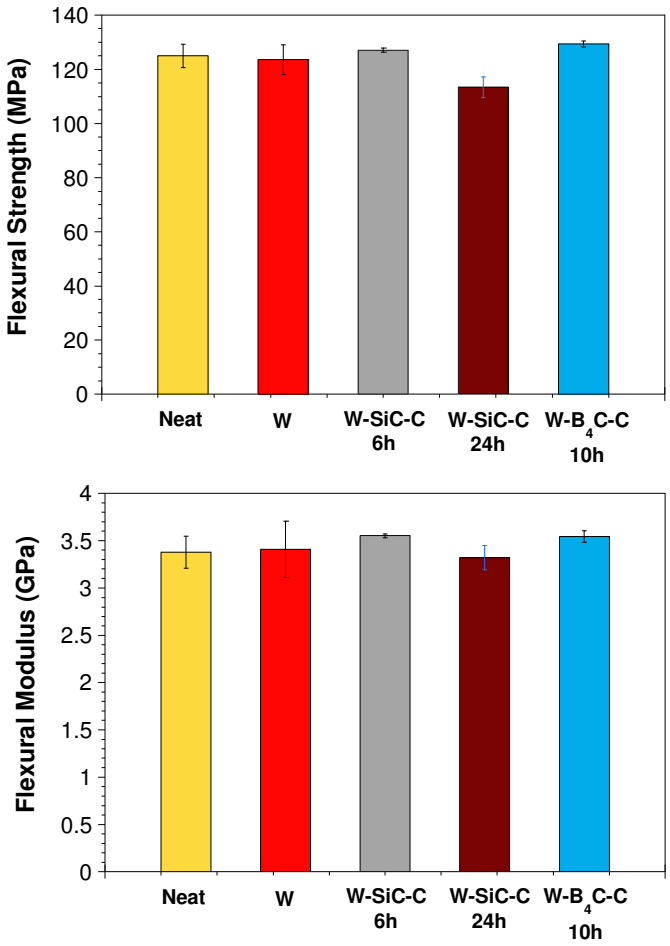

Figure 5.8. Flexural Strength and modulus values of composites containing 3 wt. % powder

In Figure 5.9, flexural properties of epoxy resin and its nanocomposites containing various types of powders at 5 wt. % content are illustrated. At this loading rate, W-SiC-C (24h) powder incorporated nanocomposites again possessed relatively lower flexural strength and modulus as compared to neat epoxy resin and the other nanocomposites with different types of powder. In all the test specimens, increasing the amount of filler embedded into epoxy resin led to lower flexural strength and modulus in the nanocomposites.

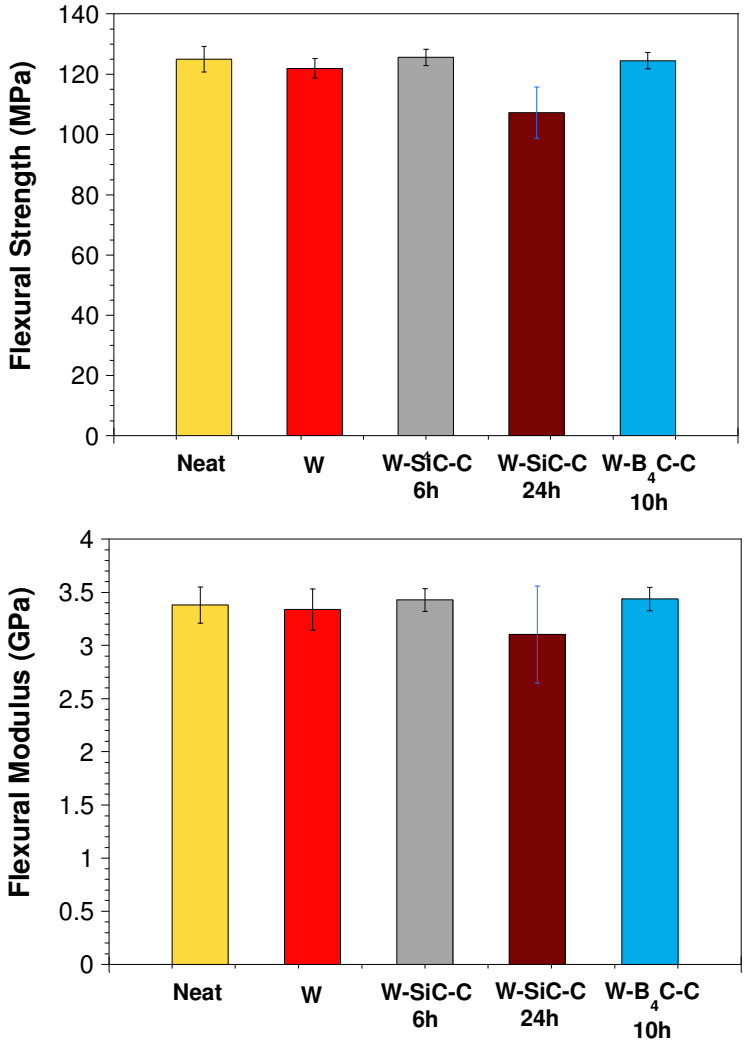

Figure 5.9. Flexural Strength and modulus values of composites containing 5 wt. % powder

5.2.3. Tensile Properties

Figure 5.10 shows the tensile strength and modulus values of nanocomposites containing 3 wt. % of tungsten based powders. The tensile strength and modulus values

of neat epoxy are 77.6 MPa and 2.8 GPa, respectively. The tensile strength values slightly increased for all specimens except for W-B_4C-C powder incorporated nanocomposite at 3 wt. %. As the increments may be due to better distribution of particles within matrix and good matrix-particle interactions, the reduction may be due to the agglomerations of the particles and thus damaged matrix-particle interactions. Tensile modulus of all nanocomposites containing 3 wt. % of powders were enhanced with the addition of powder.

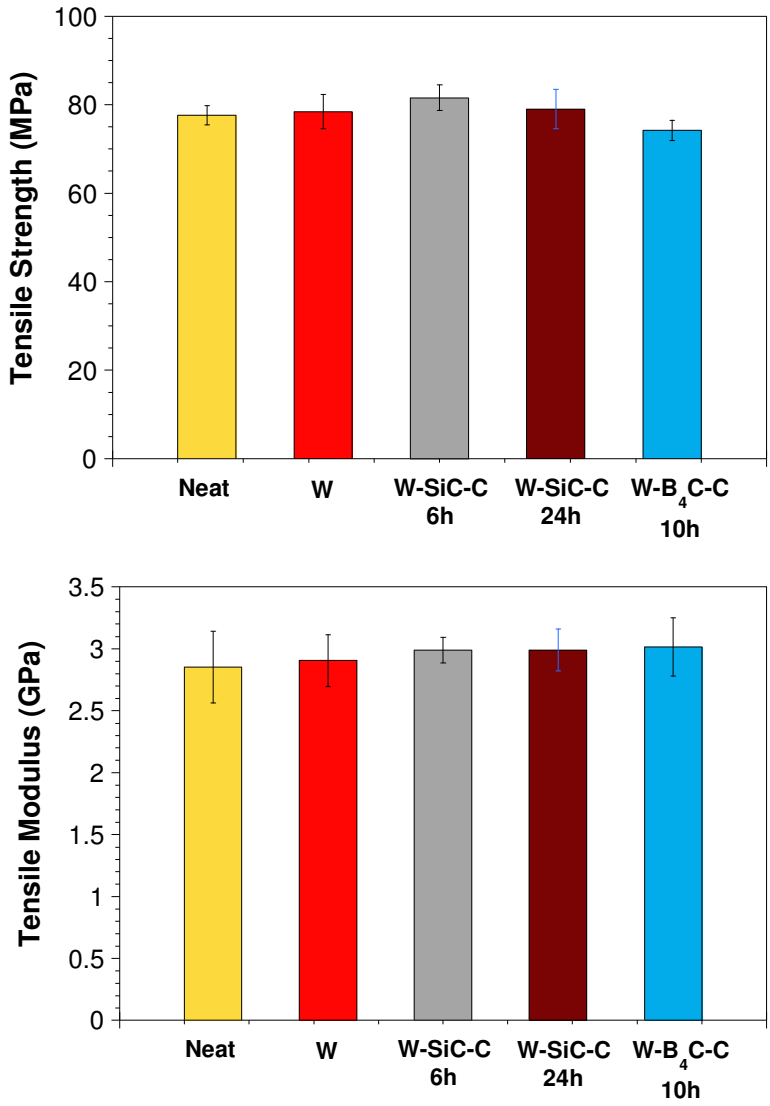

Figure 5.10. Tensile Strength and modulus values of composites containing 3 wt. % powder

Figure 5.11 shows the tensile strength and modulus values of nanocomposites containing 5 wt. % of tungsten based powders. Although the increment of the powder

content from 3 to 5 wt. % in epoxy matrix caused the tensile strength to improve for nanocomposite containing W-B_4C-C powder, other nanocomposites showed the reduction in tensile strength with the increasing of powder content. These reductions may be ascribed the higher void contents.

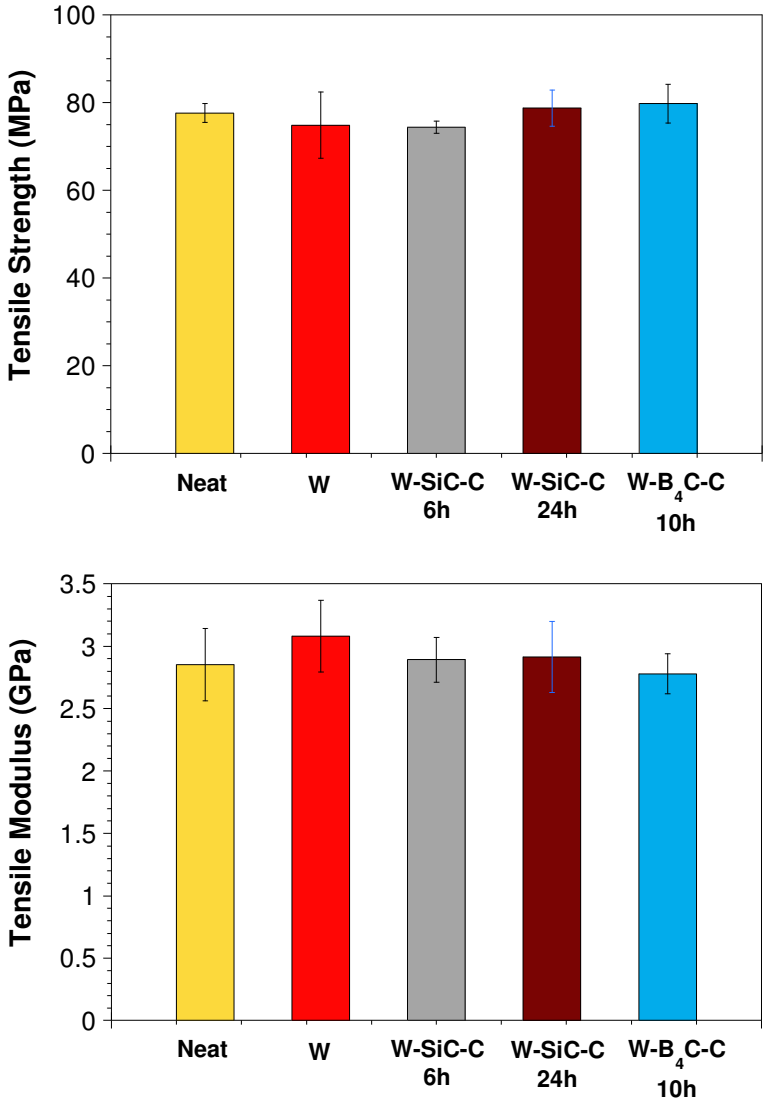

Figure 5.11. Flexural Strength and modulus values of composites containing 5 wt. % powder

5.2.4. Thermal Properties

The thermo-mechanical behaviour of the composites was evaluated by DMA. The comparison of the storage modulus of the nanocomposites is shown in Figure 5.12 and Figure 5.13. The storage modulus of the neat epoxy was measured 2.63 GPa.

Addition of all type of tungsten based powders into epoxy increased storage modulus values as compared with neat epoxy. While the specimens containing W powder demonstrated reduction in storage modulus with the increased amount of powder, no significant differences was observed in storage modulus values with the increased powder content for the other type of powders.

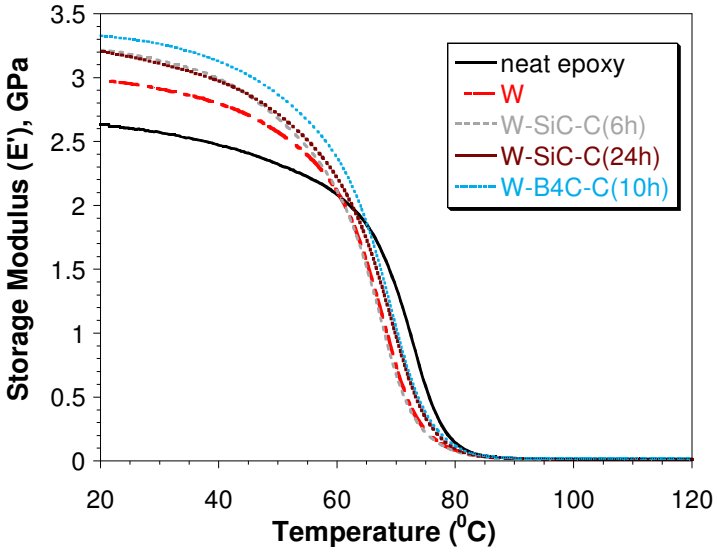

(a)

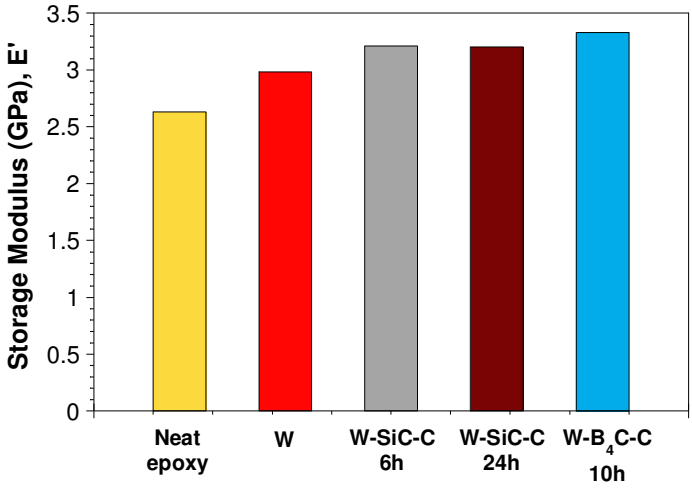

(b)

Figure 5.12. At 3 wt. % loading rate (a) Storage Modulus of epoxy nanocomposites (b) Storage Modulus values at 20 ^{0}C

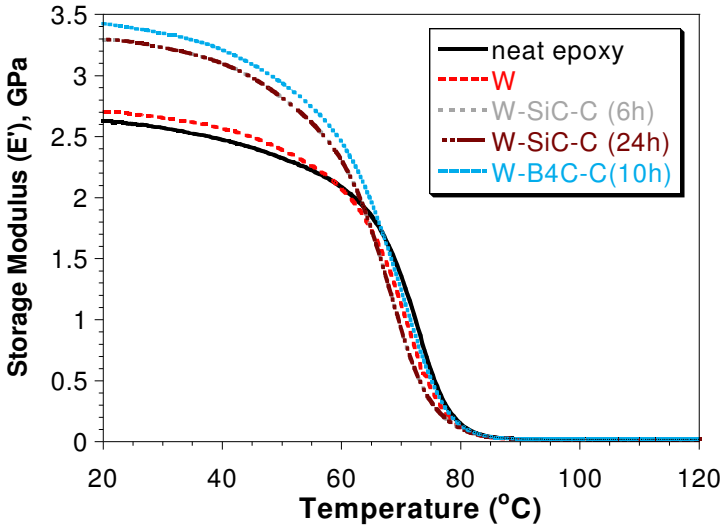

(a)

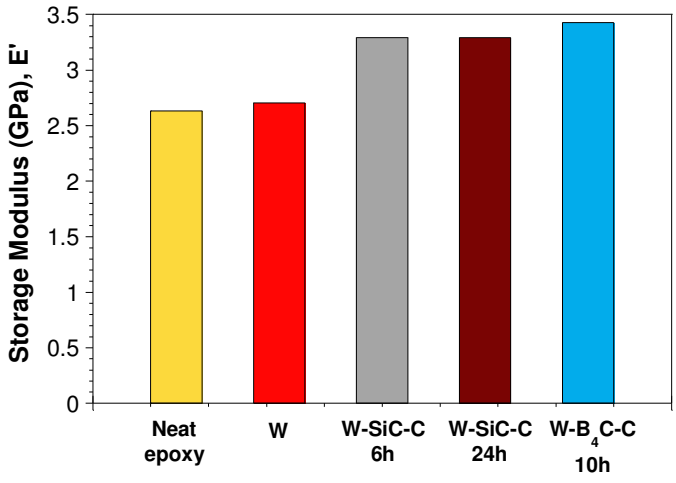

(b)

Figure 5.13. At 5 wt. % loading rate (a) Storage Modulus of epoxy nanocomposites (b) Storage Modulus values at 20 ^{0}C

In Figure 5.14, tan δ values of nanocomposites are illustrated for comparison. Based on the tan δ peak temperature, the glass transition temperature (T_g) of neat epoxy was determined as 82.56 °C. At 3 wt. % loading rate, T_g values of the nanocomposites containing tungsten based particles scatter more or less around that of neat epoxy. At 5 wt. % loading rate, the T_g values of all specimens are also close to neat epoxy, except for nanocomposite containing W-SiC-C (6h) nanopowder. With the increase in content of this powder, the T_g value of the specimen reduced. At low nanoparticles content, the dispersion homogeneity of the particles is high in general (Rong et al. 2003). Among the powders used in this study, because W-SiC-C (6h) powder has the lowest density, it occupies more volume in epoxy resin as compared to that of the other powders. Therefore, inhomogeneity

and agglomarations may be formed in epoxy for this powder and these can be the underlying reason for reduction in the T_g value of epoxy with addition of the powder.

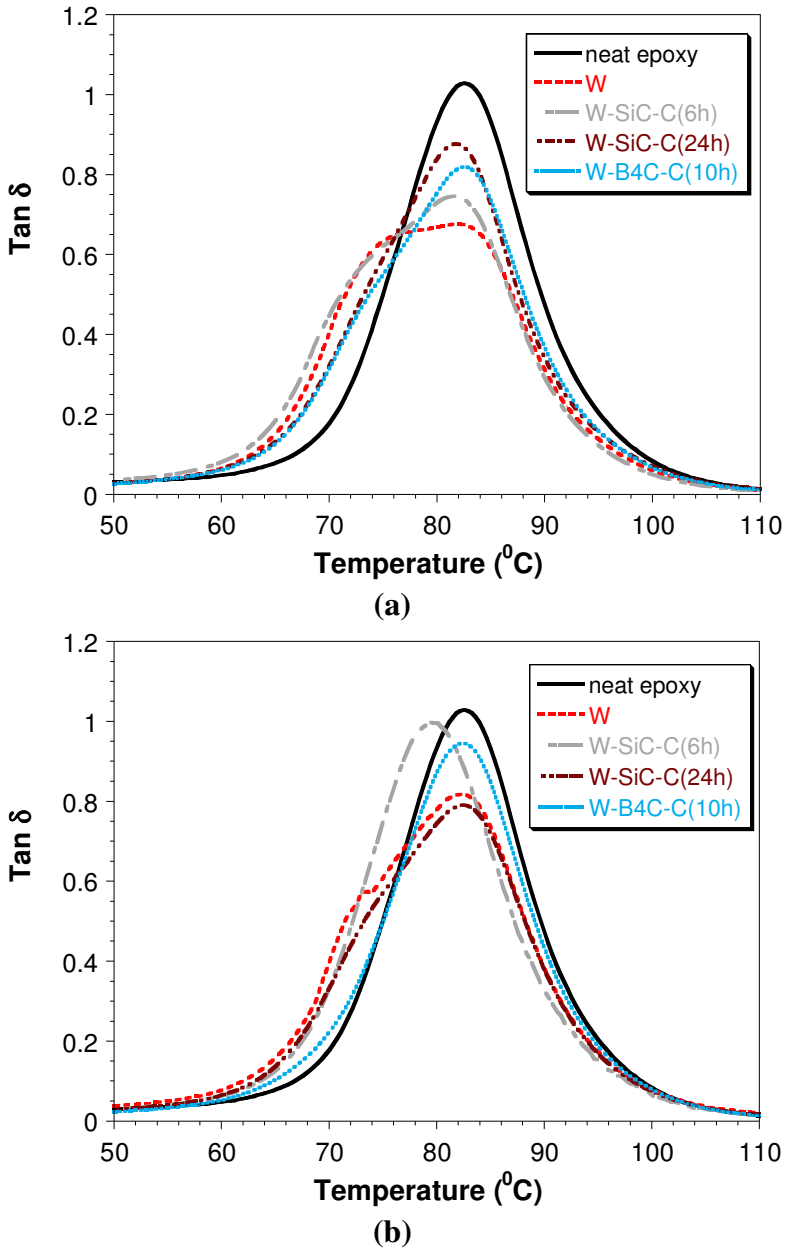

Figure 5.14. Comparison of Tan δ values of epoxy nanocomposites containing (a) 3wt. % and (b) 5 wt. % tungsten based powders

Glass transition temperatures (T_g) of nanocomposites were measured from DSC analysis. The effects of the tungsten based powders and their content on the T_g values are shown in Figure 5.15. The T_g value of neat epoxy was measured as 71.8 °C. At 3 wt. % loading rate, the nanocomposites containing W and W-SiC-C (6h) showed reduction in T_g values even though the T_g value of the neat epoxy remains almost constant with

the addition of other powders. As the filler size decreases, the interfacial area between the fillers and polymer matrix increases dramatically. It is possible that increasing the interfacial area may influence the polymer chain mobility and, therefore, change T_g of composites (Sun et al. 2004).

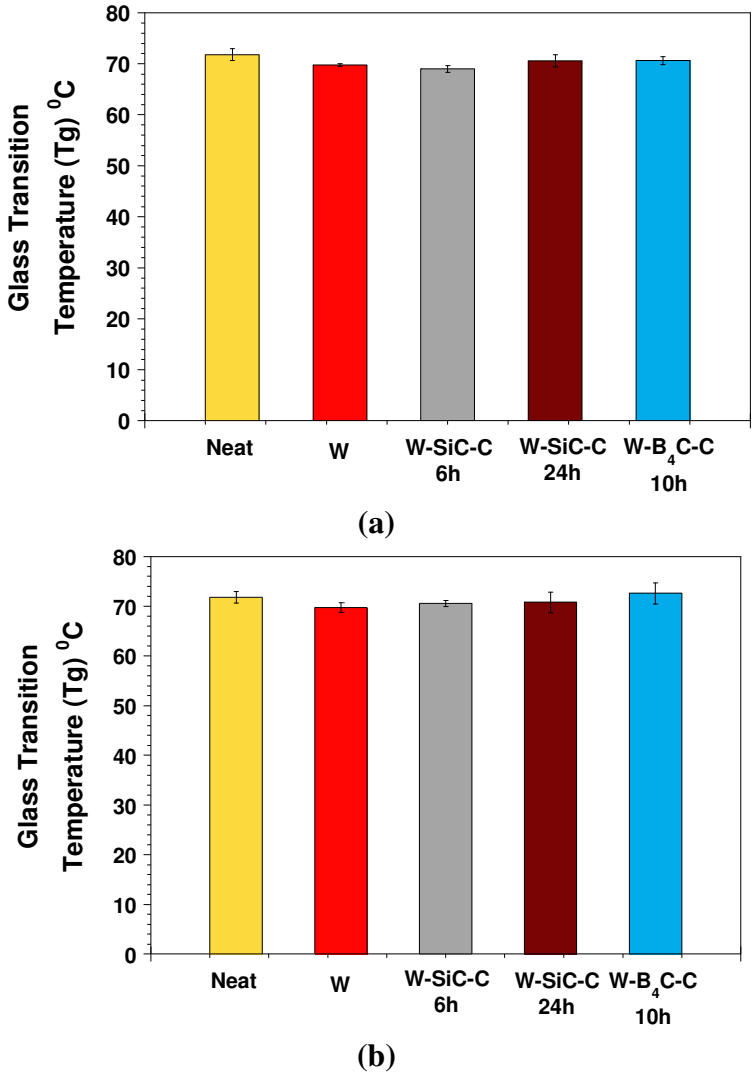

Figure 5.15. Glass Transition Temperatures (T_g) of epoxy nanocomposites containing (a) 3wt. %, (b) 5 wt. % of tungsten based powders

5.3. Fiber Reinforced Nanocomposites

5.3.1. Wear Performance

The volume loss values of non-crimp glass fabric reinforced composites (FRCs) containing 3 and 5 wt % of powder are tabulated in Table 5.2 and the specific wear rates

of FRCs are exhibited in Figure 5.16 and 5.17. Incorporation of fillers into the surface layer of fiber reinforced composites improves the wear resistance. It was found that, at 3 wt. % of powder additions, all of the specimens exhibited improved wear resistance since they showed lower wear rates as compared to those with neat epoxy. Among the different types of the powders, addition of 3 wt. % of W-SiC-C (24h) exhibited the highest improvement (approximately 2.5 times better wear rate than neat epoxy) on the wear rate. On the other hand, W and W-SiC-C (6h) exhibited relatively close values with neat epoxy.

Table 5.2 The Volume Loss Values of Fiber Reinforced Composites

Fiber Reinforced Composites	**Volume Loss (µm)**
Without Filler	1.51×10^{-6}
3 wt % loading rate of powder	
W	1.32×10^{-6}
W-SiC-C (6 h)	1.45×10^{-6}
W-SiC-C (24 h)	5.79×10^{-5}
W-B_4C-C (10 h)	1.24×10^{-6}
5 wt % loading rate of powder	
W	2.11×10^{-6}
W-SiC-C (6 h)	1.47×10^{-6}
W-SiC-C (24 h)	4.27×10^{-5}
W-B_4C-C (10 h)	1.44×10^{-6}

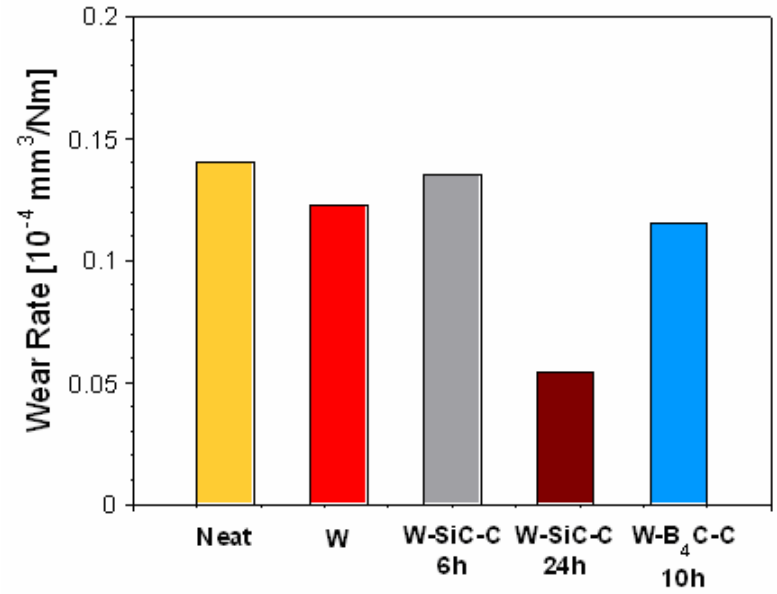

Figure 5.16. Comparison of the specific wear rates of fiber reinforced nanocomposites containing 3 wt. % of tungsten-based powders

With the increase of powder content from 3 wt % to 5 wt %, it was observed that the wear rate of the composite system that contains W-SiC-C (24h) is further reduced. However, the wear rate of the composites containing W increased even above of composites with neat epoxy. The wear rate for composite containing W-B_4C-C and W-SiC-C (6h) remained close to the values for composite with neat epoxy.

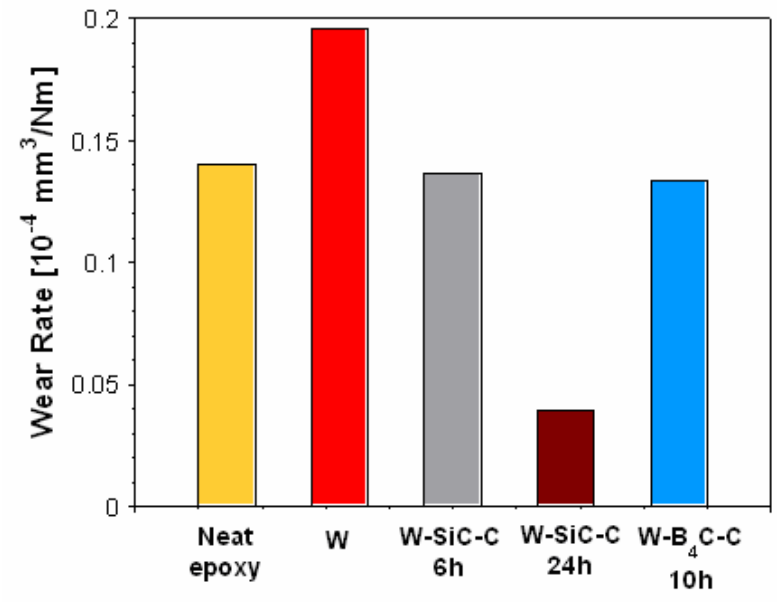

Figure 5.17. Comparison of the specific wear rates of fiber reinforced nanocomposites containing 5 wt. % of tungsten-based powders

The effect of powders and fibers on the friction coefficient values of composites is illustrated in Figure 5.18. On the contrary of wear rates, neat epoxy showed almost the lowest friction coefficient values. This might be because of the fact that it does not contain hard particles, thus wear debris of neat epoxy produced during the sliding is softer as compared with other composites and this soft wear debris has lower resistance to sliding.

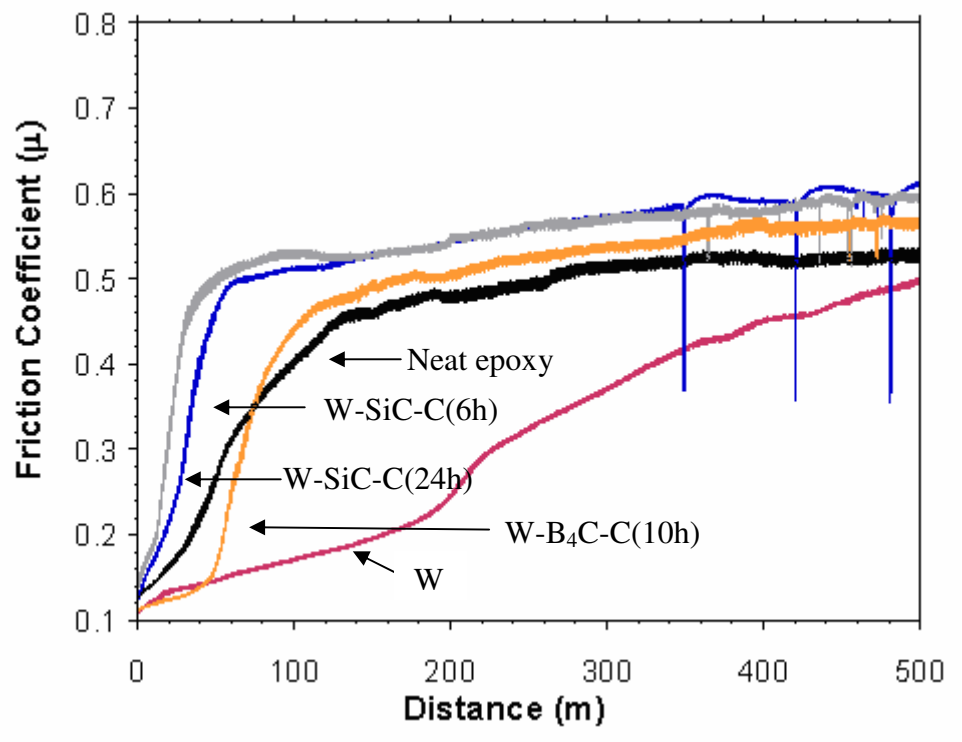

(a)

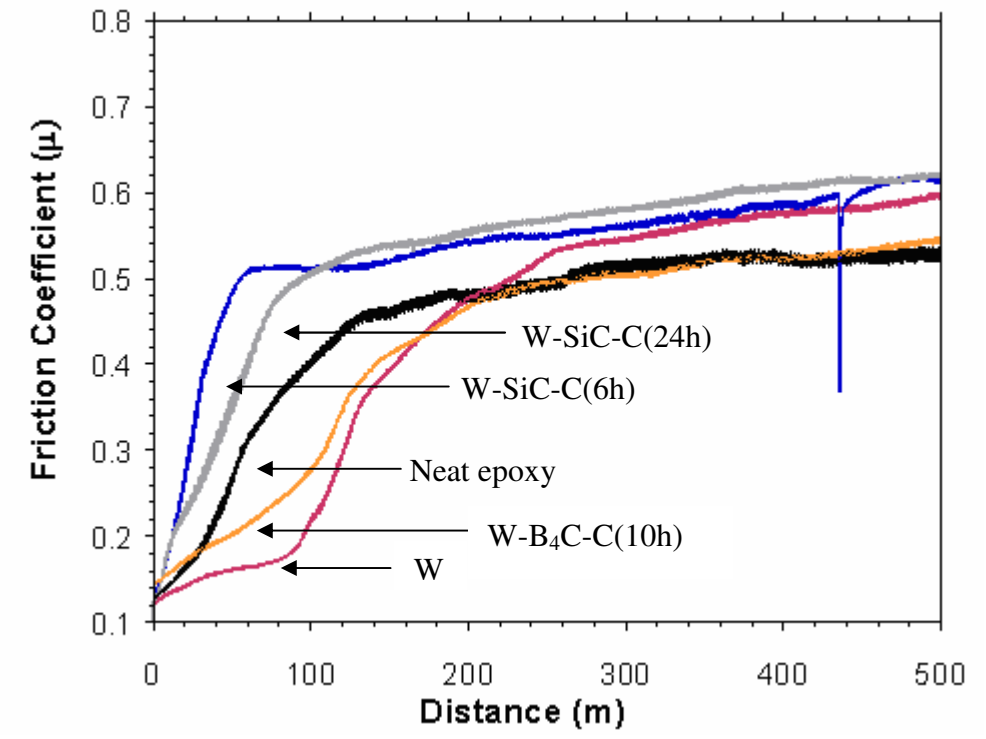

(b)

Figure 5.18. Comparison of the Friction Coefficient values of non-crimp glass fabric reinforced epoxy-based nanocomposites containing (a) 3 wt. % and (b) 5 wt. % tungsten-based powders

The topographic image of fiber reinforced composite (FRC) and 5 wt. % W-SiC-C (24h) powder incorporated FRC taken from 3-D profilometer after wear test is

illustrated in Figure 5.19. In this study, the highest wear resistance was obtained from this composite specimen. If worn surfaces of this specimen and neat epoxy are compared, it is observed that the depth of the wear groove for epoxy is higher.

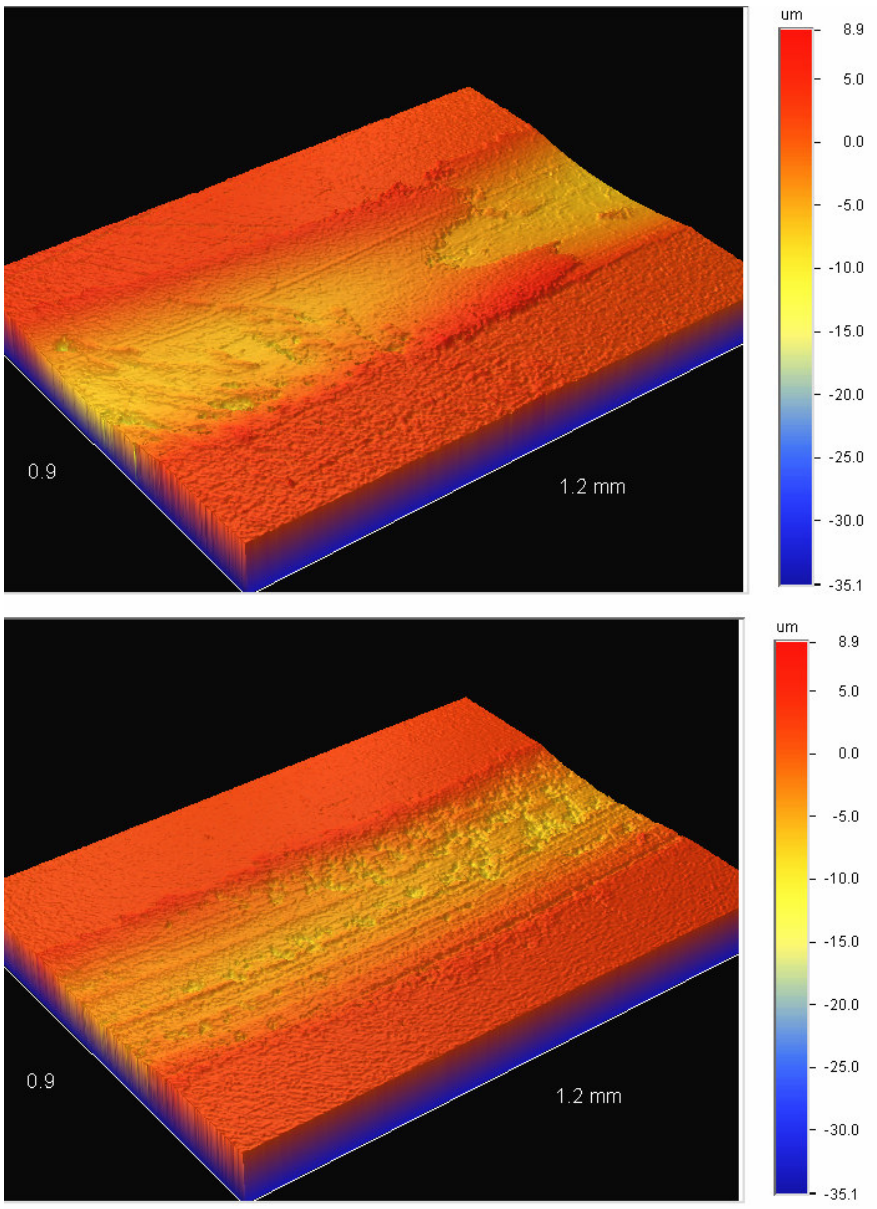

Figure 5.19. The surface topology for worn surfaces of non-crimp fabric reinforced (a) neat epoxy (b) epoxy nanocomposite containing 5 wt.% W-SiC-C (24h) powder

As seen from SEM images shown in Figure 5.20, fiber grinding and breakage was observed in epoxy composites after wear test. In other samples, an increased surface roughness was observed. Similar to nanocomposites, in FRCs, fatigue wear mechanism seems to be the dominative wear mechanism. This mechanism is based on

the sub-surface cracks nucleation due to shear deformation of the softer surface induced by the traction of the harder asperities (Zhang et al. 2002). Quintelier et al. studied the importance of the fiber orientation on wear propeties for the fiber reinforced polyester composites. They observed some wear mechanisms such as the fiber-matrix debonding. This mechanism consists of two parts. First one is the fiber-matrix debonding where matrix material is removed nearby the fibers. The other one is exposing the fiber, where matrix material above an underlying fiber is removed. The fiber-matrix debonding is dependent on the fiber orientation, mainly in the direction of the fiber. In the parallel orientation, this is due to the characteristics of the fiber, where the fibers move aside into direction parallel to applied load. In the perpendicular orientation, this is due to the possible bending of the fibers (Quintelier et al. 2006).

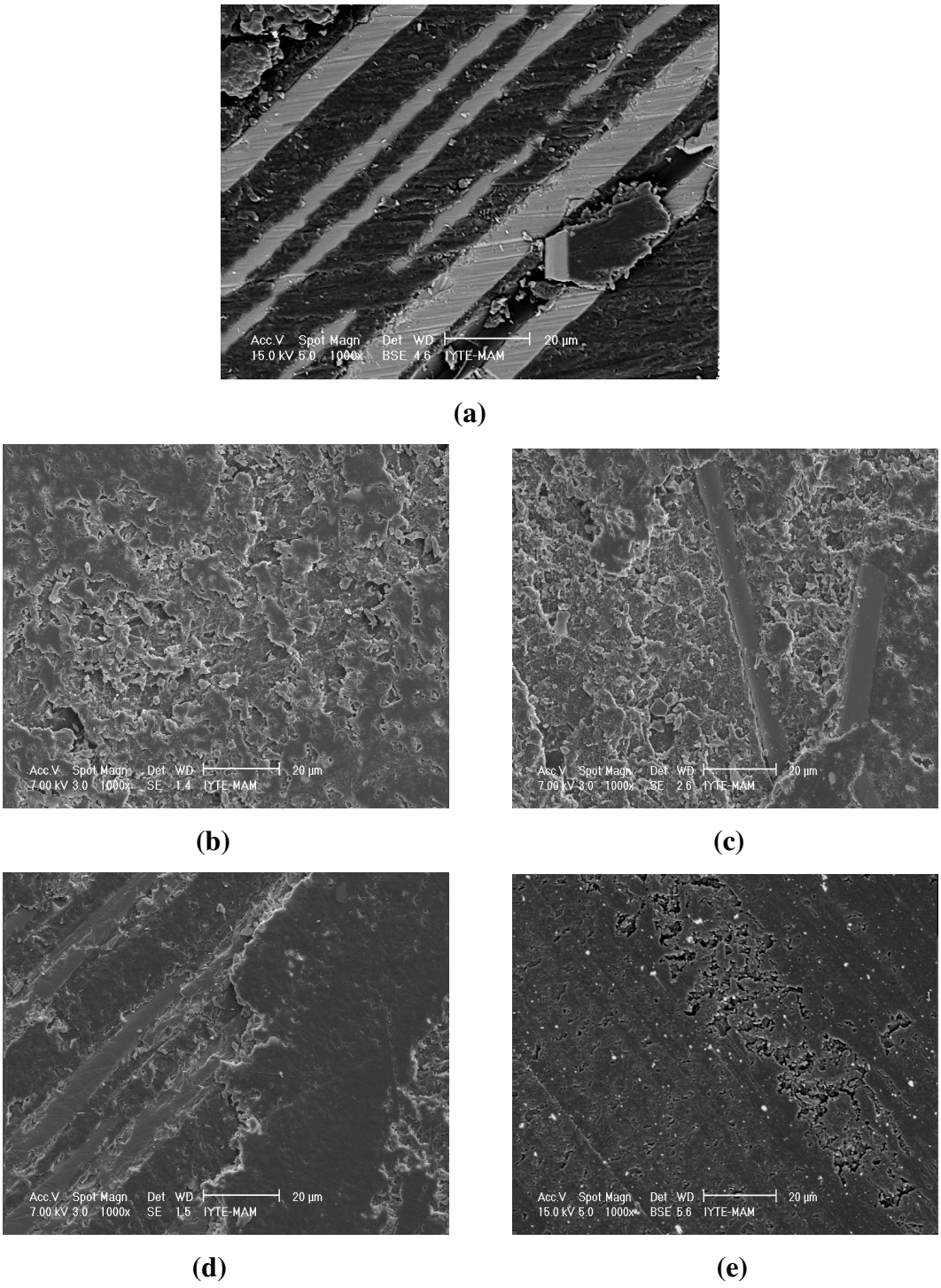

Figure 5.20. SEM images of worn surfaces of glass fabric reinforced composites containing epoxy matrix with (a) no powder addition (neat epoxy), (b) 3wt.% W, (c) 3 wt. % W-SiC-C (24h), (d) 5wt. % W and (e) 5 wt. % W-SiC-C (24h)

As surface hardness is principally regarded as one of the most important factors that govern the wear resistance of materials, Vickers microhardness values, Hv, of the composites were measured and they were given for comparison in Figure 5.21. As

mentioned earlier in section 5.2, the hardness values and wear resistance properties are related to each other. The composite containing 5 wt. % of W-SiC-C (24h) has the highest hardness value, thus resulting in the lowest wear rate value.

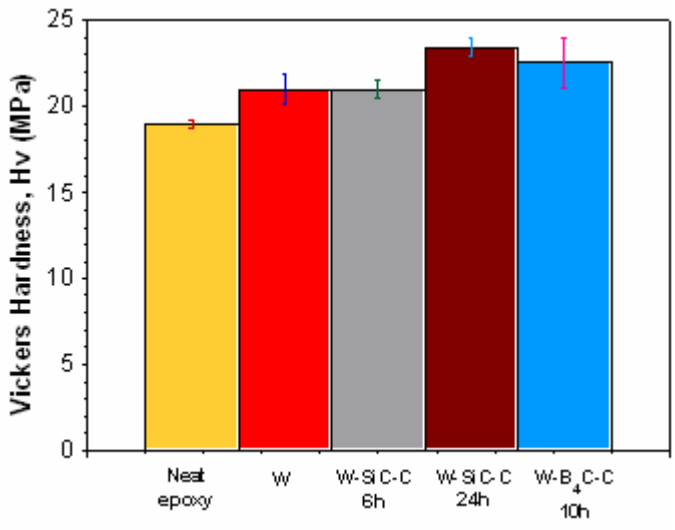

(a)

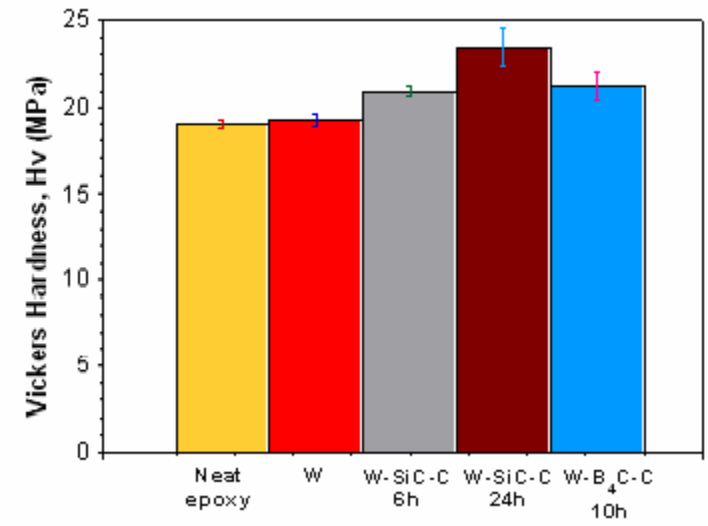

(b)

Figure 5.21. Microhardness of fiber reinforced epoxy nanocomposites containing (a) 3wt. %, (b) 5 wt. % of tungsten based powders

5.3.2. Flexural Properties

Figure 5.22 and 5.23 exhibit the influence of filler on the flexural strength and modulus values as a function of tungsten based powder loading. Flexural strength and modulus values of composites prepared without nanofiller addition were measured as,

357 MPa and 11.89 GPa, respectively. Flexural strength and modulus values decreased with the addition of powder loading. The reduction in the flexural strength may be ascribed to increasing void content with the addition of powder as highlighted in optical micrographs.

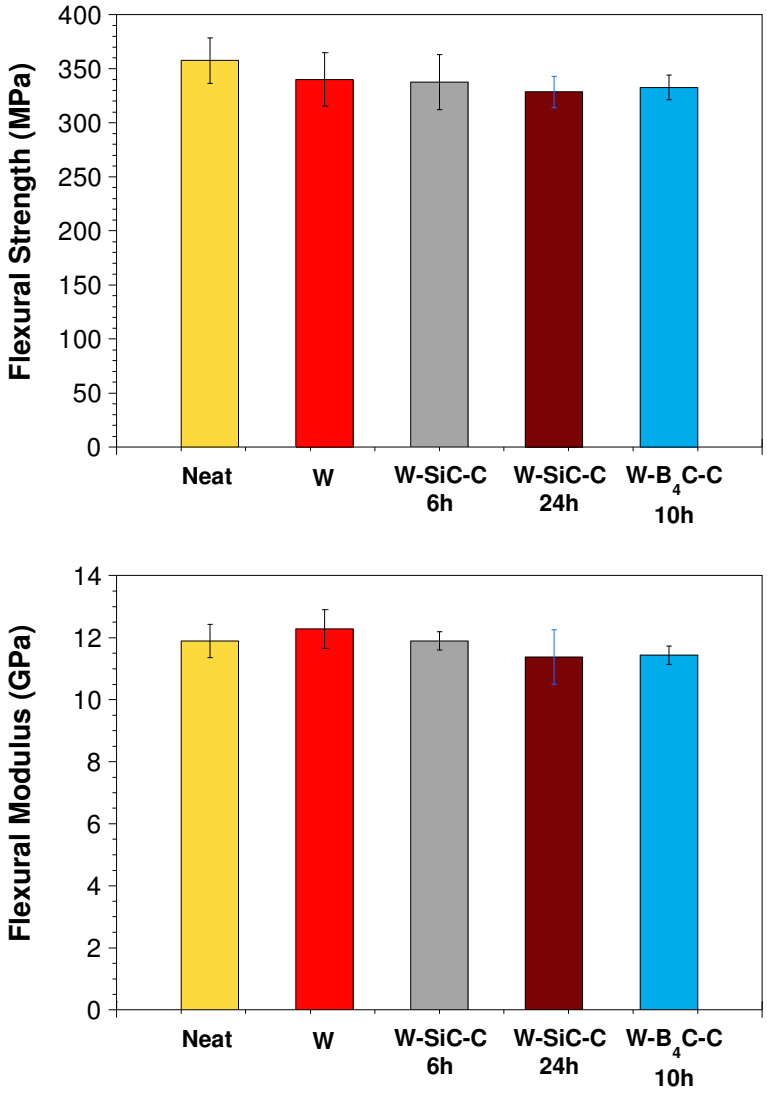

Figure 5.22. Flexural Strength and modulus values of glas fiber reinforced composites containing 3 wt. % powder

With a rise in the concentration of the nanoparticles, there is no drastic variation observed in strength values.

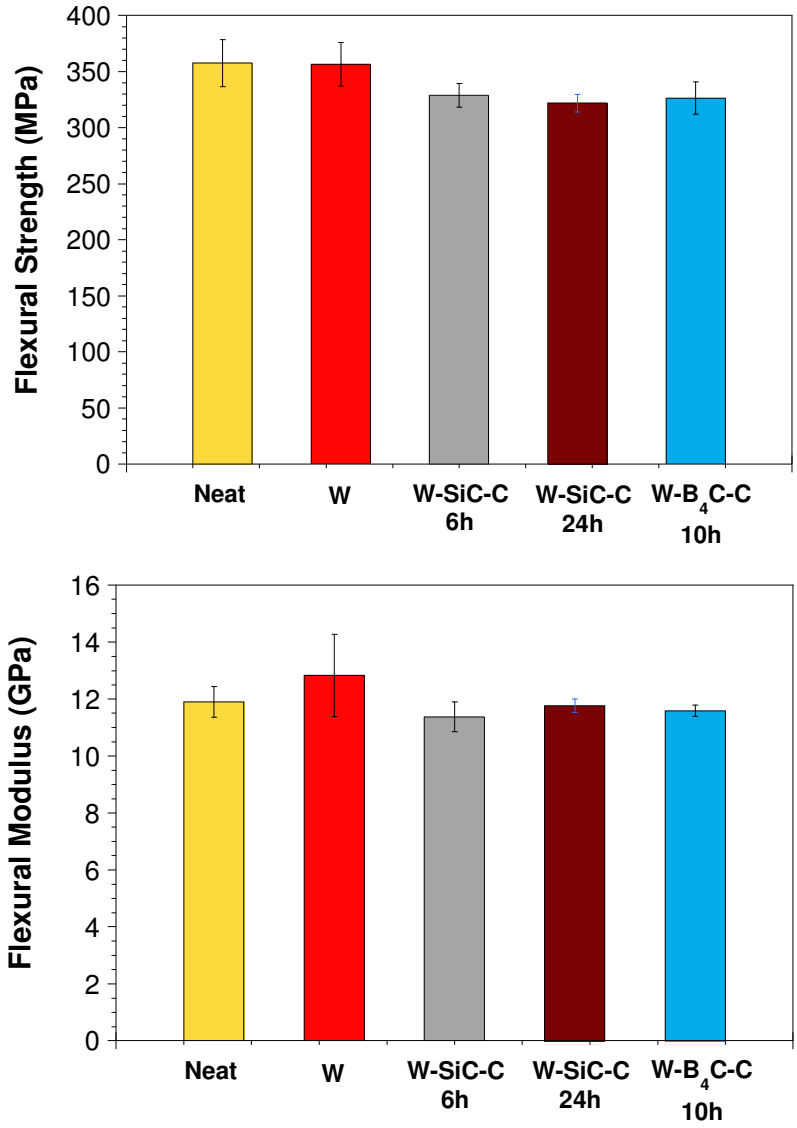

Figure 5.23. Flexural Strength and modulus values of composites containing 5 wt. % powder

Figure 5.24 shows the optical micrographs of fiber reinforced composite (FRC) without particle and with 5 wt. % W powder addition. The grinding and polishing techniques were conducted in order to take the following optic microscope images of failed specimens under flexural loading. According to these images, the reduction of the flexural strength and modulus can be ascribed to amount of void content.

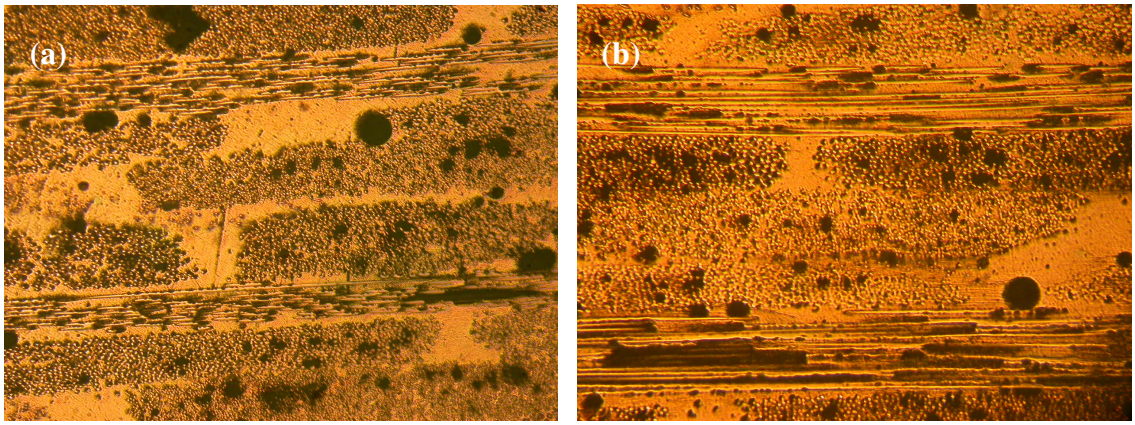

Figure 5.24. Optical micrographs of a) Fiber reinforced composite without filler, b) Fiber reinforced composite containing 5 wt. % of W

5.3.3. Thermomechanical Properties

The effects of fiber reinforcement and nanofiller additives on the thermomechanical properties of epoxy matrix composites are evaluated with DMA. The dynamic storage modulus (E') and tan δ versus temperature for FRCs prepared with neat epoxy and nanocomposites containing 3 and 5 wt. % powder are shown in Figures 5.25 to 5.26, respectively. Although both fibers and nanoadditives have significant effect on storage modulus, this study showed that the fiber is the main reinforcement compared with nanofiller to enhance the thermomechanical properties of epoxy. Increasing the nanofiller content from 3 to 5 wt. %, the storage modulus values of the composites with nanopowders are slightly lower, except for the specimen containing W-B_4C-C powder.

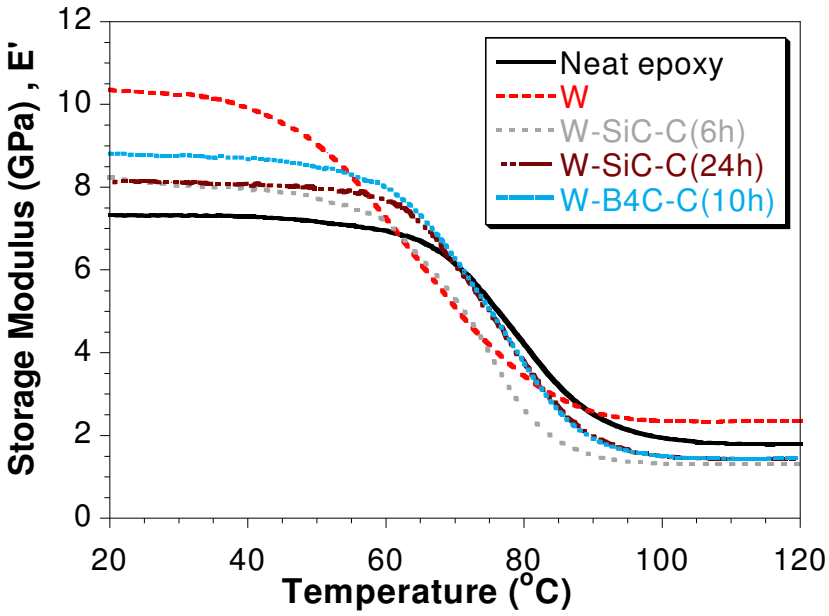

(a)

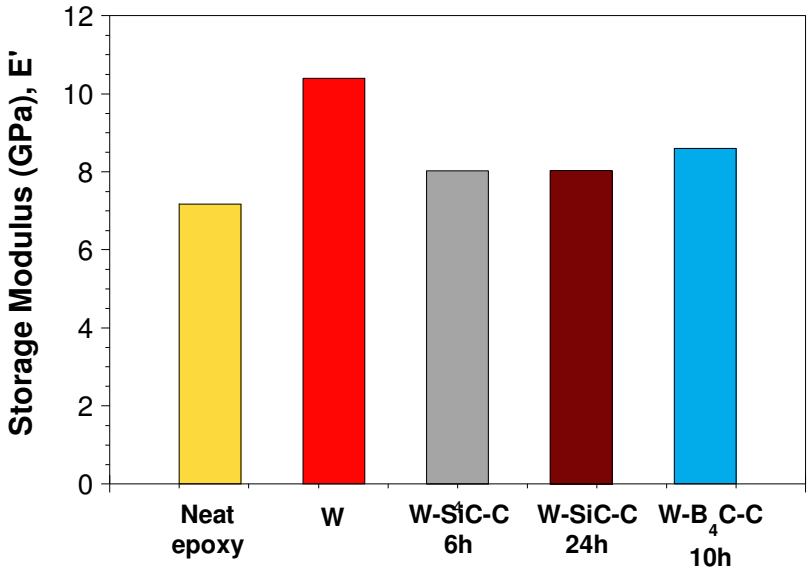

(b)

Figure 5.25. At 3 wt. % loading rate (a) Storage Modulus of fiber reinforced epoxy composites (b) Storage Modulus values at 20 ^{0}C

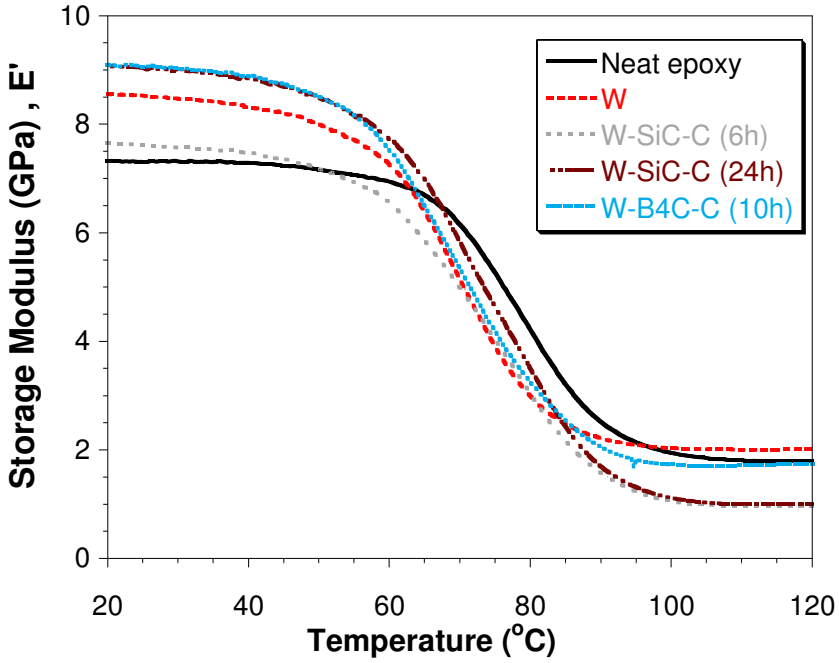

(a)

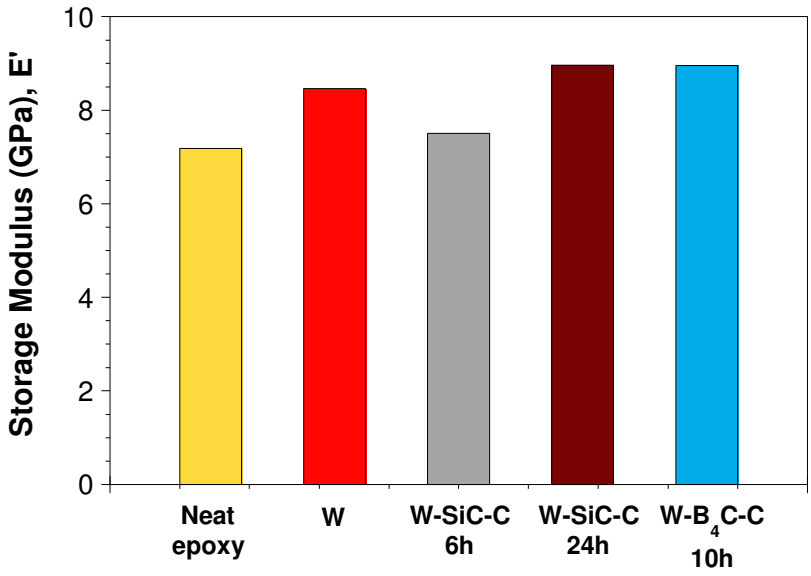

(b)

Figure 5.26. At 5 wt. % loading rate (a) Storage Modulus of fiber reinforced epoxy composites (b) Storage Modulus values at 20 ^{0}C

Tan δ values of non-crimp fiber reinforced composites are illustrated in Figure 5.27. At the glass transition temperature, the material can absorb more heat because of the increased mobility of polymer chains. Based on the tan δ peak temperature, the glass transition temperature (T_g) of composite without filler was determined as 87.53 °C. As incorporation of 3 wt. % of W and W-SiC-C (6h) into epoxy reduced the T_g values, the

other filler additions did not influence the T_g value of the neat epoxy. With the increase in content of powders, while the T_g values of the composites containing W and W-B_4C-C reduced, in other composites, the T_g values increased slightly.

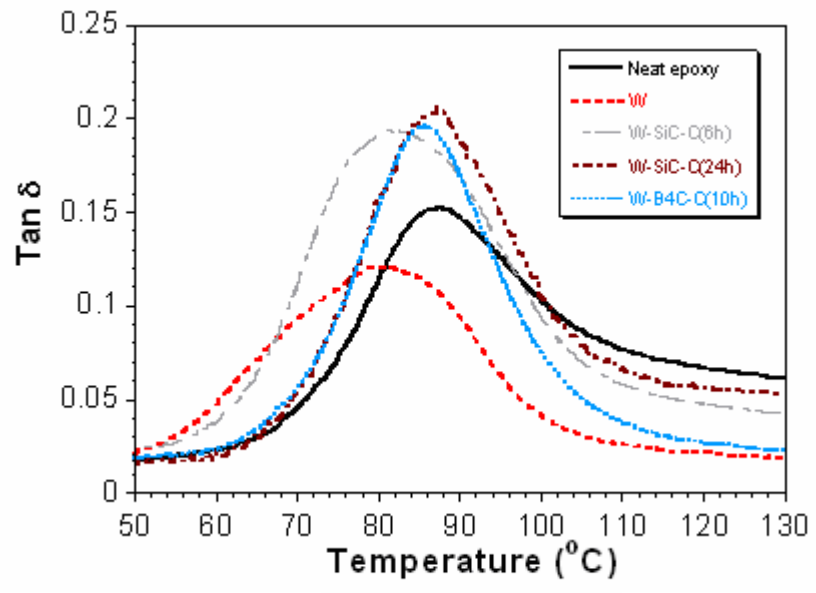

(a)

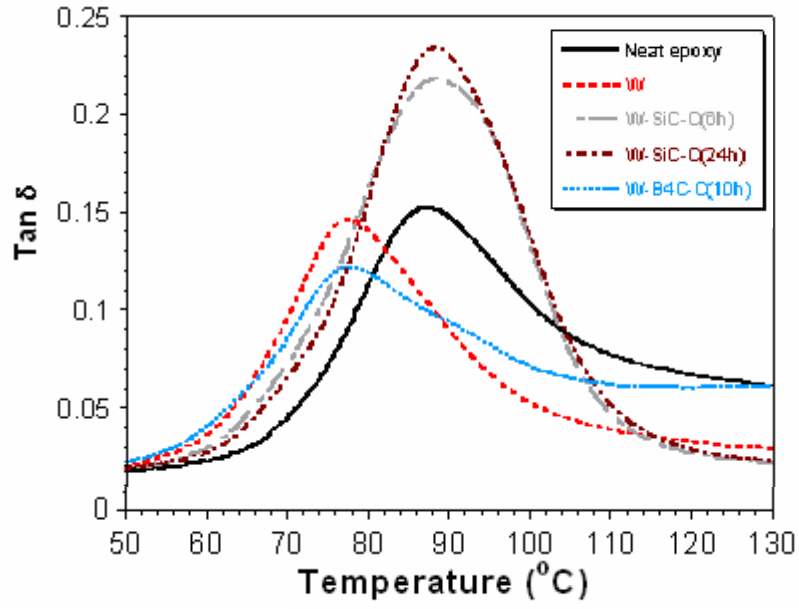

(b)

Figure 5.27. Comparison of Tan δ values of fiber reinforced epoxy nanocomposites containing (a) 3wt. % and (b) 5 wt. % tungsten based powders

CHAPTER 6

CONCLUSIONS

In the present study, the effects of tungsten based powders on the tribological, mechanical and thermal properties of the epoxy resin and stitched quadriaxial non-crimp glass fiber reinforced epoxy composites were investigated. Tungsten based powders with different composition were prepared by mechanical alloying. Based on the alloying parameters, different particle size distribution of the powders were obtained. With the incorporation of tungsten based powders into epoxy resin, resin suspensions containing 3 and 5 wt. % of various types of powders including W, W-SiC-C (6 and 24 h milled), W-B_4C-C (10 h) were obtained. The suspentions were casted in a mold and cured to obtain nanocomposites. The prepared suspensions were also used as a matrix to manufacture fiber reinforced epoxy composites.

Incorporating of all type and content of fillers into epoxy resin was found to significantly improve wear resistance of the nanocomposites. As on example, 3 wt. % of W-SiC-C (24h) powder filled nanocomposite exhibited the highest wear resistance among all of the samples, which was about 8 times higher than those of neat epoxy. Furthermore, vickers micro hardness values of the nanocomposites were investigated and consequently the highest hardness value was obtained from the same composition (nanocomposite containing 3 wt. % W-SiC-C (24h) of powder). From that point of view, it is reasonable to conclude that hardness values of nanocomposites are in relation with the wear resistance values.

It was found that the mechanical behaviour of the composites are not significantly affected by the incorporation of the nanopowders in composites. It is expected an improvement on the wear properties of the composites while there is no important decrease of the mechanical properties by the addition of nanoparticles into composite structures. The flexural strength and modulus values were slightly reduced with respect to increasing content of powders incorporated into epoxy resin. This may be related with the void content of nanocomposites that was found to increase with the addition of tungsten based powders into epoxy resin. In addition, incorporation of 3 wt. % W-SiC-C powder (6 hours milled) into epoxy resin resulted in % 9.5 higher tensile strength values in the nanocomposites relative to neat epoxy resin. Although thermo

mechanical properties of nanocomposites were enhanced to some extend with the addition of powders, their glass transition temperature (Tg) values were not significantly influenced with the presence of powders within the resin system.

Fabric reinforced composites were successfully fabricated utilizing tungsten based powder modified epoxy resin as matrix materials by conducting hand lay-up technique. The corresponding composites were then allowed to cure at room temperature followed by post curing at 80 and 150° C for 1 h and 2 h, respectively. Incorporation of fillers into the top surface layer of fiber reinforced composites improves wear resistance. While specimens containing 3 wt. % W and W-B_4C-C powder enhance the wear resistance, incorporation of 5 wt. % of these powders decreases wear resistance of the specimens. Flexural strength and modulus values of fiber reinforced composites were slightly reduced with respect to increasing content of powder incorporated into epoxy resin.

In brief, modification of the epoxy resin network by the incorporation of tungsten based nanoparticles did not lead to substantial improvements upon the mechanical properties of the nanocomposites and fiber reinforced epoxy composites. It was found that the effect of powders is more pronounced on the wear resistance as well as thermomechanical properties of the nanocomposites. In addition, tungsten based powders embedded into epoxy resin has no significant effects on the T_g values of the corresponding nanocomposites.

In the future studies, surface of tungsten based powders may be modified by using chemicals in order to tailor the interfacial interactions at interface between filler and matrix enhancing the chemical compatibility in between. Moreover, high speed mechanical stirring with higher shear rate can be employed in order to disperse the powders at nano-scale in a more succesful manner within thermosetting polymers such as epoxy or polyester.

REFERENCES

ASM International, 1992. "Friction, Lubrication, and Wear Technology", Wear, Ludema K.C., Vol.18.

Bijwe J., Neje S., Indumathi J., Fahim M. 2002. "Friction and wear performance evaluation of carbon fibre reinforced PTFE composite", *Journal of Reinforced Plastics and Composites*. Vol. 21, pp. 1221-1240.

Bloom P.D., Baikerikar K.G., Anderegg J.W., Sheares V.V. 2003. "Fabrication and wear resistance of Al-Cu-Fe quasicrystal-epoxy composite materials", *Materials and Engineering A*. Vol. 360, pp. 46-57.

Bondioli F., Cannillo V., Fabbri E., Messori M. 2005. "Epoxy-Silica Nanocomposites: Preparation, Experimental Characterization, and Modeling"

Cao Y.M., Sun J., Yu D.H. 2002. "Preparation and Properties of Nano-Al_2O_3 Particles/Polyester/Epoxy Resin Ternary Composites" *Journal of Applied Polymer Science*, Vol. 83, pp. 70–77

Chand N., Naik A., Neogi S. 2000. "Three-body abrasive wear of short glass fibre polyester composite", *Wear*. Vol. 242, pp. 38–46.

Chang L., Zhang Z. "Tribological properties of epoxy nanocomposites: II. A combinative effect of short carbon fibre and nano-TiO2", *Wear*. Submitted for publication.

Chang L., Zhang Z., Breidt C., Friedrich K. 2005. "Tribological properties of epoxy nanocomposites. I. Enhancement of the wear resistance by nano-TiO2 particles", *Wear*. Vol. 258, pp. 141–148.

Chowdhury F.H., Hosur M.V., Jeelani S. 2006. "Studies on the flexural and thermomechanical properties of woven carbon/nanoclay-epoxy laminates", *Materials Science and Engineering A*. Vol. 421, pp. 298–306.

Dangsheng X. 2005. "Friction and wear properties of UHMWPE composites reinforced with carbon fiber", *Materials Letters*. Vol. 59, pp. 175–179.

Dobrza´nski L.A., Drak M. 2006. "Properties of composite materials with polymer matrix reinforced with Nd–Fe–B hard magnetic particles". *Journal of Materials Processing Technology*. Vol. 175, pp. 149–156.

El-Tayeb N.S.M., Yousif B.F. 2007. "Evaluation of glass fiber reinforced polyester composite for multi-pass abrasive wear applications", *Wear*. Vol. 262, pp. 1140-1151.

El-Tayeb N.S.M., Yousif B.F., Yap T.C. 2006. "Tribological studies of polyester reinforced with CSM 450-R-glass fiber sliding against smooth stainless steel counterface", *Wear*. Vol. 261, pp. 443-452.

Friedrich K. 1993. “Tribology of polymer composites”, *Advanced Composites ’93*. p. 11.

Guang Shi, Ming Qiu Zhang, Min Zhi Rong, Bernd Wetzel, Klaus Friedrich 2004. “Sliding wear behavior of epoxy containing nano-Al_2O_3 particles with different pretreatments” *Wear*. Vol. 256, pp. 1072–1081

Guijun Xian, Rolf Walter, Frank Haupert 2006. “Friction and wear of epoxy/TiO2 nanocomposites: Influence of additional short carbon fibers, Aramid and PTFE particles” *Composites Science and Technology*. Vol. xxx. pp. xxx–xxx

Khedka J., Negulescu I., Meletis E.I. 2002. “Sliding wear behavior of PTFE composites”, *Wear*. Vol. 252, pp. 361–369.

Li X., Gao Y., Xing J., Wang Y., Fang L. 2004. “Wear reduction mechanism of graphite and MoS_2 in epoxy composites”, *Wear*. Vol. 257, pp. 279–283.

Lin J.C. 2007. “Compression and wear behavior of composites filled with various nanoparticles”, *Composites: Part B*. Vol. 38, pp. 79-85.

L. Chang, Z. Zhang, C. Breidt, K. Friedrich 2005. “Tribological properties of epoxy nanocomposites I. Enhancement of the wear resistance by nano-TiO2 particles” Wear. Vol. 258. pp. 141–148

L. Chang, Z. Zhang 2006. “Tribological properties of epoxy nanocomposites Part II. A combinative effect of short carbon fibre with nano-TiO_2”, *Wear*. Vol. 260, pp. 869–878

Quintelier J., De Baets P., Samyna P., Van Hemelrijck D. 2006. “On the SEM features of glass–polyester composite system subjected to dry sliding wear”, *Wear*. Vol. 261, pp. 703-714.

Rong M.Z., Zhang M.Q., Shi G., Ji Q.L., Wetzel B., Friedrich K. 2003. “Graft polymerization onto inorganic nanoparticles and its effect on tribological performance improvement of polymer composites” *Tribology International*. Vol. 36, pp. 697–707

Shi G., Zhang M.Q., Rong M.Z., Wetzel B., Friedrich K. 2003. “Friction and wear of low nanometer Si_3N_4 filled epoxy composites”, *Wear*. Vol. 254, pp. 784–796.

Shi G., Zhang M.Q., Rong M.Z., Wetzel B., Friedrich K. 2004. “Sliding wear behavior of epoxy containing nano-Al_2O_3 particles with different pretreatments”, *Wear*. Vol. 256, pp. 1072–1081.

Suresha B., Chandramohan G., Prakash J.N., Balusamy V., Sankaranarayanasamy K. 2006. “The role of fillers on friction and slide wear characteristics in glass-epoxy composite systems”, *Journal of Minerals and Materials Characterization and Engineering*. Vol. 5, pp. 87-101.

Vasconcelos P.V., Lino F.J., Baptista A.M., Neto R.J.L. 2006. "Tribological behavior of epoxy based composites for rapid tooling", *Wear*. Vol. 260, pp. 30–39.

Web_1, 2006, Farmingdale University web site, 17/05/2006, http://info.lu.farmingdale.edu/depts/met/met205/composites.html

Web_2, 2006. Composite Reinforcement Fabrics web site, 14/05/2006, http://www.vectorply.com/reinforcement.

Wetzel B., Haupert F., Friedrich K., Zhang M.Q., Rong M.Z. 2002. "Impact and wear resistance of polymer nanocomposites at low filler content", *Polymer Engineering Sciences*. Vol. 42, pp. 1919–27.

Wetzel B., Haupert F., Zhang M.Q. 2003. "Epoxy nanocomposites with high mechanical and tribological performance", *Composites Science and Technology*. Vol. 63, pp. 2055–2067.

Xian G., Walter R., Haupert F. 2006. "A Synergistic Effect of Nano-TiO2 and Graphite on the Tribological Performance of Epoxy Matrix Composites". *Journal of Applied Polymer Science*. Vol. 102, pp. 2391–2400.

Xian G., Walter R., Haupert F. 2006. "Friction and wear of epoxy/TiO_2 nanocomposites: Influence of additional short carbon fibers, Aramid and PTFE particles", *Composites Science and Technology*

Xing X.S., Li R.K.Y. 2004. "Wear behavior of epoxy matrix composites filled with uniform sized sub-micron spherical silica particles", *Wear*. Vol. 256, pp. 21–26.

Yu L., Bahadur S., Xue Q. 1998. "An investigation of the friction and wear behaviors of ceramic particle filled polyphenylene sulfide composites", *Wear*. Vol. 214, pp. 54-63.

Zhang M.Q., Rong M.Z., Yu S.L., Wetzel B., Friedrich K. 2002. "Effect of particle surface treatment on the tribological performance of epoxy based nanocomposites", *Wear*. Vol. 253, pp. 1086–1093.

Zhang Z., Breidt C., Chang L., Haupert F., Friedrich K. 2004. "Enhancement of the wear resistance of epoxy: short carbon fibre, graphite, PTFE and nano-TiO2", *Composites A*. Vol. 35, pp. 1385-1392.

Zhang H., Zhang Z. 2004. "Comparison of short carbon fibre surface treatments on epoxy composites II. Enhancement of the wear resistance". *Composites Science and Technology*. Vol. 64, pp. 2031–2038.

Zhang L.C., Zarudi I., Xiao K.Q. 2006. "Novel behaviour of friction and wear of epoxy composites reinforced by carbon nanotubes". *Wear*.